Novel features in Accelerometer-based Gait analysis for long-term monitoring of Parkinson's disease: A Signature of Gait.

Michael Dunne-Willows

Thesis submitted for the degree of

Doctor of Philosophy

School of Mathematics, Statistics & Physics

Newcastle University

Newcastle upon Tyne

United Kingdom

August 2021

I dedicate this thesis to Anne-Marie and Mark, my parents, whose avid interest in my research sustained me, for being my unconditional emotional anchor throughout; to Alexander, my brother, whose friendship and keen wit lifted me in moments of discouragement; to Walter Willows, my Grandad, himself cruelly taken from us by Parkinson's Disease, and to Mary the champion of learning that was my beloved Nanna, and of course to Sarah Jane, my beautiful fiancée, for her enduring patience and love.

Acknowledgements

I would like to thank to my supervisors Dr Silvia Del Din, Dr Jian Qing Shi, Dr Kevin Wilson, Dr Pete Philipson, and Dr Alan Godfrey for their invaluable advice, continuous support, and patience during my PhD study. Their immense knowledge experience have encouraged and supported me throughout my research.

I would like to express my gratitude to the EPSRC for Doctoral Training in Cloud Computing for Big Data and in particular to Professor Paul Watson, Jennifer Wood, Oonagh McGee and Dr Matthew Forshaw. I am also very grateful to Professor Lynn Rochester and all the wonderful people at the Brain and Movement Research Group for such a diverse PhD experience. Lastly, I would also like to thank the assessors of the Incidence of Cognitive Impairment in Cohorts with Longitudinal Evaluation study and the participants involved in this study without whom this research would not have been possible.

Abstract

Parkinson's Disease (PD) is a neurodegenerative disease that can lead to restricted or slowed movement, gait impairments and increased risk of falling. Over recent decades, instrumented gait analysis (IGA) has contributed much to the understanding of gait impairments in PD. Due to the complexity of gait and high clinical interest a plethora of features have been suggested for gait analysis in the literature pertaining to several groups such as: traditional spatio-temporal (e.g. gait speed), frequency domain, etc. A subset of these traditional gait features has been proposed and validated in PD and older adults as a comprehensive model of gait comprising five factors: pace, rhythm, asymmetry, variability, and postural control. Analysis of gait may be grouped into the assessment of two types of variability, namely, within-subject variability which is needed for personal disease management and inter-subject variability which is useful in quantifying the overall impact of PD on gait. Advances in wearable technology have led to much smaller devices (e.g. accelerometers) being commercially available in conjunction with greatly increased battery lives to the degree that not only lab-based but also continuous recordings over 7 days (real-world) are possible. Wearable technology-based gait analysis is indeed emerging as a powerful tool to detect early disease and monitor progression. Data recorded as part of the ICICLE-GAIT [1] study provides acceleration data for over 100 people with PD and age-matched control subjects in both lab and real-world conditions. These datasets form the basis for the development of a new Phase

[1]ICICLE-GAIT is a collaborative study with ICICLE-PD, an incident cohort study (Incidence of Cognitive Impairment in Cohorts with Longitudinal Evaluation—Parkinson's disease). The ICICLE-GAIT study was supported by Parkinson's UK ((J-0802, G-1301)) and by the NIHR Newcastle Biomedical Research Centre

plot methodology for gait analysis in PD. In this thesis I present a novel methodology for both assessing PD and tracking individual disease progression over multiple timescales. To accomplish this, I introduce a new feature domain, the Phase domain, based on a particular type of recurrence plot known as a Poincaré plot. Poincaré plots are sometimes referred to in the literature as return maps, self-similarity plots or Phase plots. Phase plots were being used in the early 1990s in ECG studies to produce self-similarity plots of beat-to-beat intervals. This technique proved to be reliable in detecting atrial fibrillation. The rare instances of its application to other fields are very limited and do not demonstrate any modification or development beyond that which has been used in ECG studies for decades. I develop methodology for application to gait analysis and, indeed, any cyclical biosignals. In this thesis I used the data from the ICICLE-GAIT study to demonstrate that with specific modifications and newly identified features (comprising the Phase domain), this novel Phase plot methodology is highly applicable to gait analysis within PD and provides a framework for: (i) identifying and characterising PD and (ii) individual disease tracking over the years following diagnosis. Throughout these analyses, traditional gait features serve as an established reference and benchmark. I employ statistical methods, such as non-linear mixed effects models and Statistical Parametric Mapping, to model PD progression and assess the clinical utility of Phase plots. I also used Discrete-Time Markov chain modelling, longitudinal analyses, and functional principal components analysis to demonstrate that Phase plots provide an objective, personalised, and clinically relevant signature of gait. In the case of PD patients (and controls to a lesser extent) four distinct Phase plot Types emerge and occur with high within-subject reproducibility, hence the signature interpretation. Many features within the Phase domain proved to be highly sensitive to the disease (people with PD versus controls). Using lab-based data, the Phase domain

features outperformed traditional spatio-temporal features in classifying PD. Each domain of features performed similarly well in the prediction of MDS-UPDRS [2] (a useful proxy for PD progression). Specifically, part III of the UPDRS scale was used as this relates to motor function. In real-world conditions Phase plot features showed sensitivity to disease state and physical capability across multiple timescales e.g., daily fluctuations, and also across 18-month follow up time points. The Phase plot-based signature of gait is validated under lab-based conditions to reflect participants' capacity for gait as well as under real-world conditions as a compact means of monitoring PD and walking performance through gait.

[2]Movement Disorder Society Unified Parkinson's Disease Rating Scale

0.1 Publications, Presentations, awards

1. Dunne-Willows, M., Watson, P., Rochester, L., Shi, J., Del Din, S., "A Novel Parametrisation of Phase Plots for Monitoring of Parkinson's Disease." Full paper publication - IEEE Engineering in Medicine and Biology Society (EMBC). IEEE, 2019.

2. Dunne-Willows, M., Shi, J., Hickey, A., Watson, P., Rochester, L., Del Din, S., "Validation of a novel light-weight template-based algorithm for free-living gait detection." Abstract accepted and poster presented at the 6th International Conference on Ambulatory Monitoring of Physical Activity and Movement (ICAMPAM) in Maastricht, Netherlands, 2019.

3. Dunne-Willows, M., Watson, P., Rochester, L., Shi, J., Del Din, S., "Multivariate Gaussian Mixture Model Approximation of Phase Plots for Monitoring of Parkinson's Disease." Accepted to the IEEE journal of Engineering in Medicine and Biology and presented at the 40th annual international conference of the IEEE engineering in medicine and biology society 2018.

4. VetSens Business Voucher 2018. A collaborative business voucher between Clinical Ageing Research Unit and VetSens. Developed a light-weight set of algorithms for gait analysis in canine subjects.

5. Del Din, S., Dunne-Willows, M., Godfrey, A., Shi, J., Coleman, S,. Burn, B,. Rochester, L., "Effect of medication on habitual gait in people with Parkinson's disease: a feasibility study". Accepted to the 2017 International Society of Posture and Gait Research (ISPGR) World Congress and Presented as poster.

Contents

Chapter 1

Background

In this chapter we provide a background of statistical and clinical methodologies within wearable sensor-based gait analysis.

1.1 PD and Instrumented Gait Analysis

Parkinson's Disease (PD) can lead to impaired/slowed movement, gait impairments and increased risk of falling. Wearable technology-based gait analysis is emerging as a powerful tool to detect early disease and monitor progression [1–3]. Normal gait describes the variety of walking patterns found in healthy populations [4]. Even healthy subjects' gait may present us with a degree of variability resulting from physical differences like age, height and other anatomical factors [5, 6]. Analysis of gait is complicated by significant intra-subject variability. The same person's gait may vary depending on location, activity and on the measurement techniques themselves [7]. At a high level of abstraction, analyses of gait may be grouped into the assessment of two types of variability, namely, the above mentioned intra-subject variability, and the inter-subject variability. The latter is more relevant to quantifying the impact of disease and pathology on gait. Instrumented gait analysis has

benefits including objectivity during unrestricted activities of daily living. However, there is significant heterogeneity among subjects e.g. demographic, age, height, weight, comorbidities [8, 9] etc. which require very versatile bio-markers to be developed for valid tracking of disease progression. Before development of specialist tools and sensors, gait analysis was limited to using in-person visual observations. While limited in detail, this was sufficient for clinicians in the 17th century to identify distinct phases of the human gait cycle based on gait events (GEs) like the initial contact (IC or heel strike) and final contact (FC or toe-off) [10]. IC and FC events are still used today for gait segmentation. In the 19th century more detailed methods of gait cycle segmentation were proposed including the stance (when a foot is in contact with the ground) and swing (not in ground contact) phases. The pendulum theory of locomotion was also proposed at this time [11]. This theory regards the swing phase of gait as an entirely passive phase, where the leg's motion can be described as an inverted pendulum pivoting about the pelvis. This theory, also referred to as the inverted pendulum model, is still used today for calculating reliable measures of step length and other features in the spatio-temporal domain [12]. The kinematics of gait (the evaluation of position, velocity, acceleration of limbs and joints during walking) were later studied using photographic methods. This was effective for analysing gait but was time-consuming. In the 1890s Braune et al studied the angular displacement of the lower limbs using an early method of three-dimensional motion analysis via light-emitting markers [13]. Several methods were later developed for measuring the kinetics of gait. Note here the *kinetics* of gait refers to the forces being applied and acting on limbs during walking whereas the *kinematics* refers only to the motion of said limbs. From the 1940s, more concepts of engineering, anatomy and orthopaedics were being brought into the field of gait analysis. This led to the use of electromyography (EMG) to measure the elec-

trical activity of muscles during walking, and additional means of measuring gait kinematics including force plates, and accelerometers. Each of these methods have undergone significant developments over the decades as their respective technologies have been developed. For example, in the case of accelerometers, devices are now small enough (see Figure 1.2 for an example) to be worn discretely and unobtrusively while also continuously recording at frequencies over 100Hz in three axes of acceleration for over a week without recharging. This particular development is crucial for objective gait analysis as it allows for subjects to wear accelerometers on their person in free-living conditions. Over recent decades, instrumented gait analysis has contributed much to the understanding of gait abnormalities and moreover the study of the physical manifestations of neurological conditions such as Parkinson's disease which can be characterised by its impact on walking. Another well-known method of assessing Parkinson's disease and, in particular its progression, is Positron Emission Tomography, also known as a PET scan. This is used to assess the ability of a patient's brain to absorb Levadopa, an important compound for producing dopamine, a neurotransmitter which is reduced in the case of Parkinson's disease. These scans are expensive and may be impractical to repeat regularly for elderly patients, hence the clinical and research interest in instrumented gait analysis [14]. Effective gait analysis relies on the combination of both statistical and clinical methodologies. Two feature domains in particular dominate the literature, namely the spatio-temporal domain [15] including intuitive and easily interpreted features such as stride length and cadence, and the frequency domain, which has a proven utility within PD particularly in those patients with a tremor (shaking), one of the main symptoms of the disease. In this thesis I present a novel methodology for both assessing the management of PD and tracking disease progression on an individual basis over time periods of several years. To accomplish this, I introduce

a new feature domain, the Phase domain, based on a particular type of recurrence plot known as a Phase plot. Phase plots are sometimes referred to in the literature as: return maps, self-similarity plots or Poincaré plots. For simplicity's sake, phase plot is the chosen term throughout this thesis. Phase plots were being used in the early 1990s to assess variability in cardiovascular data [16]. In short, a feature of interest would be extracted from each heartbeat in an ECG recording- each successive feature was then plotted against the feature immediately prior. The spread of the resulting 2-dimensional cluster of points would then be quantified as a measure of beat-to-beat variation. This has proven to be reliable in detecting atrial fibrillation (rapid and/or irregular heartbeats) which can lead to heart failure. Today, ECG remains the most prevalent application of phase plot analysis. The relatively rare instances of its application to other fields e.g. EEG [17], and indeed gait analysis [18], are very limited and do not demonstrate any modification or development of the phase plot methodology beyond that which has been used in ECG studies for decades. I assert and demonstrate in this thesis that with specific modifications and newly identified features (comprising the Phase domain), this novel phase plot methodology is highly applicable to gait analysis within PD and provides a framework for individual disease tracking over the years following diagnosis, while also demonstrating the methodology's sensitivity to day-to-day fluctuations in gait. In addition, within both of these time scales, Phase plots can quantify and account for the impact of ageing on an individual's disease state.

1.2 Wearable Technology for Gait Analysis

Research into gait analysis in biomedical disciplines started with visual systems typically consisting of multiple cameras synchronised with force plates which capture ground reaction forces [19, 20]. These systems have been successfully developed

but require specialised and expensive gait labs and also rely on substantial post-processing. Spatial limitations also lead to restricted and unrealistic subject activity. Wearable sensors, or "wearables", have offered an alternative which mitigates several of these issues such as cost but more crucially they allow for deployment into real-world conditions. Wearables are transforming the clinical research. Wearable accelerometers, for example, offer a non-invasive and inexpensive means of continuously monitoring the wearer's activity [21, 3]. These properties of wearables allow for realistic performance measuring in real-world conditions [2, 3]. Being able to monitor participants in real-world environments during unscripted activities of daily life (ADL) is a major advantage. Hillel et al [22] showed that there is a substantial performance gap when comparing gait recorded in scripted lab-based activities with that of real-world ADL. In general real-world gait can be regarded as a more objective measure of the wearer's performance whereas lab-based gait should be treated as a measure of their capacity for gait [23, 24], i.e. a potentially unrealistic example of the wearer's ideal gait performance. Wearable sensors have been shown to be a robust tool for quantifying gait in lab-based environments [25, 15].

Wearable technology includes sensors from simple accelerometers to Inertial Measurement Units (IMUs) which include gyroscopes (for gathering rotation and angular momentum data) and Magnetometers which detect absolute orientation (relative to the local direction of the Earth's magnetic field). In this thesis we will focus on the use of a triaxial accelerometer which records the acceleration of force applied to an object in three directions. Real-world sensor data recorded during unscripted activities has been shown to be more sensitive to gait impairments such as those resulting from PD [26, 1, 24]. The accelerometers used to produce the data for the analyses in this thesis were configured so that these three directions (or axes) where consistent with the axes of the wearer's body (see Figure 1.1).

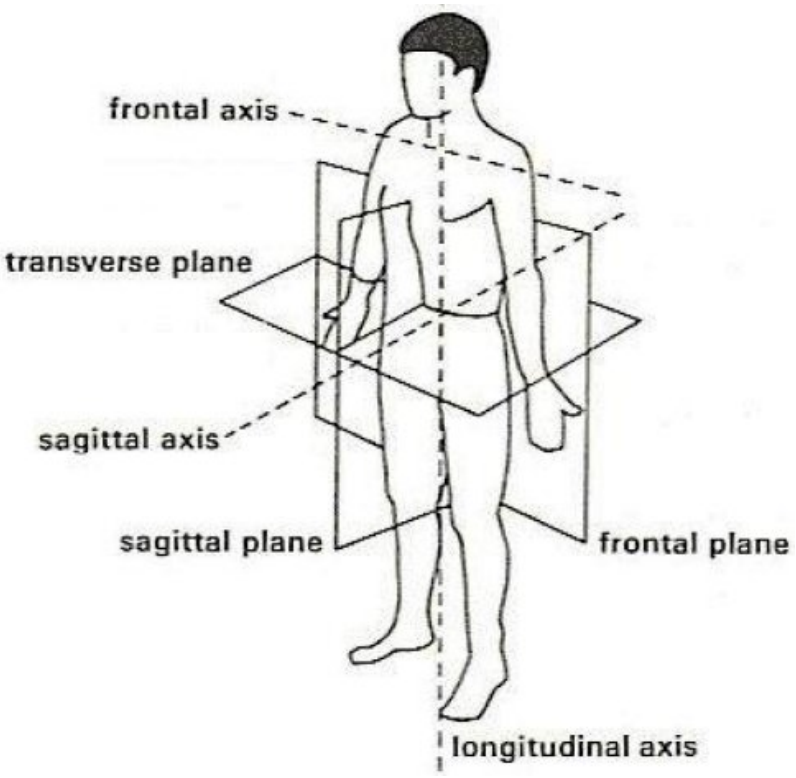

Figure 1.1: The three planes and axes of the body [27]

For a given triaxial accelerometer signal, $\mathbf{X}$, we define $\mathbf{X} = (\underline{x}_1, \underline{x}_2, \underline{x}_3)$ where $\underline{x}_j = (x_{ji})_{i=1}^{n}$ and n is the number of observations in the signal. $\underline{x}_1$ corresponds to the medio-lateral (ML or left-right) acceleration, $\underline{x}_2$ to the anterior-posterior (AP or forward-backward) signal, and $\underline{x}_3$ to the dorso-ventral (DV or vertical) signal. This DV or vertical signal is particularly useful for gait segmentation (distinguishing the phases of gait) as it is sensitive to gait events like initial contacts, due to the spike in acceleration caused by the heel striking the ground. An example of this axis of acceleration during steady gait can be seen in Figure 2.3.

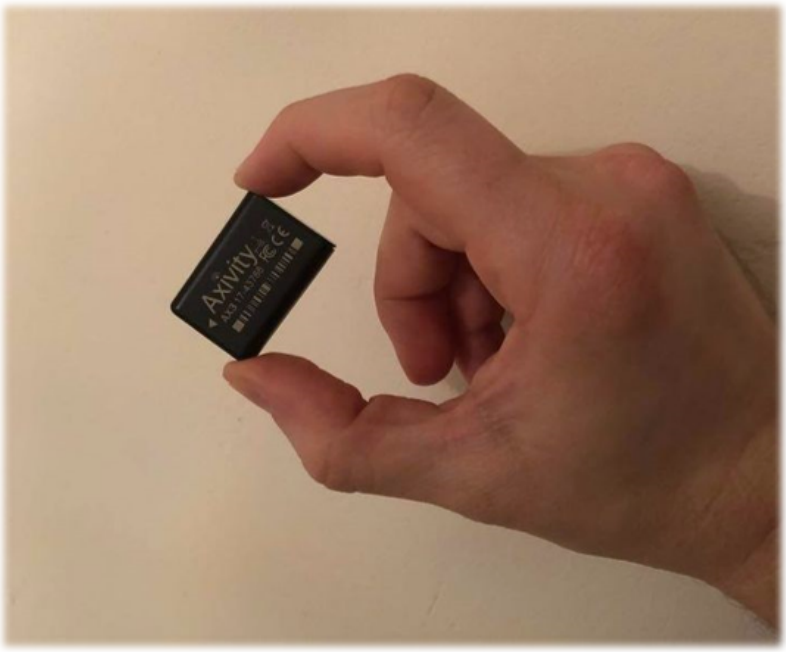

Figure 1.2: An accelerometer sensor- Axivity AX3.

1.3 Thesis Contributions

The main contribution of this thesis will be to introduce a novel domain of gait features, the Phase domain, based on a modified Phase plot methodology. While simple Phase plots have previously been constructed from accelerometry in PD, no attempts have been made to adapt the technique for accelerometry and the number of Phase domain features in the literature remains limited.

We will validate this domain's clinical relevance and utility in monitoring Parkinson's Disease (PD) progression via wearable accelerometer sensors.

In addition to demonstrating the utility of the features in monitoring of PD, we will also show that these adapted Phase plots represent a reproducible and individual signature of gait.

As part of validating this modified Phase plot methodology, we will provide a framework by which Phase plot analysis could be applied to various periodic bio-signals.

This will in turn greatly expand the clinical application of Phase plots, which has previously been almost exclusively limited to ECG analysis.

Given the novelty of the features comprising the Phase domain, it is appropriate to incorporate traditional features into this thesis. Established features of the well-known Spatio-temporal (ST) [15] domain serve as a reliable reference throughout our assessment of the Phase domain. These previously validated features also provide a benchmark for quantifying the Phase domain's performance in various contexts. By comparing with traditional features in this way, we will demonstrate that the Phase domain and the associated Phase plots provide a compact summary of gait with performance comparable to that seen in the ST domain, and in some cases even better.

Environment, or recording setting, is a recurrent them in gait analysis with clear distinctions being made between controlled lab-based environments, in which scripted gait tasks are conducted, and real-world environments, where gait is recorded in the context of unscripted ADL. We investigate the performance of both Phase and ST domain features in both of these contexts.

The presence of ADL in real-world settings is a source of substantial heterogeneity and variability among subjects. To address this we also incorporate activity levels in our analyses and assess the effect of activity on the distribution of gait features.

Disease classification, or the ability of a feature domain to discriminate PD subjects from Controls, is assessed throughout to demonstrate the Phase domain's clinical utility.

A key property of the Phase domain is the compactness of the associated Phase plots. We aim to validate these Phase plots as representing a reproducible and personal signature of an individual's gait.

Traditional features (e.g. ST domain) are an invaluable reference throughout our

analyses. However, as well as benchmarking the performance of Phase domain features, we also demonstrate that the Phase domain is indeed providing additional information not accounted for in the ST domain.

Due to the demographic typically associated with PD, the impact of ageing cannot be ignored. By including age-matched controls we will more accurately quantify the sensitivity of Phase domain features, and the progression thereof, to pathology while controlling for the ageing process. Healthy ageing represents an area of high clinical interest, we will perform longitudinal analysis to assess the interacting effects of PD and ageing i.e. the degree to which PD is accelerating the natural ageing process.

Chapter 2

Phase Plots

In this chapter, we define a novel Phase Plot methodology for feature extraction from periodic signals such as accelerometry recorded during steady-state walking (gait). The methodology presented here is applicable to any periodic signal and, unlike previous applications, does not require any prior extraction of features.

At the centre of this novel feature extraction is the fitting of conic sections (2.1) to either full or partial phase plot orbits (see Figure 2.4 for an example) allowing for highly detailed assessment of asymmetries and variances in the associated physical system which in this case is individuals' walking. Asymmetries in gait are of significant clinical interest in the case of gait disorders and various neurological conditions including Parkinson's Disease (PD). Equation (2.1) shows the general Cartesian form of a conic section with real variables (x, y) and coefficients a-f with at least one of a, b, c non-zero.

$$ax^2 + by^2 + cxy + dx + ey + f = 0 \tag{2.1}$$

2.1 Definition

Given a signal $h(t)$ over times $t = 1, 2, ..., n$ which exhibits periodicity, a phase plot of $h(t)$ is essentially a scatter plot of $y(t)$ against $x(t)$ where $y(t)$ and $x(t)$ are defined as in 2.2. A smoothed curve can be found via interpolation to produce a continuous orbital plot. In this definition, a parameter ν is required which reflects the periodicity of the signal. For example, in the case of human gait data ν can be chosen to segment adjacent gait cycles [28], or if $h(t)$ is an ECG signal ν is chosen to segment adjacent sinus rhythm waveforms, often referred to as R-R cycles [29]. In general we can denote our data as:

$$\mathcal{D} = \{x(t) = h(t - \nu),\ y(t) = h(t), t = 1, ..., n\} \tag{2.2}$$

Phase plots offer a method of embedding data into higher dimensional state spaces. Within this thesis, a phase plot formed of gait accelerometry is defined as the graph of $x(t)$ vs $y(t)$ as defined above, along with their associated interpolated curve. In general these are recognisable as clusters of ellipses such as in Figures 2.4, 2.3 and 2.12. Feature extraction is performed on these clusters and their respective constituent orbits.

2.1.1 Examples

ECG ($\nu = 1$ case)

Take an ECG signal which includes approximately 22 full sinus waveforms (see Figure 2.1). Let $h_t, t = 1, ..., 22$ be the duration of the waveforms. In this case we have a single feature per cycle in the data and as such we take $\nu = 1$. The phase plot in this case is simply a plot of each waveform duration h_t as a function of the previous i.e. $x(t) = h_{t-1}, y(t) = h_t, t = 2, ..., 22$. Although simple, this method has

been used repeatedly in the literature [30, 31, 29]. In general, however, few features can be extracted from phase plots constructed this way and only two are discussed in any detail. These are the standard deviations along the axes defined by the lines $y = \pm x$ (provided in Figure 2.2). This is an example of a phase plot formed from cycle features rather than the signal itself. As a result, no orbits or dynamicacy is exhibited in phase plots derived in this manner and further analysis is limited to single two-dimensional cluster analyses.

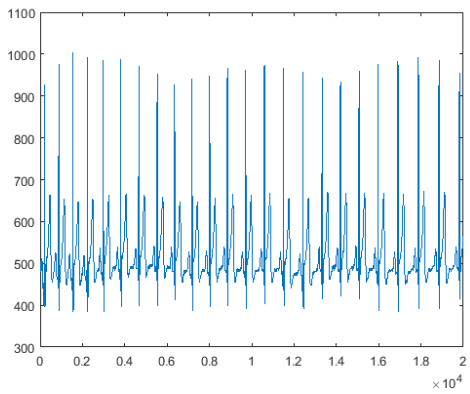

Figure 2.1: Example ECG data with clear R-R intervals.

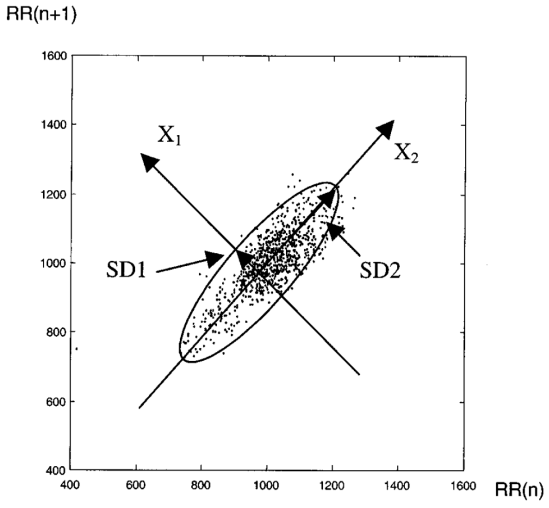

Figure 2.2: Fig. 1. An example Poincaré plot. The standard deviation of the distance of the points from each axis determines the width (SD1) and length (SD2) associated with the Poincaré plot.

Poincaré plots are a particular type of recurrence plot which are sometimes referred to in the literature as: return maps, self-similarity plots or Phase plots.

Accelerometry ($\nu \neq 1$ case)

Now let $h(t)$ be the vertical acceleration signal of a subject's centre of mass (CoM) during steady state gait as shown in Fig 2.3. We aim to form a phase plot of the original periodic signal itself, rather than of features derived from it. Some prepro-

cessing is required before plotting is possible. Most importantly, the accelerometry of all gait cycles are numerically interpolated to ensure they each consist of the same number of data points. This ensures a constant value of ν can be applied throughout the signal. For example, a subject walking with an initial contact (IC) or heel-strike frequency of 2Hz would yield a ν value of approximately $\frac{100}{2} = 50$ assuming 100Hz accelerometer sampling.

Remark. The sequence of cycle lengths can be easily recorded prior to numerical interpolation so no information loss is caused by constraining all cycles to be of equal duration.

Taking the two example cycles (adjacent) of this signal in Figure 2.3 we can construct the simplest phase plot consisting of a single *orbit* as shown in Fig 2.4. Repeating the process for all available cycles in a bout of walking completes the phase plot (see, for example, Figure 2.12). The centres of successive orbits within a complete phase plot oscillate about the line $y = x$, similarly the inclination θ of each orbit from the x-axis oscillates about $\frac{\pi}{4}$ radians (45°). This oscillation is introduced by differences in subjects' alternating (left-to-right) gait cycles.

Remark. These *orbital* phase plots are far richer in terms of features and information but require context-specific pre-processing. Non-orbital phase plots (as in Figure 2.2) are simpler in this respect but offer less insight into the physical system.

Esser et al [18] constructed phase plots from the vertical CoM excursion. Opting for vertical acceleration rather than excursion (deviation in height) avoids the issue of integration drift when estimating vertical position via double integration of acceleration signals.

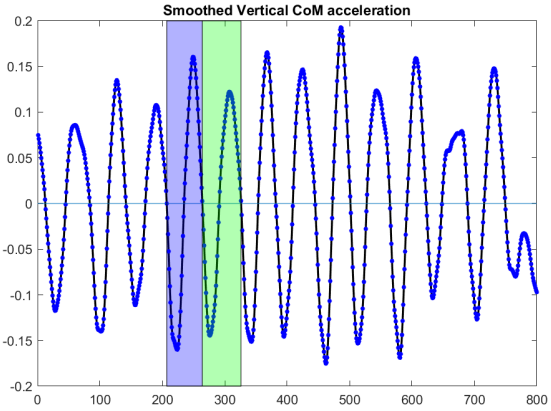

Figure 2.3: Vertical accelereation signal (smoothed) recorded from waist-worn device. Two adjacent gait cycles highlighted.

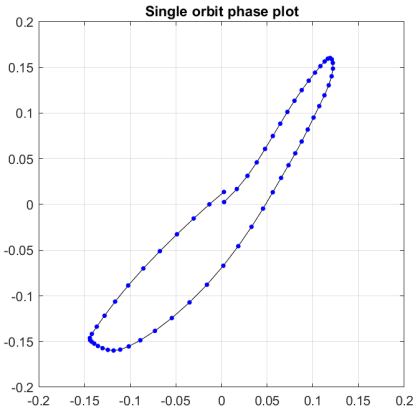

Figure 2.4: Simple Phase plot consisting of a single orbit formed of two adjacent gait cycles shown in Fig 2.3

2.1.2 Meaning of a Phase Plot

Phase plots are closely related to the assessment of variability and autocorrelation of a signal on various scales, such as cycle-to-cycle or across larger intervals. In fact, a set of lagged phase plots can form a complete description of the autocovariance function [29]. The vast majority of relevant literature only concerns non-orbital phase plots in the context of ECG signals, which do not generalise in terms of interpretation and inference. Broadly speaking however, features and variation thereof along the $y = x$ axis correspond to long-term variations in the system while those along $y = -x$ correspond to short term (cycle-to-cycle) changes in the system. In the case of orbital phase plots we instead consider the variation of orbits' major and minor radii lengths (see following section on Conic ellipse models) as respectively corresponding to long and short term change in the system. Further interpretation depends largely on the physical system in question as well as the choices of preprocessing and segmentation (how we define the boundary between cycles) which are not standardised.

While phase plots are mainly to be found in the context of ECG studies, the

methodology has been applied to gait signals, but only to vertical excursion signals and without conic, or indeed any kind, of model fitted to the data to exploit the cyclic nature of gait. Ellipses have been used in the context of phase plot analysis but only as a visual aide and to illustrate two commonly extracted features, SD_1 and SD_2 [18, 29]. This approach is very limited and often inappropriate in the case of more complex phase plots which do not exhibit consistently elliptical orbits. Although work has been done to augment these features such as that by Fishman et al [32] who introduced temporal Poincaré variability (TPV) to compliment traditional Poincaré analysis, the bulk of the literature concerns only SD_1, SD_2 and their ratio which, as previously explained often produce an over simplified and impractical measure of temporal variability in complex physical systems. Many previous applications of phase plots or Poincaré analysis would have lent themselves very well to ellipse fitting with the neccesary pre-processing steps. As we will demonstrate for the case of accelerometry, such pre-processing allows for ellipse fitting and analysis by preserving the elliptical form of the data rather than summarising each cycle with point values as is common practice within ECG studies. This allows for much more detailed features to be extracted and for complexities of the associated physical system(s) to be reflected in the phase plot. In the case of accelerometry, this leads to a unique subject-specific phase *portrait* or *fingerprint* of subjects' gait.

This shift towards individualised analysis is of great clinical interest. The valid application of gait analysis at the level of the individual is vital for informing clinical decision-making. A small number decision support tools (DSTs) and medication change proposers (MCPs) have been proposed for management of PD using wearable technology [33].

2.2 Conic Ellipse Models

After computing the phase data we can take the general orbit such as the one in Figure 2.4 and define our data $\mathcal{D}$ as in equation (2.2). We propose a novel method of characterising phase plots based on the fitting of ellipses to orbital phase plot data. We can define the general ellipse with radii, r_1, r_2 centred on (g, k) using equation (2.3). Using this method intriduces parametrisation dependence but also has the benefit of simple geometric interpretation.

$$\frac{(x-g)^2}{r_1^2} + \frac{(y-k)^2}{r_2^2} = 1. \tag{2.3}$$

In general, ellipses fitted to phase plot orbits have a non-zero inclination, θ. For this reason, we introduce the rotated coordinate system:

$$x' = (x-g)\cos(\theta) + (y-k)\sin(\theta),$$

$$y' = (y-k)\cos(\theta) - (x-g)\sin(\theta).$$

From this we derive the equation of an ellipse rotated anti-clockwise by θ about its centre

$$\frac{((x-g)\cos(\theta) + (y-k)\sin(\theta))^2}{r_1^2} + \frac{((y-k)\cos(\theta) - (x-g)\sin(\theta))^2}{r_2^2} = 1. \tag{2.4}$$

The representation (2.4) is equivalent to the conic representation (2.1) subject to the constraint $f = 1$. The constraint $a - c = 1$ is also possible. However in the context of fitting ellipses, the former choice is less prone to eccentricity bias [34]. In short, eccentricity bias is the tendency of conics fitted to elliptical data to *favour*

regions of low curvature where the cost function is steeper.

The conic form of the ellipse equation is more convenient in terms of estimation but does not have a clear geometric interpretation. We show in Section 8.3.1 that the angle of inclination θ is related to the conic coefficients by

$$\theta = \frac{arctan(\frac{c}{b-a})}{2}. \tag{2.5}$$

After finding estimates of $\hat{\mathbf{A}} = (\hat{a}, \hat{b}, \hat{c}, \hat{d}, \hat{e})'$ we can calculate estimates of r_1, r_2, g, and k by expanding equation (2.4) and equating coefficients with conic definition in equation (2.1) (see full working in Appendix 8.3.1).

2.2.1 Estimation

We aim to estimate $\mathbf{A} = (a, b, c, d, e, f)'$ in equation 2.1 using the data as defined in 2.2. Ordinary least squares is sufficient, however a suitable normalising constraint must be made to avoid the trivial result $\hat{\mathbf{A}} = \mathbf{0}$. Two common methods are to set $a - c = 1$ or $f = 1$. Throughout these analyses the latter ($f = 1$) is used as this has been shown to be less prone to eccentricity bias, which occurs due to the cost function having greater slope in regions of low curvature. In the case of more eccentric phase plot orbits, this can lead to fitted ellipses favouring the linear regions of the data parallel to the major axis rather than the vertices. We define the model as in Equation (2.1) which, with the added constraint $f = 1$, can be written as

$$\mathbf{XA} + \mathbf{1} = \mathbf{0} \tag{2.6}$$

where $\mathbf{X}$ is the n by 5 design matrix with columns $x_i^2, y_i^2, x_i y_i, x_i, y_i$ for $i = 1, ..., n$ and $\mathbf{1}$ is the 1-vector of length n. The following least squares objective function is

popular within the literature

$$C_s = \sum_{i=1}^{n} \epsilon_i^2 = (\mathbf{XA} + \mathbf{1})^T(\mathbf{XA} + \mathbf{1}). \tag{2.7}$$

where ϵ_i is the distance of each data point i from its associated fitted value. Minimising the above objective function leads to following

$$\hat{\mathbf{A}}' = -\mathbf{1}^T\mathbf{X}(\mathbf{X}^T\mathbf{X})^{-1}$$

Despite the choice of normalisation constraint (f = 1), the above least squared error (LSE) methodology is still prone to eccentricity bias and is also not guaranteed to produce an ellipse i.e. a conic estimation satisfying the condition $c^2 - 4ab < 0$. Alternatively, we can carry out the estimation step subject to this constraint however, it will prove useful to instead fit conics without enforcing this constraint and record instances when it is violated on a per subject basis. In this novel methodology and application, we cannot assume all phase plots constituent orbits are necessarily well-modelled as an ellipse and as such it would be inappropriate to apply this constraint. In the rare case of non-elliptical conics being fit to Phase orbits, these conics are not used feature extraction. This issue is related to goodness-of-fit and is covered in a later section. It should be noted that, despite the method of estimation presented here, the parametrisation of an ellipse and the fitting of an ellipse to data are essentially unrelated issues.

Error functions

Conic sections are often visualised as the intersection of a plane with one or two cones as shown.

For the purposes of fitting conics to elliptical data, fitting values of $\mathbf{A} = (a, b, c, d, e)'$

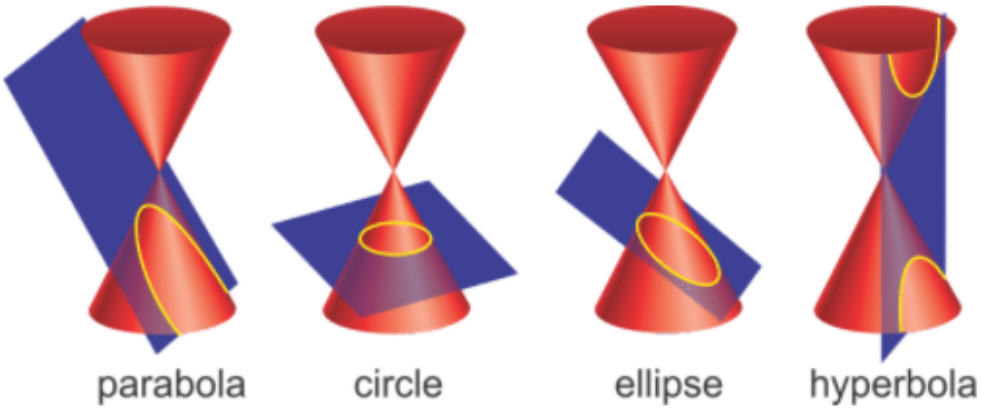

Figure 2.5: The three possible conic sections shown as the intersection of a plane with cones. The circle is a special case of an ellipse with eccentricity equal to zero.

as in 2.1 corresponds to estimating the function whose intersection with the plane $z = 0$ minimises the cost function given in Eq. 2.7

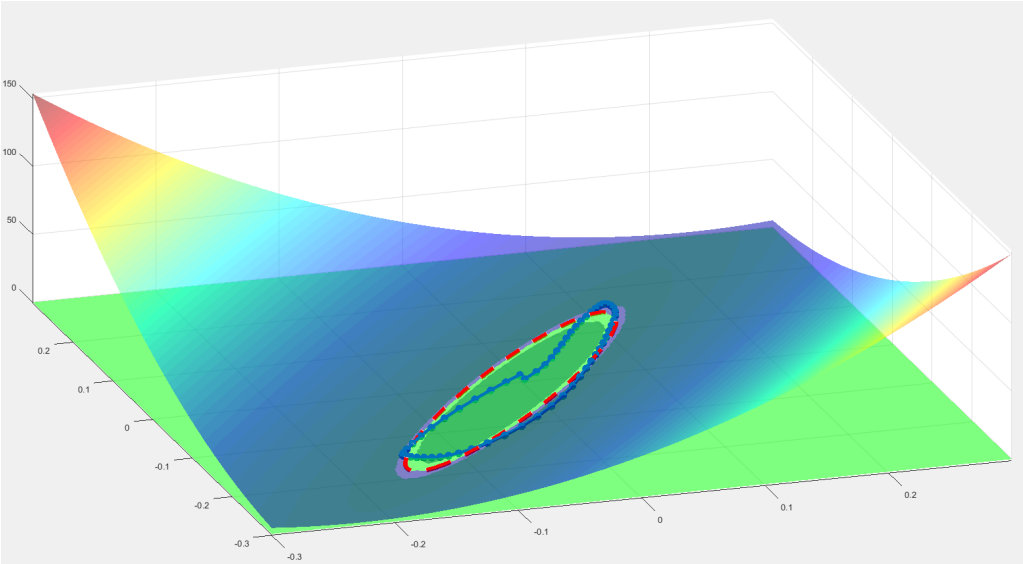

Figure 2.6: The fitted ellipse (red) corresponding to 2.1 with $f = 1$ fitted to data (blue).

As previously mentioned, ellipses fitted in this way are prone to eccentricity bias. This is due to the relatively high gradient of the cost function in regions of the ellipse with low curvature. This is best shown in contour plots (see below) where the contours near regions of high curvature are more spaced out. The example

below demonstrates how the fitted ellipse may deviate more readily from those high curvature regions of the data, hence resulting in an eccentricity bias which can be either positive or negative.

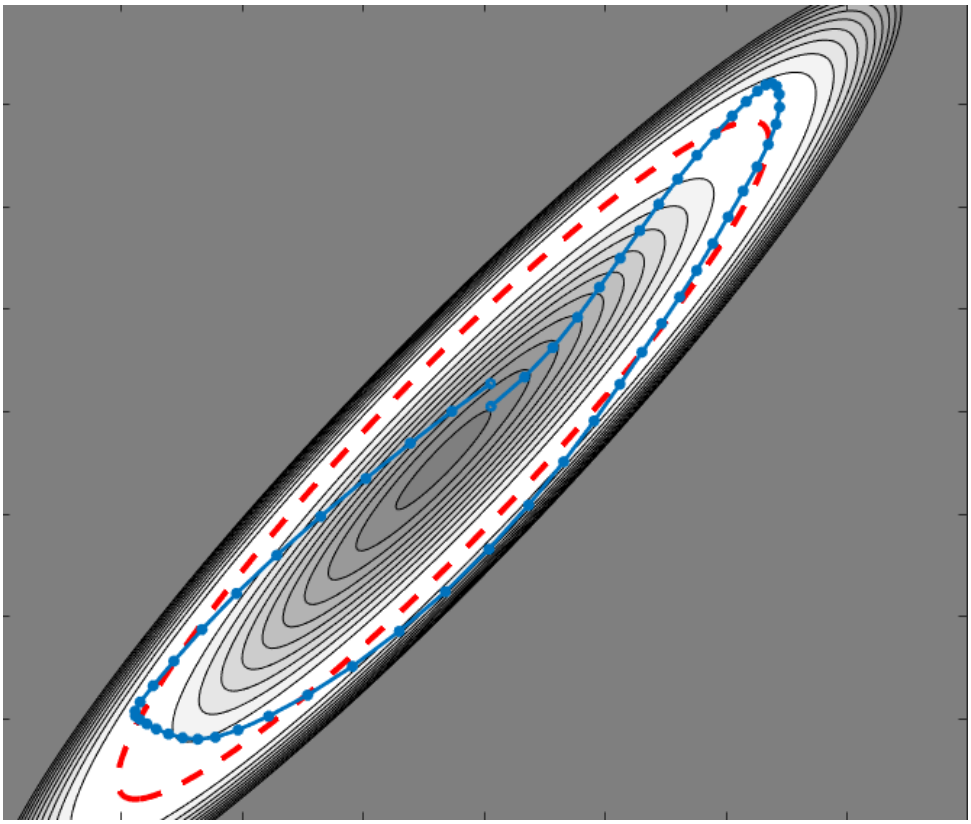

Figure 2.7: Contour plot of conic fitted in 2.6 showing considerably higher gradient in regions of low ellipse curvature

Other error functions are available which can mitigate this bias in ellipse fitting. For example, we may weight the previous cost function 2.7 by the inverse of the magnitude of its gradient, $|\nabla(C_s)|$ resulting in a new error function given by the surface in Figure 2.8 and the contour plot 2.9.

The ability of this non-standard error function to mitigate eccentricity bias is again best shown in a contour plot where we can see the contours are being *pulled* in near high curvature regions (see Figure 2.8).

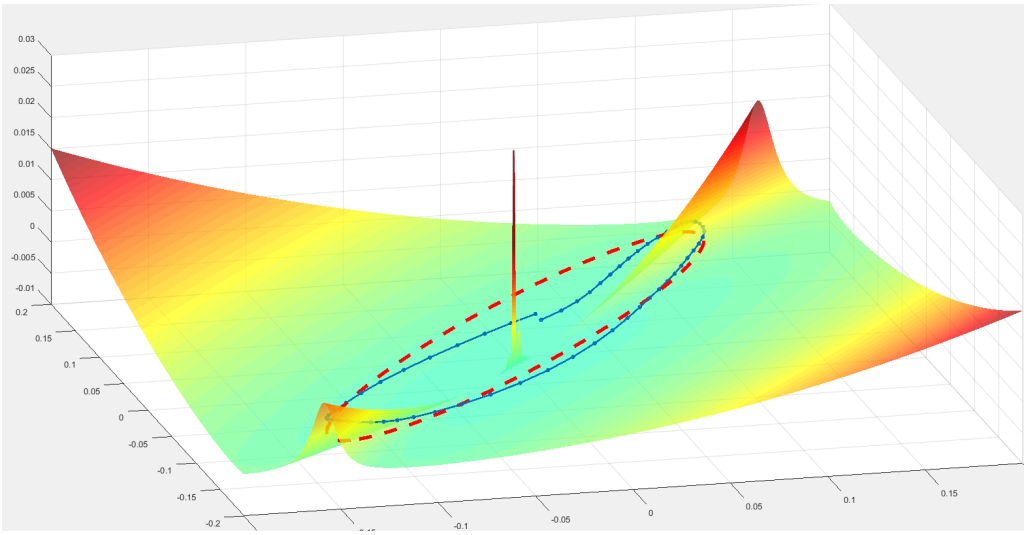

Figure 2.8: A non standard error function for conics, altered to mitigate eccentrity bias in regions of high curvature

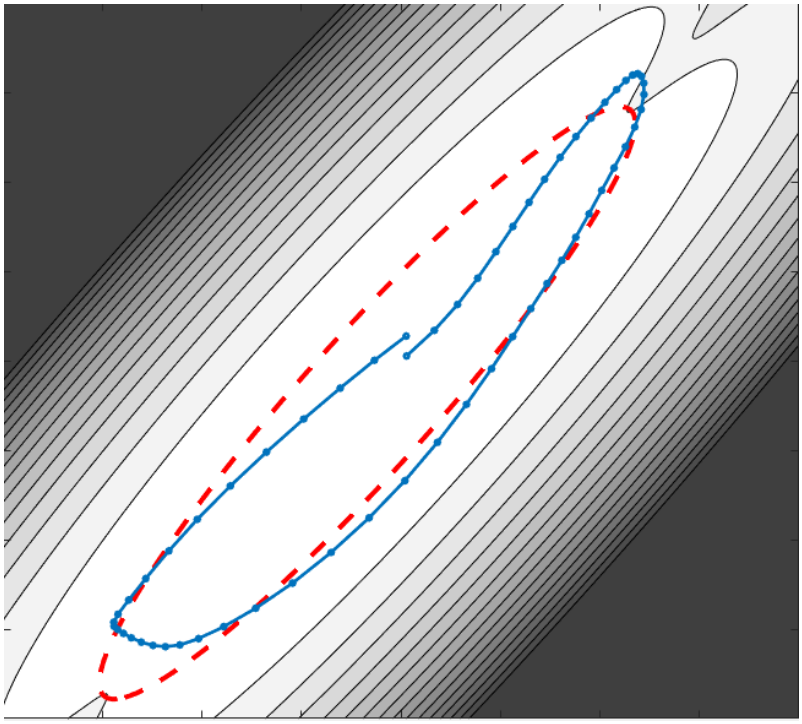

Figure 2.9: Contour plot of 2.8 showing increased gradient in regions of high curvature to reduce eccentricity bias

2.2.2 Goodness of Fit

Regardless of estimation method and objective function, the goodness of fit of estimated conic sections is important to monitor in this new methodology. The average radial distance is an intuitive measure of goodness-of-fit of the conic section model to phase plot data.

The following function can be evaluated on a per phase plot basis and used to compare the goodness-of-fit of conic models. It it based on the radial distance of the data points from the fitted ellipse.

$$G_r = \sum_{i=1}^{n} \epsilon_{r_i}^2 = \sum_{i=1}^{n} |p_i - f(\mathbf{A}, p_i)|^2 \tag{2.8}$$

where $p_i = (x_i, y_i)$ and $f(\mathbf{A}, p_i)$ is the point on the ellipse intercepted by the ray originating from the centroid of the ellipse defined by $\mathbf{A}$ and passing through p_i. Using this radial distance in the context of conic sections has been mentioned briefly by Rosin et al [34]. These rays are shown in Figure 2.13. After defining this radial goodness of fit measure, it may be temping to use a similar method to perform ellipse fitting. One significant issue with this approach would be that the previously mentioned eccentricity bias would not be addressed.

Remark. When plotting an ellipse and radial rays it is helpful to note the relation between the parameter θ in (2.4) and the actual angle from the x-axis ϕ, which is given by:

$$\phi = \tan^{-1}(\frac{m}{M}\tan(\theta)) \tag{2.9}$$

where m and M are the semi-minor and semi-major axes of the fitted ellipse respectively.

Anatomical factors such as height may impact the scale of phase plots so to make

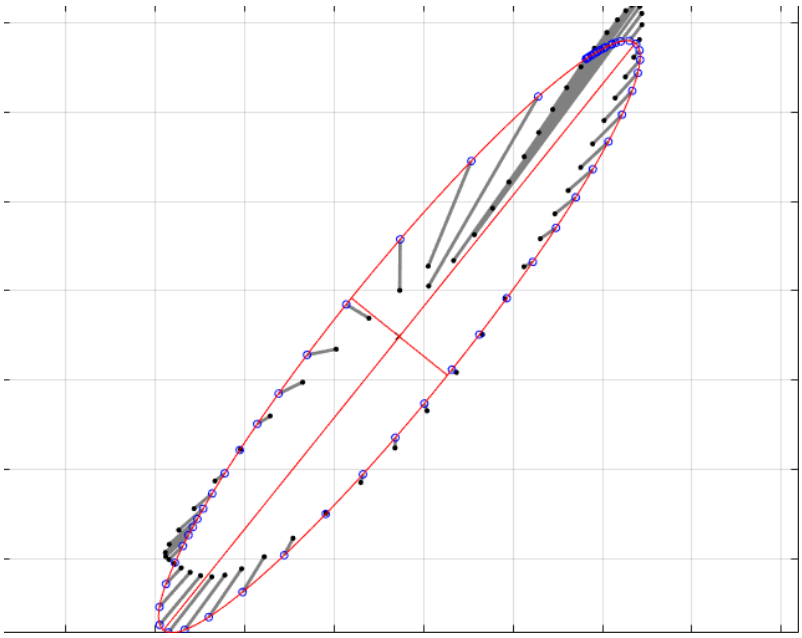

Figure 2.10: Ellipse (red) fitted to gait data (black) with radial distances (absolute) showing the distances used to calculate radial GoF

this measure of fit is consistent across different scales the following function based on the proportional radial distance is used.

$$G_{rp} = \sum_{i=1}^{n} \epsilon_{rp_i}^2 = \sum_{i=1}^{n} |f(\mathbf{A}, p_i)|/|p_i|^2. \tag{2.10}$$

Conic sections as defined in 2.1 can take any of three non-degenerate forms (ellipse, hyperbola or parabola) based on the value of the discriminant, $c^2 - 4ab$. The condition for an elliptical conic is

$$c^2 - 4ab < 0 \tag{2.11}$$

This constraint can be incorporated into fitting procedures to ensure that every fitted conic is an ellipse however this leads to volatile values of derived features

It is not certain that all phase plot orbits are well-suited to an elliptical conic model. Some phase plot orbits with particularly high eccentricity may yield a better

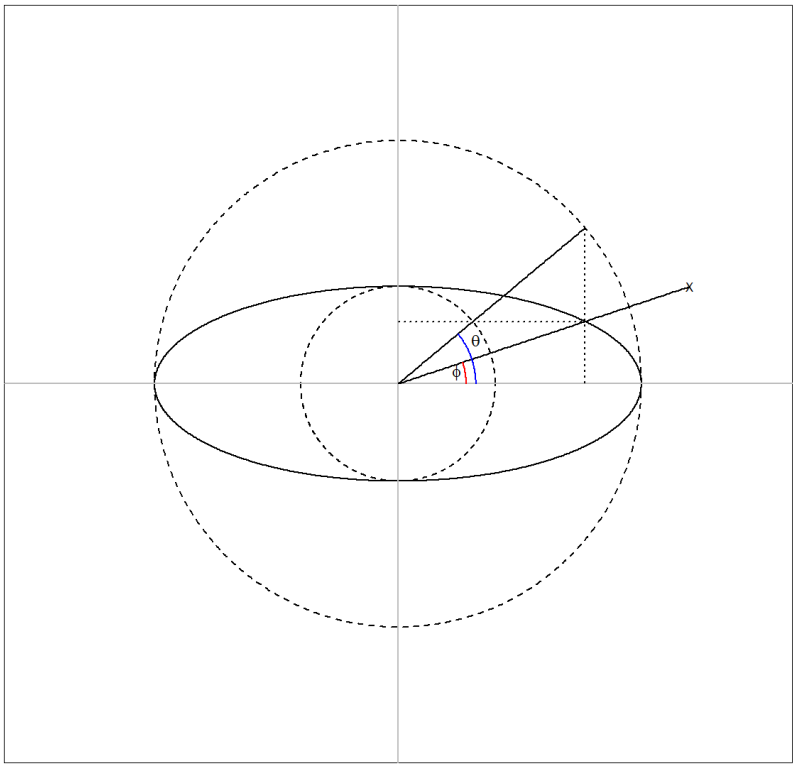

Figure 2.11: Geometric relation between argument of data point and closest point on fitted ellipse.

goodness-of-fit (2.10) for a hyperbolic or parabolic conic. Instead of constraining all conics in this way, we instead reject non-elliptical orbits' features from further analysis and also record the proportion of non-elliptical conic fits per-phase plot as an additional empirical measure of goodness-of-fit.

2.2.3 Primary Features

Primary features are those derived from available ellipses fitted to complete orbits within a phase plot and are each defined in terms of the parameters of Eq. (2.4). Each of these features have intuitive geometric interpretations: Area and γ (eccentricity) are simply the area and eccentricity of the fitted ellipse. As we have

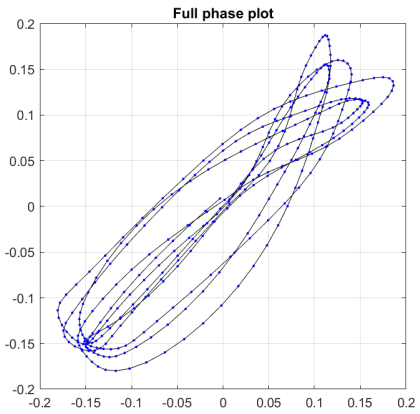

Figure 2.12: Complete phase plot comprising 7 continuous gait cycles

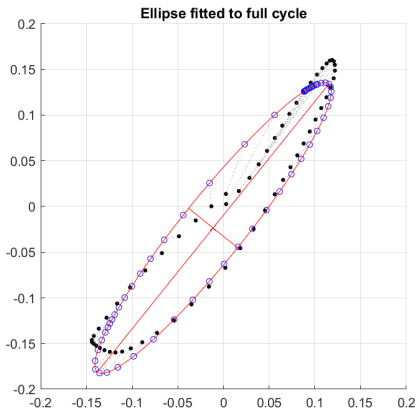

Figure 2.13: A single orbit taken from Fig 2.12 with fitted conic (ellipse) - red.

seen Phase plots generally take the form of two adjacent clusters of ellipses. These two clusters are easily distinguished by labelling during the construction stage as successive orbits become associated with each cluster in an alternating manner. The relative location and orientation of these clusters forms the basis of several asymmetry-related features within the Phase domain. In the case of full-orbit fitting for Primary features, we have Asy_θ and Asy_{Area} which are the average differences in ellipse angle (θ) and ellipse area between alternating ellipses. GoF is simply the reciprocal of the arithmetic mean of the distances shown in Figure 2.13. SD_{r_1} and SD_{r_2} are measures of the semimajor and semiminor axes of the ellipses and are similar to the measures SD1 and SD2 generally extracted as part of Poincaré analysis [18].

Primary Features	Description
Area	Fitted ellipse area equal to $\pi r_1 r_2$ where are r_1 and r_2 are the radii of the ellipse as defined in (2.4)
γ	Eccentricity of the fitted ellipse equal to $\sqrt{1-\frac{r_2^2}{r_1^2}}$.
Asy_θ	Obliqueness. The relative inclination of adjacent fitted ellipses.
Asy_{Area}	The ratio of the areas of adjacent fitted ellipses. Averaged over a full phase plot.
GoF	The goodness of fit of the conic section model fitted to the phase plot 2.13.
SD_{r_1}	The standard deviation of the semi-major axis (r_1) of the fitted ellipse. This is analogous to the measure SD_1 which is regularly cited within ECG studies incorporating Poincaré plots
SD_{r_2}	As above for the semi-minor axis r_2.

Table 2.1: Phase-plot-derived features from conic parametrisation. *Asymmetry in this context refers to mean absolute difference between features of ellipses derived from left or right step cycles. † features extracted from an ellipse fitted to a full cycle of the original phase data.

2.3 Partial Orbit Fitting

Many phase plot orbits exhibit asymmetries and non-elliptical behaviour in that curvature is not consistently reflected about their semi-major and semi-minor axes. For this reason, in addition to the previously described ellipse fitting we also derive secondary features by segmenting orbits of phase plots and fitting partial ellipses to the resulting segmented data or *half orbits*. Phase plot orbits are segmented, or *halved*, in two ways based on their semi-major or semi-minor axis (found from the ellipse fitted to the full orbit). We refer to these as Type I and Type II features respectively. Both types are still subsets of the secondary features.

2.3.1 Type I

Here we create two half-orbits by partitioning a complete orbit about its major axis. We then fit a separate conic section to each half of the cycle as partitioned by the major axis of the originally fitted ellipse.

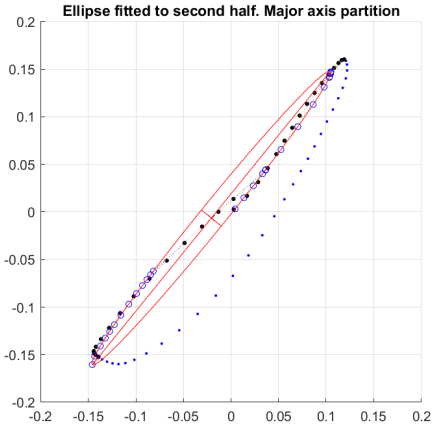

Figure 2.14

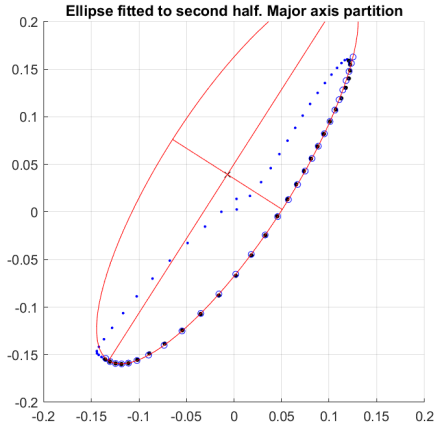

Figure 2.15

2.3.2 Type II

Here we fit a separate semi-ellipses similarly as above but partitioned by the *minor* axis of the originally fitted ellipse.

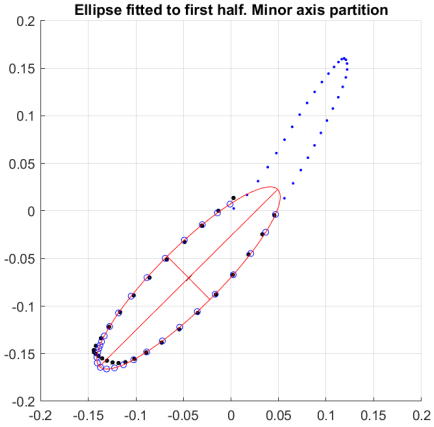

Figure 2.16

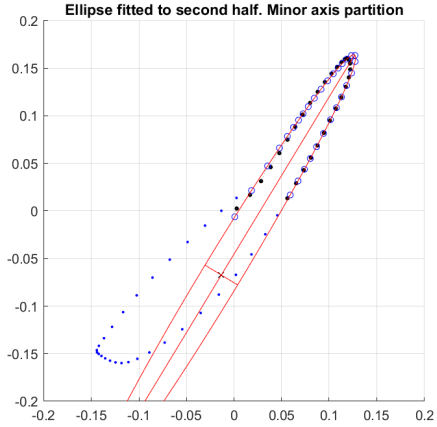

Figure 2.17

Partitioning and fitting semi-ellipses in this way addresses the issue of asymmetric or inconsistent curvature and adds a large number of potential features such as those in Table 2.2.

2.3.3 Secondary Features

Secondary Features	Description
$\text{Asy}_{\gamma_\text{m}}$	Asymmetry in eccentricity of ellipses fitted to gait cycle after minor axis partitioning Fig 2.16 and Fig 2.17.
$\text{Asy}_{\gamma_\text{M}}$	Asymmetry in eccentricity of ellipses fitted to gait cycle after major axis partitioning Fig 2.14 and Fig 2.15.
$\text{Asy}_{\theta_\text{m}}$	As above with ellipse inclination θ in place of eccentricity γ.
$\text{Asy}_{\theta_\text{M}}$	As above applied to major axis cycle partitioning
$\text{Asy}_{\text{Area}_\text{m}}$	Proportional asymmetry of ellipse areas following minor axis partitioning
$\text{Asy}_{\text{Area}_\text{M}}$	As above following major axis partitioning
GoF_m	The radial goodness of fit of the conic sections to the phase data after minor axis partitioning (2.10).
GoF_M	As above applied after major axis partitioning.
SD_GoF	The standard deviation of radial goodness of fit measures from all conic sections (fitted to full and partial cycles) through out a bout of walking.

Table 2.2: Phase-plot-derived features from conic sections fitted to partial phase cycles. Proportional asymmetry is used when reporting asymmetry in partial ellipse area asymmetries as absolute differences in area are likely highly correlated with physiological factors such as subject height

In total there are 16 features extracted from a phase plot (7 primary and 9 secondary). The 16 features of the Phase domain will be extracted from both lab-based (Chapter 4) and free-living (Chapter 5) datasets of participants' gait accelerometry. In addition to these Phase domain features, we all extract features of the well-established spatio-temporal (ST) domain consisting of 15 features. These traditional features provide an excellent reference against which the clinical relevance

of the Phase domain can be assessed. The ST domain and its associated features are described by Del Din et al [15]. Features within the ST domain, e.g. step length, step velocity, stride asymmetry etc are already valid biomarkers of physical capability. Secondary features of the Phase domain are not as intuitive and may not be as easy to visually gauge as the primary features. Take $\text{Asy}_{\gamma_\text{m}}$ for example, this should be read as the asymmetry (absolute difference) of γ (eccentricity) between the two conics fitted to a Phase plot orbit following partitioning about the minor axes (hence the lower-case m-subscript). Similarly for $\text{Asy}_{\gamma_\text{M}}, \text{Asy}_{\theta_\text{m}}, \text{Asy}_{\text{Area}_\text{m}}$ etc. GoF_m is the goodness-of-fit of the conic section to each of the resulting partitions while SD_GoF is the standard deviation of all primary and secondary GoF measures.

Note the different interpretations of *asymmetry* within the Phase domain and ST domain. For ST features, asymmetry refers to the magnitude of the difference in feature values associated to the left and right legs respectively whereas within the Phase domain asymmetry refers to absolute differences in features associated with successive orbits within a given phase plot. As demonstrated in figures 2.18 complete phase plots generally exhibit two clusters of ellipses with some degree of obliqueness. The asymmetry related features defined in 2.2 are calculated by extracting features on a per orbit basis and taking the absolute difference in mean values associated with orbits whose centroids are above and below the main diagonal $y = x$ respectively.

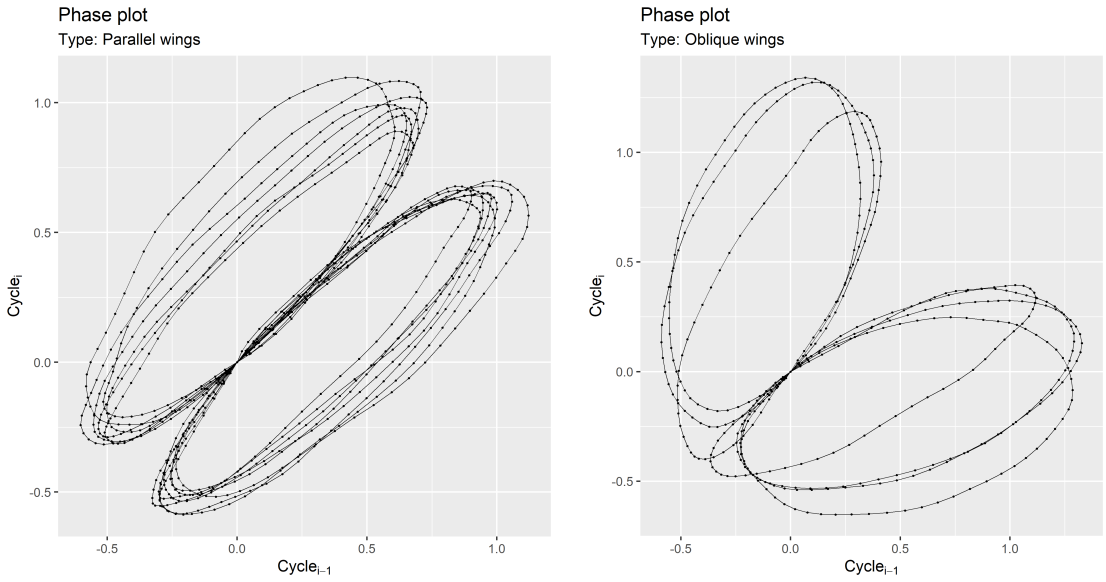

Figure 2.18: Example phase plots of type PW and OW.

We have manually featurised Phase plots to produce the previously listed primary and secondary features. These features were chosen partly to summarise the variation seen between participants' phase plots. Future studies may benefit from automating this process although this would likely be at the expense of the intuitive geometric interpretation of the features presented here.

2.4 Feature Interpretation

Phase plot features have the advantage of unambiguous geometric interpretation. For example, a phase plot whose orbits have generally high eccentricity is clearly distinguishable from one whose orbits are low in eccentricity. This is in contrast to more well-known features in the spatio-temporal domain whose intuitive interpretation is physical e.g. step lengths/durations which are easily observable.

Previous studies have not presented detailed interpretations of the features of phase plots or following Poincaré analysis, rather they explain that variation in the minor axis direction corresponds to short-term variation and in the major axis

direction corresponds to longer term variation. There are important nuances in these interpretations however, they assume that the phase plot has been constructed using point values rather than adjacent cycles as in this novel approach.

In the first instance, it is helpful to interpret newly developed features in terms of previously established features and relevant biomarkers. In our case, gait accelerometry in a PD cohort, we can calculate spatio-temporal features as a reference throughout analysis of the newly derived primary and secondary features.

SD_{GoF} is a measure of the variation in goodness-of-fit of the different ellipses fitted to different components (partitions) of a given phase cycle. Higher values imply that there exist multiple components to the phase cycle(s) in question which are elliptical themselves but that the complete orbit is not.

Chapter 3

Data and Methods

3.1 Data

The data in these analyses are taken from 203 participants of the "Incidence of Cognitive Impairment in Cohorts with Longitudinal Evaluation-GAIT" (ICICLE-GAIT) [1] study [25]. Among the included participants, 92 were people with early PD diagnosed according to the UK Parkinson's Disease Brain Bank criteria by a movement disorder specialist [35] and 111 were healthy control subjects (CL). Ethical approval was obtained from the "Newcastle and North Tyneside research ethics committee" (REC No. 09/H0906/82). All subjects gave written informed consent before participating in this study. In addition, all the methods and experiments were performed according to the declaration of Helsinki.

[1] ICICLE-GAIT is a collaborative study with ICICLE-PD, an incident cohort study (Incidence of Cognitive Impairment in Cohorts with Longitudinal Evaluation—Parkinson's disease). The ICICLE-GAIT study was supported by Parkinson's UK ((J-0802, G-1301)) and by the NIHR Newcastle Biomedical Research Centre

3.1.1 Demographic and Clinical Data

Participants' demographic characteristics such as age and height were recorded. Severity of the PD motor symptoms was assessed using part III of the modified version of the Movement Disorder Society Unified Parkinson's Disease Rating Scale (MDS-UPDRS) [36]. The UPDRS score is available only for PD subjects and serves as a valuable proxy for disease progression. The measure is calculated based on both motor and non-motor features and is designed to characterise the extent and burden of disease during ADL. All of the data are summarised in Table 3.1.

Demographic/measure	CL	PD
n	111	92
M/F	53/58	58/34
Age	71.1 ± 6.9	68.2 ± 9.8
Height	1.7 ± 0.1	1.7 ± 0.1
MDS-UPDRS	-	32.7 ± 10.2

Table 3.1: Demographic and clinical data summary.

3.1.2 Experimental Design and Protocol

Participants were instructed to walk at their preferred pace on a 10 meter walkway. Gait was sampled at 100Hz using a discretely worn accelerometer (see Figure 1.2) located at the lower back, specifically at the L5 vertebra. Participants completed four walks on a straight 10 metre walkway Figure 3.1. PD participants were assessed while in a clinically defined "ON" state, meaning their symptoms were generally under control at the time of recording. All 203 participants were also assessed in a real-world setting, completing normal ADL for 7 days while wearing an accelerometer which continuously sampled three perpendicular axes of accelerometry at 100Hz. Once returned, the data from these sensors was downloaded and fifteen traditional spatio-temporal (ST) gait characteristics were derived [15]. Sixteen Phase domain

features were also derived for all the gait data and will be presented in chapter 4. Features from both ST and Phase domains were each aggregated and are expressed as their per-bout averages. The above protocol is conducted at baseline, which can be defined as any time within six months of receiving an official PD diagnosis, and is then repeated at 18-month intervals resulting in gait data at 0, 18, 36, 54, and 72 month timepoints. As part of the lab-based experiment design, participants also completed longer continuous bouts of walking on a 25m oval-shaped walkway. These bouts and hence the associated accelerometry include a large proportion of exclusively right-hand turning between portions of straight line walking. Many of the ST features as well as the novel phase domain features are associated with asymmetries in gait and PD itself is known to have asymmetric physiological manifestations. For these reasons, the straight line intermittent bouts of walking form the focus of the lab-based analysis. Real gait does of course consist of turning and this will be reflected in the analysis of real world gait data for which we will make the reasonable assumption of no left or right preference in turning.

Inclusion criteria Two inclusion/exclusion criteria were implemented. Firstly, we only include participants who had available both lab and real-world data at one or more timepoints. Secondly, accelerometry data recorded at baseline (PD diagnosis $\pm$6 months) was excluded. This decision to not include baseline data is due to a different sensor configuration being used at participants' first visit. Considerable unknown variability may be introduced in the baseline recording. For example, the state of an individual's disease and hence the degree of impact of PD on their gait is a highly complex phenomenon and can depend on several factors including lifestyle. In particular, the impact of PD on a person's gait will depend largely on the suitability of their individual medication regime (dosage, frequency, timing) and how strictly they abide by it. Omitting the baseline timepoint gives credit to the

assumption that each of the participants present in the PD cohort are in a stable routine with regards to their individual medication regime having lived with the disease and presumably having regular check ups for approximately 18 months. this is in addition to bypassing any bias introduced by the alternate sensor configuration at baseline.

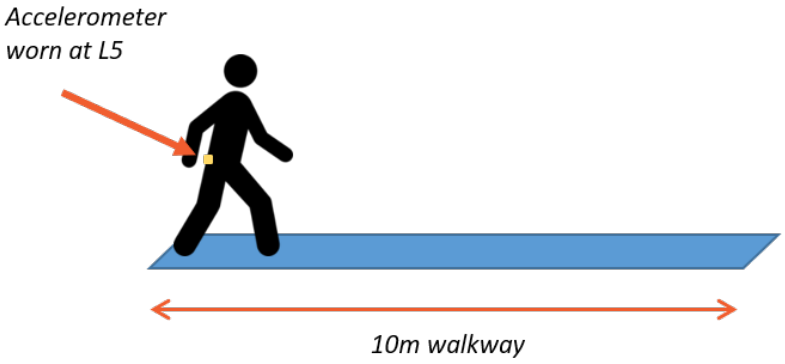

Figure 3.1: ICICLE-GAIT^2 protocol

3.1.3 Data Processing

The general bout of walking can be segmented as gait initiation followed by steady-state gait followed finally by gait termination. To allow for valid comparisons the steady-state section of bouts is where we focus our analyses. This is an important part of data processing as PD can have a significant impact on gait initiation and termination. This specific impact of the disease on the individual's gait initiation and termination is the subject of many clinical studies [37] [38] and bespoke features e.g. TUG (timed-up-and-go) [39]. To remove any such complication the first and last three step cycles from each bout of walking [15] are removed. This trimming of bouts is carried out on all real-world bouts as well.

Gait detection and segmentation (identifying periods of valid walking) in the case of real-world accelerometry was performed in MATLAB® (R2015) and followed the process flow outlined by Hickey et al [40]. This process was validated

in healthy participants who wore a body-mounted camera which was synchronised with a wearable accelerometer to provide objective context during real-world conditions. This gait detection process was carried out prior to extraction of ST and Phase domain features.

3.2 General Analysis Aims and Hypotheses

Throughout the majority of the analyses in this thesis, the control subjects serve as an age-matched reference by which the PD subjects can be assessed. Similarly, the traditional ST feature domain, which has been validated in a number of studies [15], [41], serves as an excellent standard against which the novel Phase domain of features can be assessed. We aim to demonstrate the utility of the novel Phase domain of features for the monitoring of PD via gait accelerometer-based gait analysis.

As well as the general theme of comparison between PD and CL subjects, there is also significant clinical interest in within-group and within-subject comparisons. Specifically, rather than simply comparing PD with CL, we will compare PD at time t with PD at time $t+1$ etc. This clinical interest comes from the need to monitor disease progression. Given the age range of the participants, analyses are prone to complications caused by comorbidities and other age-related sources of variation. Again, the inclusion of age-matched controls can help account for this and also shed some light on the degree to which a PD patient's decline may be attributable to the effects of ageing rather than direct results of PD. The longitudinal design of the experiment and protocol allow us to assess the feature domains in their ability to assess PD gait over multiple time scales: single bouts, days etc. and to predict disease progression over time scales of several years.

For each feature domain we will assess how lab-based gait data compares with real-world data when detecting PD or assessing PD progression. Real-world data

introduces a huge number of unknown factors due to the potential variety of ADL. While lab-based data cannot be expected to fully represent an individual's typical ADL, the controlled environment and scripted gait tasks do have the advantage of reproducibility and more straight forward between-subject comparisons, as lifestyle related factors have been largely removed. We will investigate if any particular features within either domain are generally masked by the strictly controlled lab-based setting. We will, for example, see which combination of features and environment best predict the PD subjects' UPDRS score e.g. Phase features in lab setting, ST in real-world, or some combination etc. Throughout these analyses it is important not to assume that lab-based can be seen as a subset of real-word gait i.e. a straight 10m walk in a real word setting is not necessarily comparable to the lab-based 10m walk.

There are several properties of gait Phase plots that we will demonstrate to validate its interpretation as a signature of gait. Firstly, we require reproducibility of Phase plot type across environments and between bouts at a given timepoint. Secondly, we will demonstrate sufficient between-subject variability that the signature offers enough detail to inform decisions at the level of the individual. Lastly we will show that this signature is clinically relevant - the established ST domain will be used to demonstrate that an individual's Phase plot type is of clinical interest and that any changes to this signature likely represent a change in physical capability and/or disease state.

3.3 Methods

Statistical t-tests are used for between group differences (PD vs CL). Prior to t-tests, the distribution and characteristics of features from both domains will be assessed, and transformed if need be, to better satisfy the assumptions of t-tests e.g.

normality and homogeneity of variance. In addition to transforming the data we will also include a Bonferonni correction where appropriate to account for multiple measures. This is necessary in this case as the large number of features significantly increases the probability of a type-1 error, when a true null hypothesis is rejected by chance.

Logistic regression is a popular statistical method for modelling the probability of an entity belonging to a certain class conditional on certain covariates, in our case the probability of a participant being part of the PD group rather than the control group. This is also a commonly used method within the related literature so we can easily compare the various models' performances with those of other studies.

Mixed Effects Models Mixed effects models (also known as mixed models or mixed error component models) are statistical models which comprise both fixed and random effects. Mixed effects models are useful when data have multiple sources of random variability, for example, when subjects are sampled multiple times (repeated measures). They are particularly useful when working with a hierarchical experiment design such as within the ICICLE dataset where participants are "sampled" in multiple locations (lab and real-world), at several timepoints (18-month intervals). Furthermore, at each visit to the lab participants complete four separate bouts of walking (more repeated measures). During the real-world gait portion of recording, we may regard each of the seven days of recording as non-independent repeated measures within each subject. Linear mixed effects models (LMEMs) can be used for predicting continuous variables such as UPDRS as a model of ST and/or Phase domain features. LMEMs will also be used to model certain gait features themselves as part of feature selection. Logistic mixed effects models can also be employed when classifying PD vs CL.

Non-linear mixed effects models (NLMEMs) have previously been used in mod-

elling of disease progression [42] [43]. The increased number of parameters of NLMEMs increases the risk of over-fitting if applying them only to lab-based data where we may only have four repeated measures per participant for each of the four timepoints included in these analyses. They are however much more applicable to real-world data. Each day of accelerometry can be segmented by hour and each hour treated as a non-independent repeated measures. Daily patterns in gait and moreover in pathology are of high clinical interest and may be valuable in informing decision support tools [44].

Depending on experiment designs it is not always immediately obvious whether an effect should be regarded as fixed or random. As a general rule the predictor variables that we wish to investigate after accounting for any random variability should be included as fixed effects. In addition random effects are those with can be regarded as being drawn from a probability distribution. For example, in clinical studies, a random effect may be included at the level of the individual to account for unknown impact of lifestyle on the variable of interest. This is often referred to as subject-level variability.

Statistical Parametric Mapping Statistical parametric mapping (SPM) is a method which allows for hypothesis testing across waveforms such as those produced from brain imaging techniques or throughout the human gait cycle [45]. SPM will be used applied to the real-world data to better characterise daily patterns in the gait features of PD and CL subjects.

In any analyses which relate to binary classification (e.g. PD vs CL), the measures of performance: specificity, sensitivity and accuracy, defined as

$$\frac{\text{true positives} + \text{true negatives}}{\text{false positives} + \text{false negatives}}$$

will be reported. Depending on the specific setting, either specificity or sensitivity can be more important. In many clinical settings a higher sensitivity is preferable even at the risk of a lower specificity as this corresponds to a reduced probability of type-2 errors (rejecting a true alternate hypotheses). The trade-off between sensitivity and specificity is controlled by threshold values associated with classifiers. These threshold values can be selected based on a number of criteria and depending on research interests. Receiver operating characteristic (ROC) curves are graphs which summarise the performance of a classifier across all possible threshold values. These ROC curves are generally summarised by their respective AUC (area under the curve) value between 0.5, equivalent to random class assignment, and 1, equivalent to perfect classification of all subjects. In the case of binary classification, k-fold cross validation was used with k = 5 corresponding to an 80%-20% split of the data into training and test datasets respectively.

Multicollinearity may occur in any analysis with a high number of features. In our case we will be working predominantly with two feature domains, ST and Phase with fifteen and sixteen gait features respectively. The variance inflation factor (VIF) of models can be used to assess multicollinearity associated with features in the context of the model. VIF can be used to assess multicollinearity within feature domains and also across all features. There are certain combinations of features that we might expect to cause high VIF values if included. For example, Step length, time and velocity are closely related via the equation $Velocity = Length/Time$ so it is likely that one or more will initially produce a high VIF value. While highly correlated variables pose no risk in a predictive context, VIF can shed light on which on any redundant features which do not bring additional information.

Principal Components Analysis Principal components analysis (PCA) is a popular method for reducing dimensionality and the number of variables needed in

analyses. PCA will be applied to both feature domains. Scree plots are a visual tool which display the proportion of variance explained by successive components following PCA and can be used to show how many principal components are needed to represent $n\%$ of the variance their respective feature domains. Function principal components analysis (FPCA) [46] is a statistical method which extends the concept of PCA to functional data. For our real-world data, we can segment daily gait features by hour and apply FPCA to the resulting time series. FPCA can then be used to identify the main patterns of variability in waveforms.

Due to physiological constraints and bounds on certain features we require transformations to meet assumptions of the above mentioned models. Box–Cox (BC) transformations are versatile. Each feature v_i has been replaced with its BC transformed values according to:

$$v_i^{(\lambda)} = \begin{cases} \frac{v_i^{\lambda}-1}{\lambda}, & \text{if } \lambda \neq 0 \\ \ln(v_i), & \text{if } \lambda = 0 \end{cases}$$

There are several benefits to using BC transformations. Two important values are included in the range of possible values of λ, namely, when λ is taken to be zero the standard log-transformation is restored, and when λ is taken to be 1 then the BC transformation is equivalent to a simple location shift.

3.4 Data Consideration on Drop-outs

Due to the uncontrollable factors, many patients were not available at all time points. Patient drop-out may confound analysis on the PD cohort however. The impact of including these individuals in the analysis is a subject of investigation as we can generally assume that patients available at all follow up time points are exhibiting

on average lower pathology i.e. less deterioration. Missingness due to drop-out or attrition is a very common issue among longitudinal studies, particularly in those with clinical aspects. To begin with lab-based analysis we must first choose an appropriate means of addressing data missingness. Correctly addressing the issue of missing data requires that we regard the entire dataset i.e. all patient data available at each time point. Further longitudinal analysis will be carried out in a later chapter. There is anecdotal evidence that those participants present at later time points within the ICICLE study may be representative of the PD cohort as a whole and that their attendance at later time points may be partly due to a more well-managed disease or less severe symptoms and pathology. These so called "super survivors" have the potential to introduce significant bias into any analyses particularly those including later time points. This is a specific case of survivorship bias [47]. In the context of medical studies with a longitudinal aspect, survivorship bias refers to the disproportionate representation of individuals in data due to their increased propensity to be present at follow-up checks. In our case, a PD subject may not be in attendance at particular time points for a number of reasons including increased pathology leading to reduced mobility or death. When assessing this attrition, it is difficult to attribute attendance to any specific features as this requires disentangling the effects of the disease from the natural deterioration we may expect from in this age group. The proportion attendance of each group is summarised in table 3.2. In a later analysis the age-matched control group provide a useful reference from which the impact of age alone may be estimated. Before addressing missing data by imputation, we must first identify the mechanism by which the data are missing. In general there are three possible mechanisms of missingness [48] [49].

- **Missing Completely at Random** (MCAR)

If data are MCAR, then the data (observed and unobserved) are independent of the fact that the data are missing. In other words, no differences exist between subjects with full data and those with missing data. If, for example, all our missing data was due to adverse whether conditions or travel restrictions unrelated to subjects' physiology then we may be able to assume MCAR. The reduced sample size reduces the power of subsequent statistical testing but crucially does not introduce any bias. In the case of MCAR, the data can be safely treated as a random sample of the full dataset in question and no systematic bias would be introduced by performing complete case analysis i.e. omitting missing or partially missing data. For these reasons, MCAR is a desirable but often unrealistic situation.

- **Missing at Random** (MAR)

  If data are MAR, then the observed data are systematically related to the fact that the data are missing. For example, if there was a tendency among male subjects to decide not to attend follow up sessions and no such tendency among female subjects, then the probability of a subject having missing data at any given timepoint is related to gender (fully observed variable) but not to the condition of their disease or their pathology. If these assumptions hold then the data are MAR. Complete-case analysis may or not be bias in the case of MAR data. In any case, the degree of biased can often be estimated and adjusted for by accounting for the observed variables (in this example, gender).

- **Missing not at random** (MNAR)

  MNAR is the when the propensity of data to be missing is dependant on the missing data itself. A common example of this is when the sickest patients in a clinical are those most likely to drop-out at later timepoints.

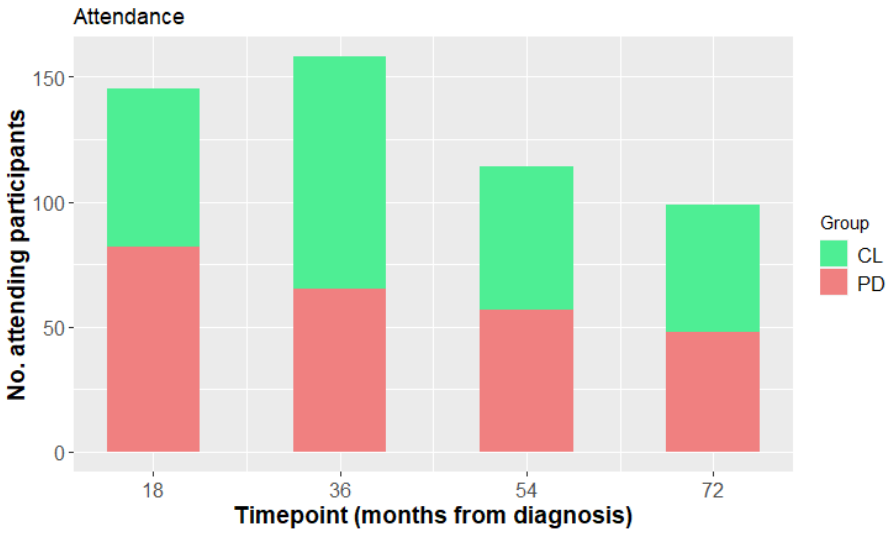

Figure 3.2: The number of participants (by group) in attendance at each follow-up timepoint

MAR and MNAR are both example of non-ignorable missingness. These mechanisms are non-ignorable due to the bias that is potentially introduced if we perform complete-case analysis. MCAR is rare in longitudinal studies - data at earlier timepoints likely hold information on the propensity of individuals to attend follow ups. It should be noted that mechanisms for missingness are not exclusive and incomplete records can be the result of a combination of these mechanisms. Figure 3.2 shows the level of attendance at each timepoint. From this we can see a steady decline in attendance across both the control and PD groups. This decline is deviated from at the 36 month timepoint when there was an increase is attendance from the control group. Figure 3.3 shows the number of participants who attended exactly, 1, 2, 3, or 4 follow-up visits. Interestingly, this shows a relatively uniform spread for the PD group but with the Controls mainly attending either 1 or 4 timepoints.

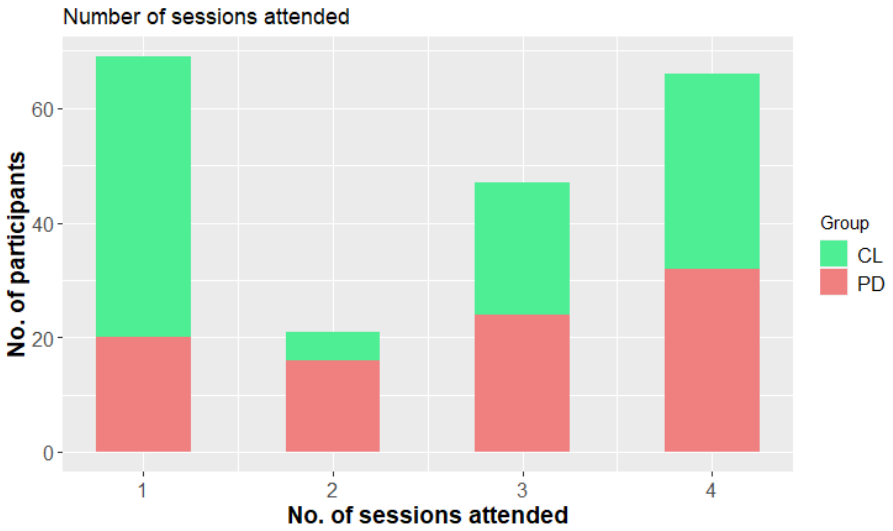

Figure 3.3: The number of participants (by group) in attendance at exactly n timepoints.

	Time point			
Group	18	36	54	72
Control	0.57	0.84	0.51	0.46
PD	0.89	0.71	0.62	0.52

Table 3.2: Attendance proportion at each timepoint by group.

3.4.1 Modelling Drop-out

We wish is investigate the propensity of participants to attend future timepoints and quantify the degree to which observed data can predict the probability of continuation. We aim to estimate $\Pr(R_{it} = 1|Y_{t-1}^{-})$ where R_{it} is an indicator variable equal to 1 if participant i is in attendance and 0 if they are absent at timepoint t. For compactness we allow Y to include Age, height, group (PD or CL), and UPDRS (where applicable). Reliably modelling drop-out in longitudinal studies is crucial to informing future studies and experiment design. Throughout our modelling of drop-out and the probability of continuation our goal will be to address the following questions:

- Do PD and CL participants differ in terms of their propensity to miss a follow up date or drop out of the study all together?
- Within the PD cohort, can an individual's continuation probability be modelled on their respective previous observed data?
- Adjusting for the impact of ageing, how does an individual's probability of dropping out vary at successive timepoints? I.e. asides from the increase in age, is there an impact of disease duration on continuation probability?

	Time point		
Group	18	36	54
Control	0.73	0.52	0.84
PD	0.70	0.71	0.75

Table 3.3: Probability of continuation given a participant's attendance at a specific time point.

Continuation probabilities Table 3.3 shows the overall continuation probability conditional on attendance at previous time points. While helpful, it should be noted that these probabilities do not actually directly relate to the absolute levels of attendance at subsequent time points because there are many participants who temporarily drop-out and return for a later session. I.e. in general we have

$$\Pr(R_{it} = 1 | R_{it-1} = 0) > 0.$$

Logistic regression Logistic regression is the extension of linear regression to binary classification problems. It seeks to model the probability of an event, in our case $\Pr(R_{it} = 1 | Y_{t-1}^{-})$, the probability of attending at timepoint t given all available (prior) information. Logistic regression models can be assessed using performance

measures: accuracy, specificity, and sensitivity, to gauge each model's utility in predicting participant continuation.

We will fit and assess logistic regression models to all extracted gait features and also separately to each feature domain.

For our dataset we have a relatively small number of discrete timepoints making it practical to conduct drop-out analysis separately for each timepoint.

Random Forest A random forest classifier is example of an ensemble method. Ensemble methods aim to improve their predictive power by producing multiple models and combining them into a more accurate model. In the case of Random Forests, these individual models are decision trees- a type of decision support tool similar to a flowchart where each node represents a query on a particular attribute of the subject in question.

Classifier	Accuracy	Specificity	Sensitivity
	All features		
Logistic	0.63	0.645	0.64
RF	0.63	0.65	0.65
	Phase domain		
Logistic	0.60	0.63	0.57
RF	0.64	0.65	0.62
	Spatio-temporal domain		
Logistic	0.59	0.61	0.56
RF	0.61	0.65	0.56

Table 3.4: Performance measure for predicting R_{it} given Y_{t-1}^{-}.

From the performance measures presented in Table 3.4 we could argue that Phase domain features are slightly better at predicting continuation than ST features for a given classifier. However, overall none of the measures are particularly impressive (all $\approx$65%). This reflects the difficulty in explaining drop-out in the case of MNAR and/or MAR. Neither Phase domain nor ST features were particularly impressive

at predicting attendance at follow-up timepoints. However this is not surprising as there are many unknowns which may impact an individual's ability to attend. Regardless, we will revisit the problem of predicting drop-out in chapter 5 to assess how real-world gait and increased ADL can improve this prediction.

3.4.2 Imputation Methods

The simplest approach to addressing drop-out in a longitudinal study is to ignore all incomplete records and base all following analysis on only those participants with complete data and full attendance. This known as complete-case analysis. This is very prone to introducing bias unless the dataset exclusively exhibits MCAR missingness in which case complete-case analysis can produce valid conclusions.

Last observation carried forward (LOCF) A marginally better method is to impute a missing observation Y_{it} as Y_{it-1} assuming $R_{it} = 0$ and $R_{it-1} = 1$. This has the benefit of increasing the amount of data available for analysis and does at least base newly imputed values on data observed for the participant in question.

Last residual carried forward (LRCF) Similarly, LRCF imputes a missing observation Y_{it} as $Y_{it-1} - \overline{Y}_t$. This represents a significant improvement over LOCF as it does more to maintain any local trends in the data.

For consecutively missed follow-ups both LOCF and LRCF can be carried out iteratively, although errors will accumulate. Each of these methods, which are based on the most recent available timepoint for imputation, are simple to implement but are criticised in the literature [50] partly due to their failure to address random variation caused by the imputation process itself.

Multiple imputation by chained equations In summary, complete case analysis is not appropriate due to the potential bias it would introduce. Similarly, both LOCF and LRCF would introduce cumulative error in any imputations.

The chosen method for addressing missingness here is multiple imputation by chained equation (MICE) also known as "sequential regression multiple imputation". In addition to those listed above, the reasons for selecting MICE are: creating multiple imputations rather than just one helps account for uncertainty in the data. The MICE methodology is flexible with regards to variable type and other complexities such as bounds [51]. This is particularly relevant to our dataset in which many features are bounded or constrained due to physiological limits or mathematical definition. For example, spatio-temporal features such as step length asymmetry defined as the mean absolute difference between left and right step length for a given bout is unlikely to be more than a small proportion of the corresponding mean step lengths. Within the Phase domain, primary or secondary measures derived from ellipse eccentricity have strict constraints due to the definition of eccentricity,

$$\sqrt{1 - \frac{m^2}{M^2}}$$

where m and M are the semi-minor and semi-major axes respectively. This means eccentricity will not exceed the value of 1. It should be noted, however, that general conic sections can have any positive value of eccentricity but we are only concerned with strictly elliptical conics here. The flexibility of MICE means we can rely on these variables' complexity being conserved. In general Multiple Imputation is more efficient where incomplete cases have some data associated with them. In our case we do have Age data and disease group as well as any previous or future attended timepoints. MICE is just one of many possible means of imputation, this method is chosen here for it's flexibility in handling different variable type and complexity in

the data.

More information on MICE is available from Azur et al [51] as well as information on other approach for multiple imputation [52] but in short the steps for implementing MICE are as follows:

1. An initial place holder imputation is made. This can be done using a simple arithmetic mean of available data for each variable to be imputed.

2. The initial imputed values for a single variable are removed (again labelled as missing data).

3. This variable is then taken as the dependant variable in regression with all other available variables as independent variables.

4. The missing values for the variable are predicted (imputed) from this regression model.

5. Repeat steps 2–4 for all variables which had missing data. Once this process has been carried out for all variables then we say we have completed one cycle or iteration and all missing values have been replaced with predictions from regression models which reflect the relationships observed in the data. It is important to note that while cycling through the variables when a variable is used as an independent variable having already been taken as the dependant variable in a previous model then both the observed and imputed values are used in the new regression model.

6. Steps 2–4 are repeated for some number of cycles and the imputations are updated at each cycle.

There is no general rule for the optimal number of cycles. Although Raghunathan et al [53] recommends that 10 should be sufficient in most cases there are

other arguments that approximately 40 cycles improve the quality of the predictions if practical given system resources. Performing multiple cycles ensures that any dependency on the order in which the variables are cycled through is removed. 30 cycles were performed while imputing the missing data taking approximately 25 minutes on the following system: Processor- Intel(R) Core(TM) i5-4460 CPU @ 3.20GHz, 8GB of RAM.

Chapter 4

Accelerometry-based Gait Analysis in Parkinson's Disease: Application of Traditional and Phase plot Gait Characteristics.

4.1 Aims

The effectiveness and practicality of novel methodology and feature domain introduced in chapter 2 can be demonstrated through its application to PD gait accelerometry. While lab-based gait data are necessarily restricted in its representation of real-world gait it can provide reliable proof of concept for this Phase plots methodology and the new Phase domain of features.

As well conducting an initial exploratory analysis of novel Phase plot features from lab-based gait, in this chapter we will answer the following questions:

- Can novel phase domain features distinguish between PD and CL patients

based solely on the accelerometry of their respective bouts of walking?

- Do individual subjects reliably reproduce the same type of phase plot across multiple bouts? I.e. is it fair to refer to phase plots as a signature of gait? If so, is this the case for both PD and CL subjects?

- How do ST and Phase plot features compare when used to classify PD and CL subjects, and does a combination of ST and Phase features out perform either domain alone?

- Do Phase plots hold additional information pertaining to an individual's gait and disease state beyond that which can be provided by traditional features such as those within the ST domain?

4.2 Data and Pre-processing

Here we focus our analyses on the lab-based portion of the ICICLE-GAIT study as described in chapter 3. In particular, we will be using accelerometry data from intermittent walks performed four times by each of 203 included participants (92 PD and 111 Control) at up to four evenly spaced timepoints.

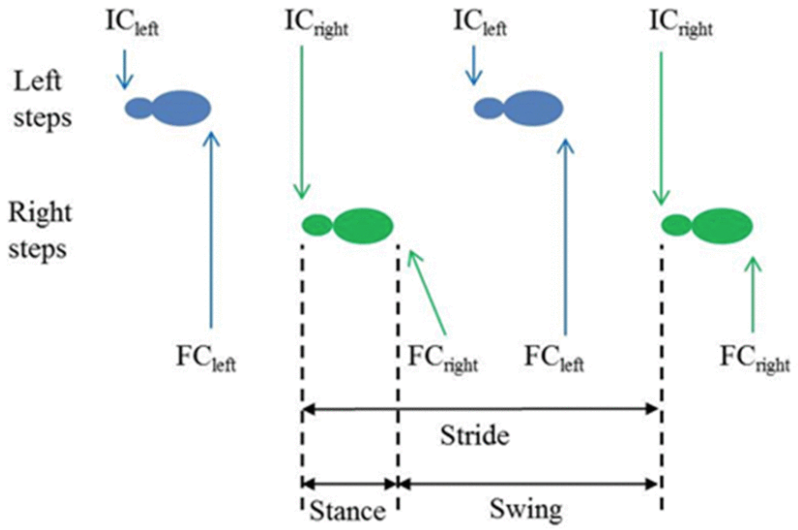

Figure 4.1: Gait cycle showing gait events (GEs). IC = Initial contact (heel strike), FC = Final contact (toe-off)

Here the data associated to each participant are one or more (depending on attendance) triaxial acceleration signals $\mathbf{X} = (\mathbf{x_1(t)}, \mathbf{x_2(t)}, \mathbf{x_3(t)})$ recorded during straight walking bouts with a waist-worn accelerometer device affixed at the L5 vertebra (see Figure 3.1). These lab-based ambulatory bouts are an example of scripted activities and as such do not require complicated gait detection. The Phase domain features here are derived from phase plots constructed from the vertical axis acceleration, $\mathbf{x_1(t)}$ employing the zero-crossing (ZC) gait cycle segmentation method detailed in 2.1

As explained in chapter 2, when constructing cyclic phase plots as opposed to those based on per-cycle features [18], we must have a method for distinguishing subsequent cycles and defining the thresholds j_n, k_n such that we associate $x_1(i)$ to cycle n if $j_n \leq i < k_n$ i.e. the boundaries of each gait cycle. Within the field of gait analysis, gait events (GEs) such as initial contact (IC) and final contact (FC) of alternating feet are utilised to segment gait (see Figure 4.1). GEs offer intuitive reference points when performing detailed gait analysis and ICs in particular can

be accurately and reliably detected with a variety of sensor set-ups. However, when segmenting gait in this way according to GEs the resulting phase plots are highly sensitive to small variations in IC timings. This is due to the sharp characteristic spike in the vertical axis of acceleration associated with heel strikes. This resulting in a disproportionate impact of IC estimate final on Phase plot features. For this reason, descending ZCs in the vertical signal were used to segment adjacent cycles i.e. cycle 1 begins at the earliest value of j such that $x_1(j) < 0$ and $x_1(j)$ is associated with valid gait. Cycle 2 begins at the earliest subsequent index j such that $x_(j-1) > 0$ and $x_(j) < 0$ and so on. Segmenting in this manner produces phase plots which exhibit within-bout stability.

Due to this non-standard gait segmentation, our definition of a gait cycle deviates somewhat from the model shown in figure 4.1 (left IC to right IC) as descending ZC events occur shortly before IC events. Essentially this ZC-based method of gait segmentation produces a slightly left-shifted gait cycle when compared to the standard IC-to-IC model. This altered gait segmentation method was needed to ensure robustness and reproducibility of Phase plots and their respective features.

4.3 Lab-based Phase Plot Analysis

Before assessing the utility of Phase plots and features within the Phase domain we should consider the number of new features being introduced. We employ Bonferroni correction [54] where appropriate to correct for multiple comparisons. Say we intend to test the hypotheses $H_{01}, ...H_{0i}$ that features 1,...,16 of the Phase domain do not differ between PD and CL patients for i = 1,...,16 (each of the phase domain features). As the number of features, i increases, so does the probability of a Type I error where by we reject at least one true H_{0i}. Intuitively, investigating more and more features extracted from a dataset increases the probability of

finding a spurious difference between PD and CL subjects appearing statistically significant. A well-known counter action for this increased probability of type 1 errors is to employ the Bonferroni correction by reducing the significance level of our tests from α to $\frac{\alpha}{i}$ where i is the number of hypotheses being tested as above. If we take the standard significance level of $\alpha = 0.05$ and given that we have 16 Phase domain features of interest our new significance level adjusted for multiple measures is $\alpha_p = 0.05/16 \approx 0.0031$ As a useful reference we will also take note of the p-values associated with well-established spatio-temporal features throughout these analyses.

4.3.1 Exploratory Analysis

Several features in both domains exhibit significant right or left skew. In several cases a log transformation was sufficient in addressing this prior to conducting t-tests. To assess normality (a key assumption of t-tests) we can plot the quantiles of the data as a function of the theoretical quantiles of a normal distribution with equal mean and SD. These Quantile-quantile plots are commonly known as qq-plots. For both PD and control subjects, Asy_{γ_m} showed significant right skew and deviation from normality. Figure 4.2 shows the impact of this transform on the data distribution. It also makes clearer the shift in position and size of the effect of disease on this feature. To formally test the impact of this transformation we can use qq-plots (Figure 4.3 and 4.4) and observe the improvement shown by comparing before and after. The quantiles of the data match closely their corresponding theoretical quantiles implying normality has been achieved. As a more formal assessment we can also perform Shapiro-Wilk tests for normality. In the case Asy_{γ_m} we see an initially failed test ($p < 0.01$) i.e. the feature is not normality distributed. The transformation $log(Asy_{\gamma_m})$, however, yields $p > 0.05$ which validates the choice of transformation for this particular feature. All features underwent a Box–Cox (BC) transformation

Feature	CL	PD	Mean difference, %	p
Phase Domain				
		Primary features		
Area	0.254	0.167	-34.1	0.045
$\boldsymbol{\gamma}$	0.945	0.937	-0.790	**<0.01***
$\mathbf{Asy_{\theta}}$	6.68	10.23	53.1	**<0.01***
$\mathrm{Asy_{Area}}$	3.62	2.48	-31.7	0.22
GoF	6.79	6.69	-1.49	0.79
$\mathbf{SD_{r_1}}$	0.040	0.0293	-27.2	**<0.01***
$\mathrm{SD_{r_2}}$	0.197	0.153	-22.0	0.159
		Secondary features		
$\mathbf{Asy_{\gamma_m}}$	0.018	0.0316	75.61	**<0.01***
$\mathbf{Asy_{\gamma_M}}$	0.0253	0.0293	15.75	**<0.01***
$\mathbf{Asy_{\theta_m}}$	9.48	12.145	28.05	**<0.01***
$\mathbf{Asy_{\theta_M}}$	5.48	6.614	20.67	**<0.01***
$\mathrm{Asy_{Area_m}}$	19.12	9.33	-51.2	0.10
$\mathrm{Asy_{Area_M}}$	456.5	72.1	-84.2	0.24
$\mathrm{GoF_m}$	29.9	30.05	0.20	0.92
$\mathbf{GoF_M}$	53.2	46.3	-12.9	**<0.01***
$\mathrm{SD_{GoF}}$	37.8	36.81	-2.65	0.32
Spatio-temporal Domain				
		Mean characteristics		
Step time	0.557	0.541	-3.04	**<0.01***
Stance time	0.721	0.703	-2.46	**<0.01***
Swing time	0.409	0.394	-3.82	**<0.01***
Step length	0.532	0.576	7.50	**<0.01***
Step velocity	0.973	1.074	9.41	**<0.01***
		Variability (var) characteristics		
Step time var	0.025	0.019	-28.8	**<0.01***
Stance time var	0.084	0.069	-21.9	**<0.01***
Swing time var	0.061	0.047	-30.2	**<0.01***
Step length var	0.0582	0.061	4.87	0.03
Step velocity var	0.109	0.117	6.70	**<0.01***
		Asymmetry (asy) characteristics		
Step time asy	0.0183	0.0136	-34.7	**<0.01***
Stance time asy	0.0470	0.0390	-20.7	**<0.01**
Swing time asy	0.0390	0.0296	-33.3	**<0.01***
Step length asy	0.0397	0.0370	-7.68	0.013
Step velocity asy	0.0713	0.0647	-10.1	**<0.01***

Table 4.1: Feature values from the spatio-temporal and phase domains. *Statistically significant following Bonferroni correction

which, as detailed in chapter 3, can include the $log()$ transform depending on the estimated value of λ. It is well known that normality may be assessed using one of many available goodness-of-fit tests such as Pearson-Chi-square, Shapiro-Wilk etc. Similarly, λ is estimated by finding the argument which maximises/minimises the criteria associated with these tests. It should be noted that the approach laid out here is not the only option, for example, non-parametric tests such as the Kernel two sample test or the Mann–Whitney test could also be conducted here.

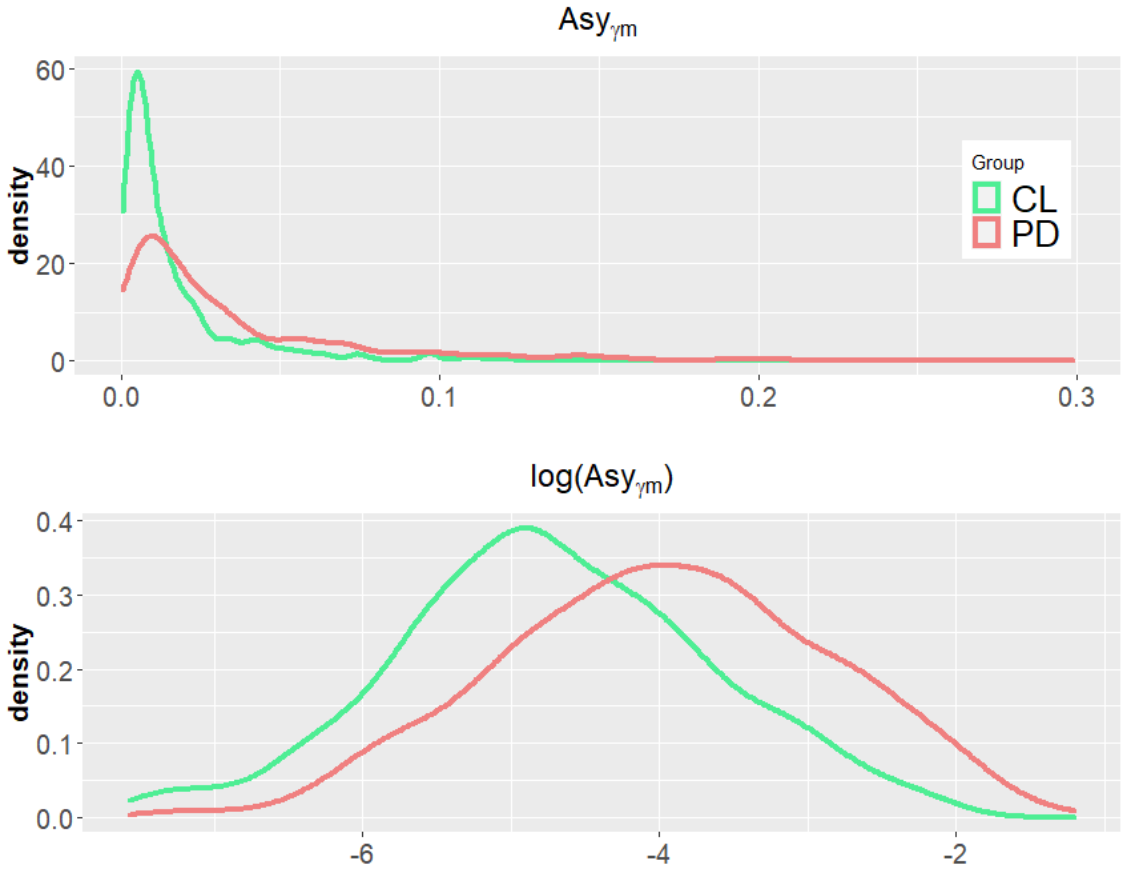

Figure 4.2: Asy_{γ_m} empirical density before and after log-transform

Table 4.1 shows the extracted values of all 16 Phase and 15 Spatio-temporal features as well as their respective signed mean differences (PD - Control). P-values are calculated via two-sample un-paired t-tests. While the study design included

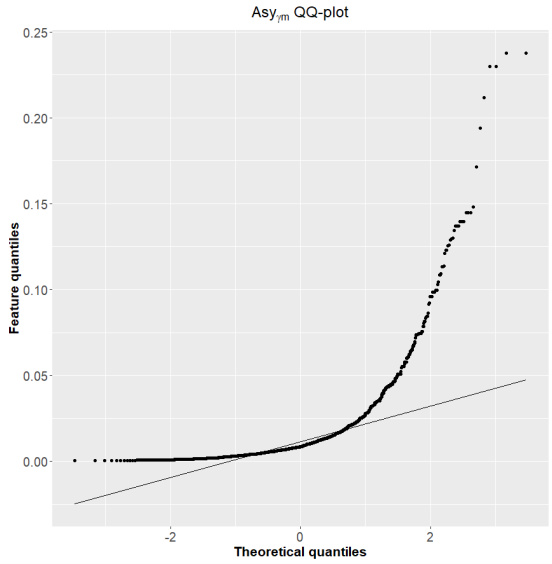

Figure 4.3: the non transformed feature shows a qq-plot typical of a feature with right skew

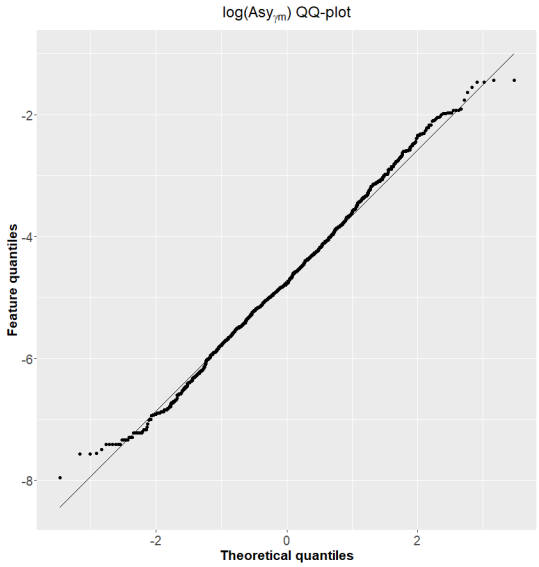

Figure 4.4: log-transformed data exhibiting normality.

age-matched controls, drop-out and inconsistent attendance in both groups weakens the case for a paired test, hence the use of an un-paired t-test. Starred p-values indicate significance at the 5% level adjusted for multiple measures.

Densities

Empirical densities offer a quick visual summary of the distribution of various extracted features among the cohorts and an indication of which features may have discriminative power in terms of detecting PD from lab-based gait.

The feature densities presented here are of untransformed data. Due to physiological limitations and specific derivations some of these features have characteristic empirical densities. For example, step length asymmetry is defined as:

$$StepLength_{Asy} = |Average_{Left} - Average_{Right}|$$

i.e. the average absolute difference between left and right step lengths. For this

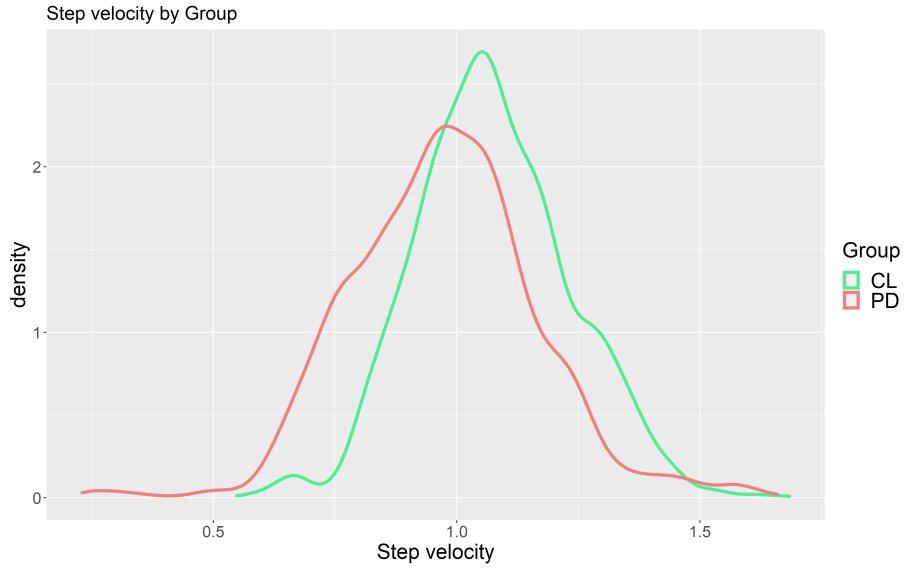

Figure 4.5: Lab based Step velocity by Group

reason, we can expect the associated feature to be bounded below at zero potentially with heavy right skew. We would also expect that the actual values of this feature would not be more than a small fraction of the average step length (about 0.55 across all participants). Indeed this is observable in the respective density (Figure 4.6) with a right skew and modal value around 0.01, about 2% the average step length. Phase domain features are also subject to similar constraints, usually as a result of their derivation from conic sections. As was previously explained, the feature γ (primary ellipse eccentricity) is strictly bounded above by 1 as visible in Figure 4.7.

Box-plots by Group and Time point

Longitudinal analysis will be conducted in detail in Chapter 6, however the following box-plots are provided by timepoint as well as disease group. The visualisations here are constructed following BC transformation of the features in question. These transformations preserve ordering of the data so all trends and between-group differences are also preserved.

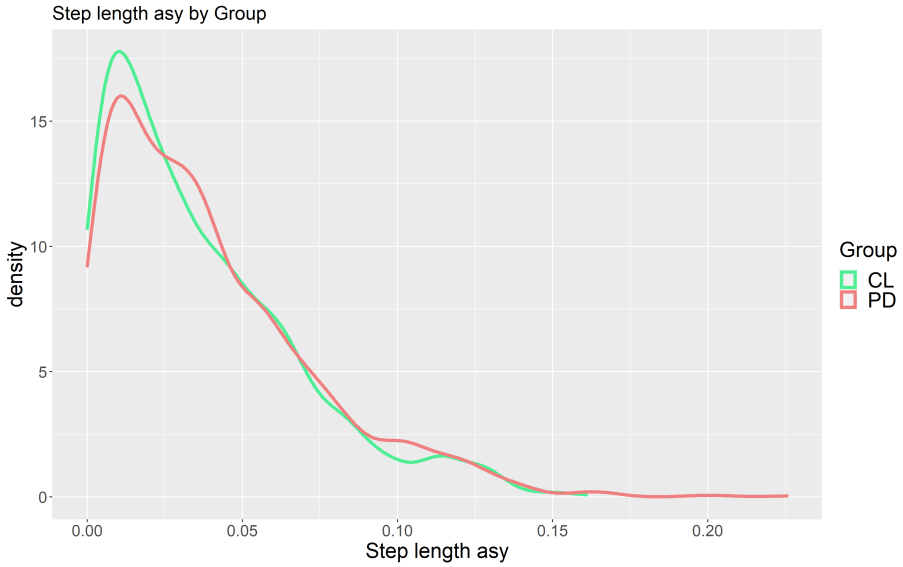

Figure 4.6: Lab based Step length asymmetry by Group

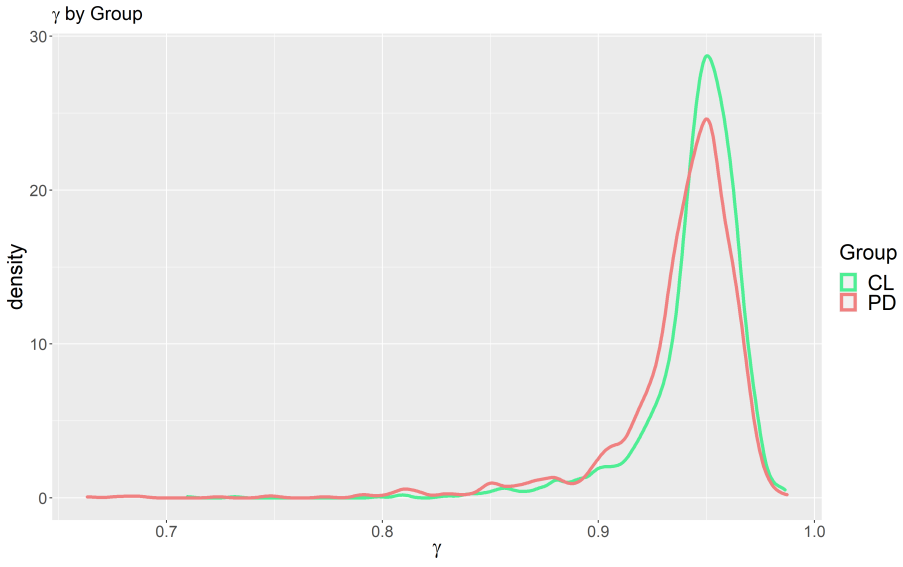

Figure 4.7: Lab based primary ellipse eccentricity by Group

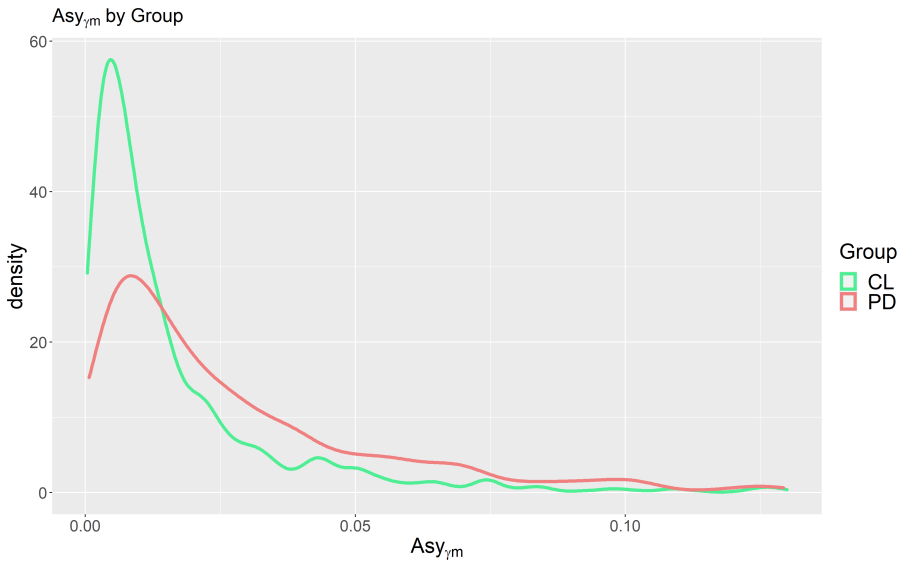

Figure 4.8: Lab based type II ellipse eccentricity asymmetry by Group

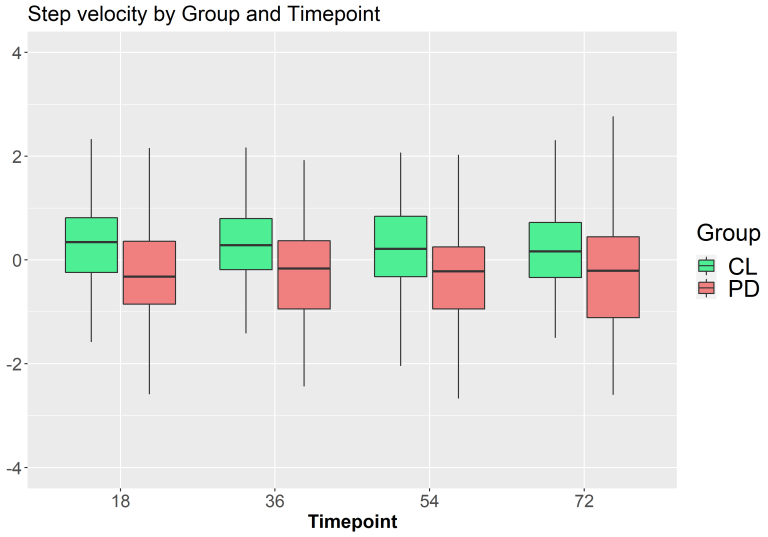

Figure 4.9: Standardised step velocity by group and time point

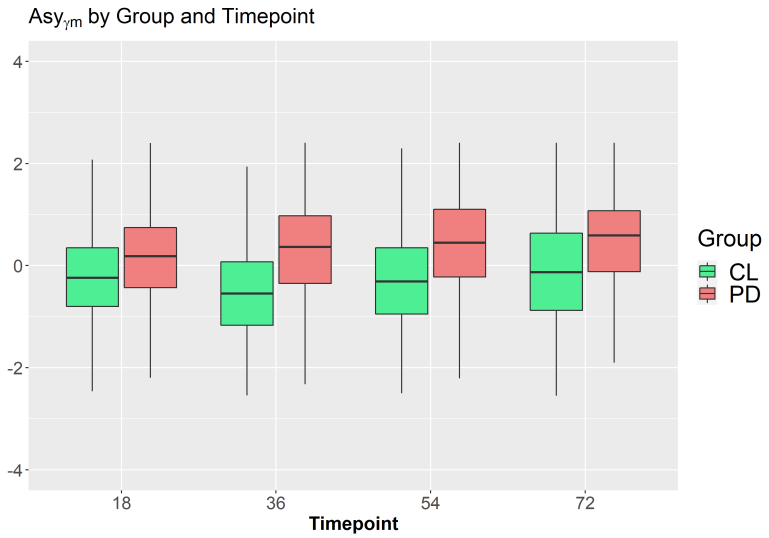

Figure 4.10: type II ellipse eccentricity asymmetry (Standardised) by Group

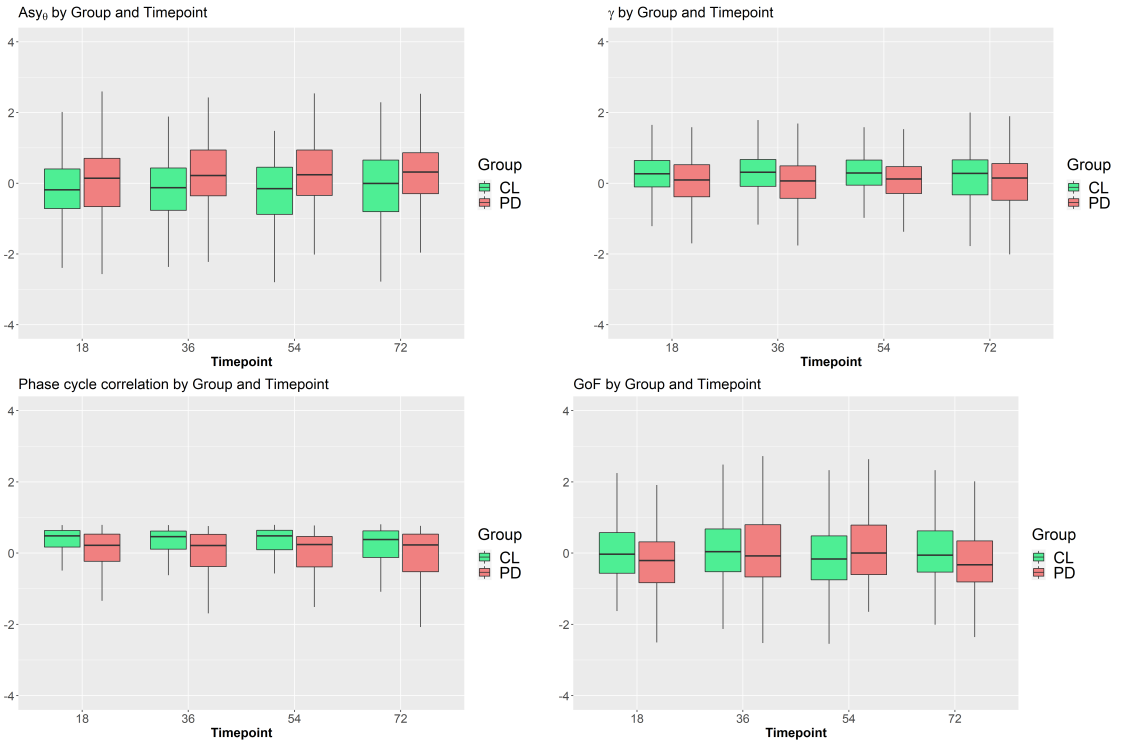

Figure 4.11: Four primary phase domain features by group and timepoint (Plotted as standardised values)

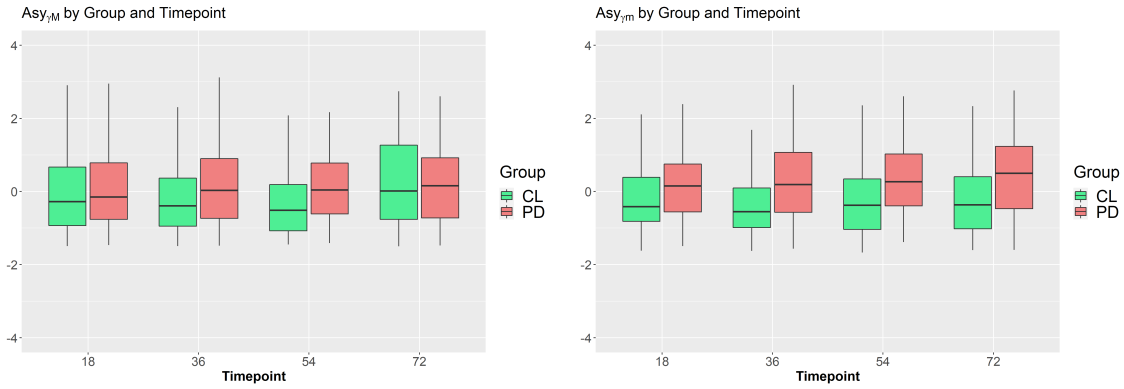

Figure 4.12: Two secondary phase domain features, type I and II ellipse eccentricity γ shown.

Multicollinearity

Multicollinearity is the presence of interdependence or high inter-correlations between independent variables. Multicollinearity can be assessed via the VIF (Variance Inflation Factor). In short, VIF is a quantity that can be calculated on a per-predictor basis which represents the degree to which the coefficient of said predictor is "inflated" due to correlations with the other predictors in the model. Opinions differ on where a cut-off should be drawn for VIF and what exactly constitutes "too much" multicollinearity but the methods for dealing with it and reducing its impact are clearer. If VIF highlights a multicollinearity issue in the data then those variables with the highest VIF may be suitable candidates for removal from the model. To assess the discriminative power of gait features in the context of PD, we may initially fit two saturated logistic regression models. Here the aim is to model the probability of being a PD participant as a function of their corresponding features in either the Phase or ST domain.

$$P(PD_i = 1) = S(\beta_0 + \beta_1 x_{i1} + ... + \beta_n x_{in}) \tag{4.1}$$

where PD_i is an indicator variable equal to 1 when participant i has a diagnosis of Parkinson's disease and 0 otherwise and x_{ij} is the value of the j-th feature for subject i.

When $S(x)$ is the sigmoid function,

$$\frac{e^x}{1+e^x} \tag{4.2}$$

then 4.1 corresponds to a linear model of the log-odds of P which is equal to

$$\log\left(\frac{P}{1-P}\right)$$

If we first take the ST feature domain, then $x_{i1}, x_{i2}, ..., x_{i15}$ correspond to the i-th subject's step length, stance time, step velocity etc respectively. Alternatively, if we instead take the Phase domain we have $x_{i1}, x_{i2}, ..., x_{i16}$ corresponding to the i-th subject's primary ellipse features (γ, Asy_θ etc.) and secondary ellipse features ($Asy_{\gamma m}$, $Asy_{\gamma M}$, GoF_m etc). These two saturated models may be used to assess the discriminative power of each feature domain applied to PD and CL gait. However, the initial purpose here is to assess multicollinearity within each of the feature domains by calculating the VIF for each feature in each logistic model (Table 4.2).

For the Phase domain we find an average VIF of **1.73** compared to an average of **12.21** for the ST domain. Upon further inspection it is clear that a small number of ST domain features contribute to this relatively large average VIF due to their physiological dependence on each other. For example, for a given step time, we have step velocity and step length, essentially proportional to each other. There is no objective cut-off value for VIF beyond which we conclude a feature should be removed and the model re-fitted however. Some researchers suggest a cut-off of 5 or below while other propose that only values exceeding 10 should be cause for concern

Feature (Phase)	VIF	VIF*	Features (ST)	VIF	VIF*
Area	1.41	1.38	**Step time**	**22.8**	-
γ	2.67	1.62	Stance time	4.57	1.70
Asy_{θ}	1.46	1.35	**Step length**	**44.9**	1.05
Asy_{Area}	1.28	1.27	**Step velocity**	**61.6**	-
GoF	1.64	1.64	Step time var	2.93	2.80
SD_{r_1}	1.41	1.39	Stance time var	3.18	2.84
SD_{r_2}	1.35	1.33	Swing time var	2.63	2.52
Asy_{γ_m}	1.82	1.69	Step length var	12.1	1.51
Asy_{γ_M}	2.08	2.06	**Step velocity var**	13.0	-
Asy_{θ_m}	2.16	2.15	Step time asy	1.75	1.74
Asy_{θ_M}	1.91	1.88	Stance time asy	2.45	2.46
Asy_{Area_m}	1.05	1.05	Swing time asy	2.42	2.39
Asy_{Area_M}	1.14	1.13	Step length asy	2.72	2.44
GoF_m	1.89	1.45	Step velocity asy	2.57	2.23
$\mathbf{GoF_M}$	3.54	-	Swing time	3.67	1.75
$\mathbf{SD_{GoF}}$	4.07	-			

Table 4.2: Phase and ST domain features' Variance Inflation Factor (VIF). VIF* shows values following sequential removal of highest scoring features until all were within the acceptable region (< 5).

in terms of multicollinearity [55]. A common theme among the relevant literature is that the consequences of multicollinearity must be assessed in terms of the analysis in question. In the case of our analyses we should therefore consider the order in which spatio-temporal features are removed from the respective logistic regression model. In particular we can see step time, step length and step velocity are all exhibiting very high VIFs (>25). After removal of the feature highlighted in table 4.1 the domain-specific VIF values reduce to **1.49** and **2.12** respectively.

From the plotted correlation in Figure 4.13 we can see several properties which support the use of the Phase domain features. Firstly, the within-domain correlation of the phase domain is considerably lower than that of the spatio-temporal domain (0.20 and 0.32 respectively). Also, the correlation between domains is very low (0.12) which gives credit to the hypothesis that this novel feature domain does indeed

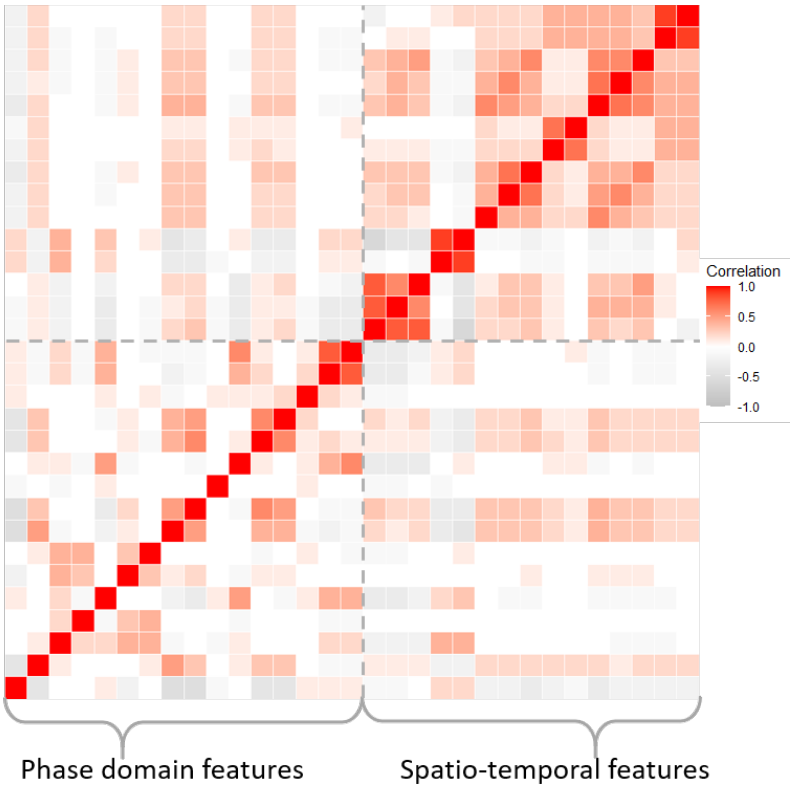

Figure 4.13: Correlation heatmap of feature of ST and Phase domains.

contain additional information beyond that contained in the ST domain alone.

Hierarchical Clustering Clustering based on gait characteristics from each domain will help address the aim detailed in section 4.1 regarding the hypothesis that Phase plots hold gait-related information not available on ST features. From Figure 4.13 we can see that clusters of features are emerging. In the case of traditional ST features, this is partially to be expected given the relationship between certain features e.g. step length, time (duration), and velocity. There is no similar intuitive clustering to the phase domain however. We perform hierarchical clustering to quantify these clusters and sub-clusters of features. We will consider agglomerative hierarchical clustering methods. Here "agglomerative" refers to the way in which we initiate the clustering method, where each observation (or feature in our case)

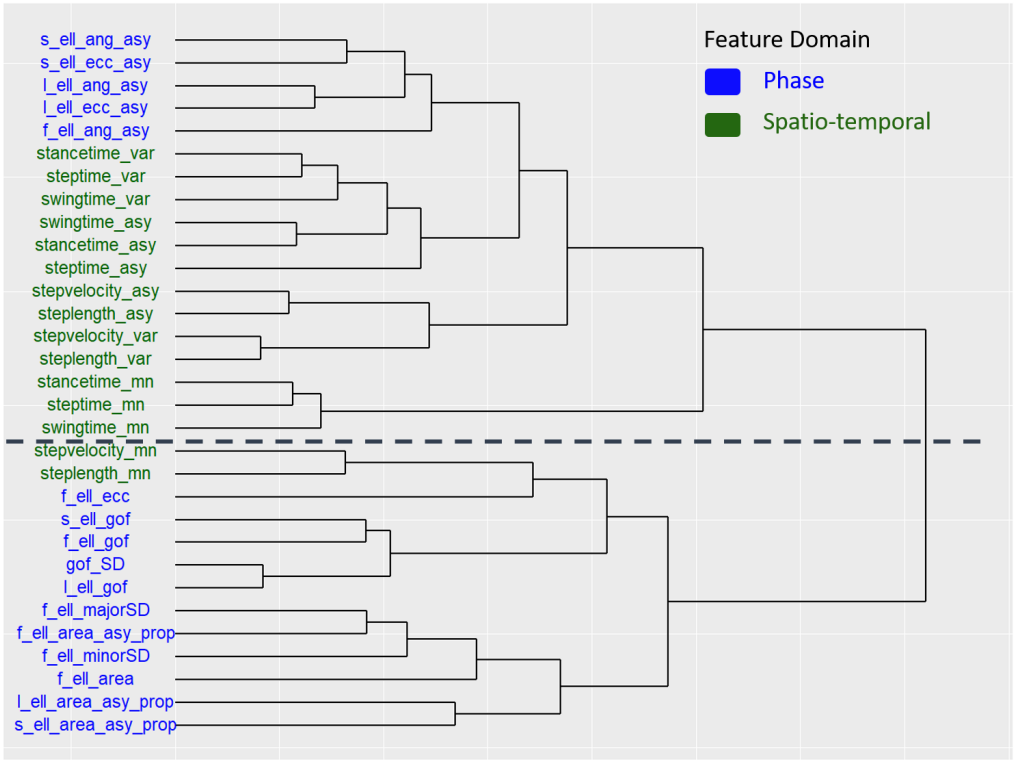

Figure 4.14: Full-linkage complete hierarchical clustering of features in Lab-based setting. Highest level clustering shown.

begins as its own cluster of size 1. This is an alternative to divisive clustering which begins with all features in a single cluster and aims to split into successively smaller clusters based on some heuristic.

There are several methods for agglomerative hierarchical clustering [56]. Here we use a method known as the complete-linkage method. Other popular methods such as Ward's method [57] [58] produce overall similar results.

As displayed in Figure 4.14 hierarchical clustering does to a large extent distinguish between the phase and spatio-temporal domains with most of the overlap being accounted for by four secondary Phase features: Asy_{γ_m}, Asy_{γ_M}, Asy_{θ_m}, Asy_{θ_M} being clustered with 13 out of 15 ST features and two ST features, step length and step velocity, being clustered with the majority of phase features. This observation is based on the second last level of clustering.

Principal Components Analysis (PCA)

Given the presence of multicollinearity and the large number of features it makes sense to perform a factor analysis at this stage. PCA is generally used to reduce the dimensionality of datasets such as those containing the Phase and ST domain features by producing a much smaller number of orthogonal and uncorrelated variables constructed as linear combinations of the original features. These new features are known as the principal components. For our purposes, it can be used to compare and contrast the two feature domains in question here by looking at the how well the top first n principal components capture the variability in their respective domains.

Scree plots in Figures 4.16 and 4.15 show the proportion of variance explained by each successive principal component. We can see that both domains have comparable PC decompositions in terms of cumulative respective variance explained as both domains have over 60% of their respective variances explained by the first five principal components.

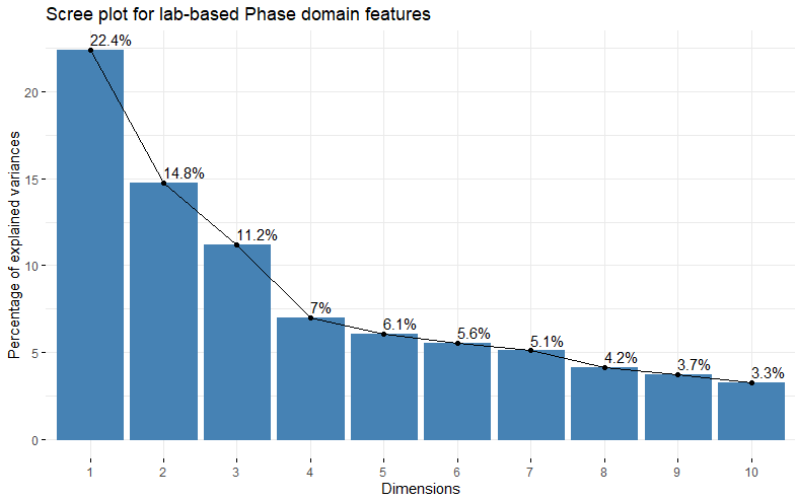

Figure 4.15: Scree plot for all Phase domain features

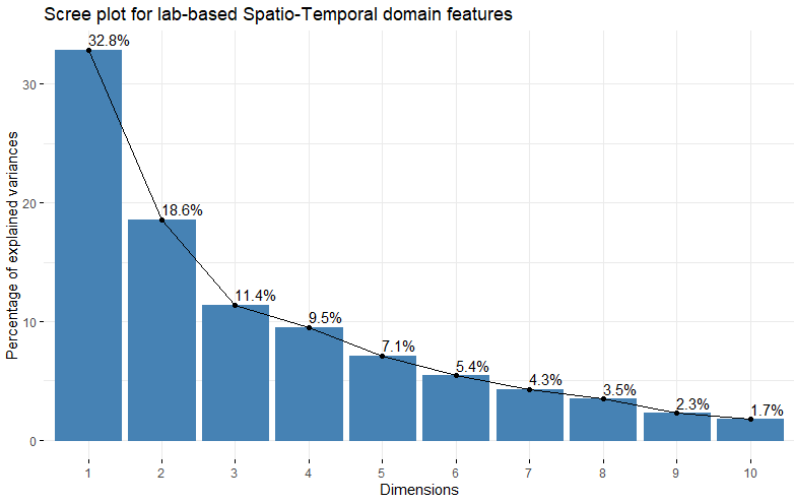

Figure 4.16: Scree plot for Spatio-temporal features.

Prior to performing PCA we centred and scaled (to have unit variance) each feature. This is best practice in the case of variables prone to significant differences in magnitudes. Following on from the Box–Cox transformations earlier, several transformed features in each domain were subject to a shift in location. Neglecting this step produces vastly different Scree plots showing $> 90\%$ variance explained by just 3 features in each domain. This would lead to a large reduction in features and model complexity moving forwards, however the subsequent disease classification analyses would not see a similar increase in efficiency. This 90% figure is only produced if we don't scale variables and allow the analysis to be distorted by those features with outlying magnitudes.

In chapter 6 we will also perform a functional principal components analysis to better explain trends in these features over the course of the study duration and assess the ability of the new Phase domain in monitoring disease progression over several years.

4.3.2 Discriminative Power in PD

Much of the clinical interest in gait features is directed at diagnostic power and reliability of certain features in identifying PD gait vs healthy gait. It must be noted, however, that "healthy" is an ambiguous term here and refers to the gait of age-matched controls who are by no means completely free from comorbidities themselves.

Following on from the two saturated logistic regression models in the previous section, it is standard practice to remove those variables identifies as having correlations with other independent variables or high VIFs. Following their removal, we can construct Receiver Operating Character (ROC) curves to help assess each domain's utility in detecting PD. The ST and Phase plot (PP) feature domains show slightly different characteristic ROC curves but almost equal AUC (area under the curve) values. AUC can be interpreted as a combined measure of both specificity and sensitivity i.e. a high AUC value implies simultaneously a low false positive rate and low false negative rate. In the context of this analysis, this corresponds to correctly classifying both PD and CL subjects. The ST and Phase feature domains show noticeably different characteristic ROC curves, provided in Figure 4.17. The ST domain gave an AUC value of ≈ 0.66 compared with ≈ 0.71 for Phase plot features. From this it appears both domains are approaching the "acceptable" range generally defined as 0.7-0.8 in the literature [59]. The crucial context of this is the environment in which the gait data was recorded - a highly controlled unnatural lab-based setting. The slight difference in the feature domains' respective ROC curves shows that depending on a choice of threshold, the Phase domain may have a reduced specificity compared to the ST domain or a slightly superior specificity and sensitivity.

There are several available methods for defining an *optimal* threshold from the

ROC curve. Common criteria involve selecting a point at which the sensitivity and specificity of the classifier are simultaneously close to the AUC and to each other.

In addition to the standard logistic regression model we also implement a Naive Bayes (NB) classifier [60]. NB classifiers have several properties which make them suitable for our purposes:

Insensitivity to irrelevant features. It is plausible that given multicollinearity in the phase domain and features with similar definitions in the ST domain that several features are not necessary in disease classification.

Scalable. It will be helpful to apply the same classification method to the free-living dataset in a later chapter where the vastly increased data size may carry more computation time consideration than the relatively small lab-based dataset. There are also downsides to this classifier such as the assumption that each feature makes an equal and independent contribution to the prediction class which may not hold here.

Classifier	Accuracy	Specificity	Sensitivity
	All features		
Logistic	0.65	0.74	0.54
NB	0.65	0.53	0.75
	Phase domain		
Logistic	0.64	0.74	0.53
NB	0.60	0.41	0.76
	Spatio-temporal domain		
Logistic	0.60	0.75	0.41
NB	0.61	0.41	0.76

Table 4.3: Performance measures for predicting disease status by feature domain (top 4 PCs) and classifier type

Table 4.3 shows the performance of three logistic regression models for assessing the ability of each feature domain to predict PD status in lab-based gait. These models are fitted using only the first 4 principal components (PCs) of their respective

domains. For this dataset and classification task, the choice between a Naive Bayes and logistic regression for detecting PD represents a trade-off between specificity and sensitivity. Which of these is preferable depends on the context. Within clinical studies and diagnostics, we may wish to err on the side of caution and accept a higher than ideal false positive rate (lower specificity) in order to avoid high false negatives (low sensitivity). One of the motivations for this is that it reduces the probability of missed diagnoses. Overall the measures shown in table 4.3 are not excellent with several around the 0.5 region - which might expect to achieve with random guessing.

In terms of domain comparison, the Phase domain appears to perform at least as well as the ST domain for both classifiers. These results must be seen in the context of the environment in which the associated gait took place. The unnaturally restricted and scripted bouts of walking necessarily restrict the variety of physical movement and it is unreasonable to assume that ST features based on variability of gait e.g. step length variability are representative of an individual's general gait during ADL. The impact of environment on gait features from each domain will be investigated in chapter 5. We can safely hypothesise that features within the ST domain such as step length (variability) will exhibit notably different distributions in the real-world environment due to ADL and variety of gait. However, in the case of the novel Phase domain, it is unclear how the transition from lab-based to free-living may impact feature distributions and the general appearance of phase plots. While these results appear to show some promise for the performance of Phase domain features, it must be noted that the results in Table 4.3 are based only on the first 4 principal components of the respective featured domains. While this method is helpful in reducing the number of variables in a model, there is no guarantee that the full predictive power contained in each feature domain is represented in just 4

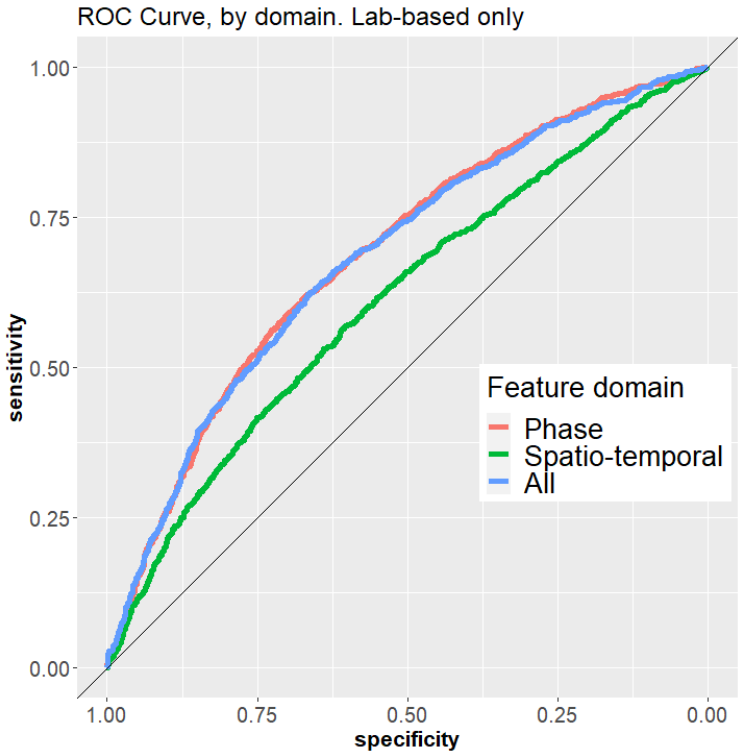

Figure 4.17: ROC curves for the Phase and ST feature domains.

PCs.

4.3.3 Phase Plots as a Signature of Gait

A small subset of the Phase domain features can be used to categorise all phase plots into one of four easily recognisable and clearly distinct types. These features are the angle subtended by successive phase plot orbits Asy_θ, the primary ellipse eccentricity γ and the Euclidean distance between adjacent successive orbits, d. Human fingerprints can all be categorised as one of a small number of types (see Figure 4.18) while still containing enough distinctiveness to accurately identify a single individual. We aim to demonstrate that gait, and specifically Phase plots, offer a similar categorisation while holding subject-specific information. This level of individualisation is of particular clinical interest as it is a vital component in

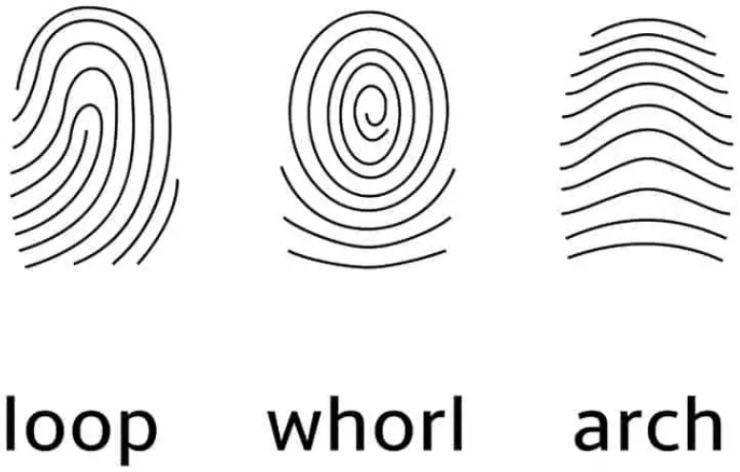

Figure 4.18: The three main fingerprint types

any decision support tool [44] or indeed any automated means of individual disease management.

Remark. While this "fingerprint" analogy is helpful, it should be noted that while fingerprints are immutable and unchanging, gait is not and therefore, an individual's Phase plot type is not necessarily fixed over time. In later analysis in chapter 6 we aim to show the clinical utility of regarding phase plots as snapshots of subjects' gait at a particular time and disease state. For this reason it is more appropriate to regard a Phase plots as a **signature** of gait in the context of the subject's current disease state.

Furthermore, the group sizes and longitudinal experiment design allow us to observe any transitions between phase plot types in free-living environments where we can rely on other gait measures to contextualise these transitions similar to the way shown in Table 4.4.

The flow diagram provided in Figure 4.19 shows a proposed method for grouping phase plot types named: oblique wings (OW), parallel wings (PW), oblique lines (OL), and single line (SL), examples of each can be seen in Figure 4.20 for PD and

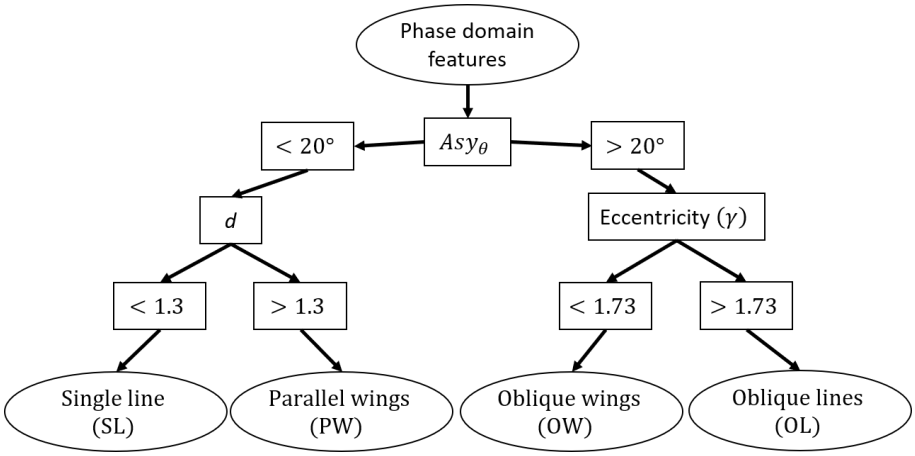

Figure 4.19: Flow diagram for categorising complete Phase plots.

CL. This categorisation is designed manually to reliably distinguish between the four apparent Phase plot Types. The regime can be validated by inspecting the corresponding feature values in the ST domain, see table 4.4. We can see several combinations (pairings) of plot types which represent significant changes in specific SP characteristics. We deduce from table 4.4 that a transition from OL to PW correlates to significant increases in both step length and velocity which reliably measure physical capability [61]. From this we might intuitively hypothesise that transitions to SL (the modal phase plot type) would represent positive changes in ST characteristics. However, our results imply that walking with such a gait pattern as to produce a PW type phase plot as opposed to SL can result in improved gait parameters among PD subjects. This algorithm for categorising Phase plots is not fully objective as it was designed based on subjective observations of many Phase plots across the PD and CL cohorts.

An additional requirement to validate this *fingerprint* interpretation of gait-derived Phase plots is intra-subject consistency i.e. will a participant only produce a single type of phase plot across multiple bouts of walking? We have the data to test this as the experiment protocol of the ICICLE-PD study involved participants

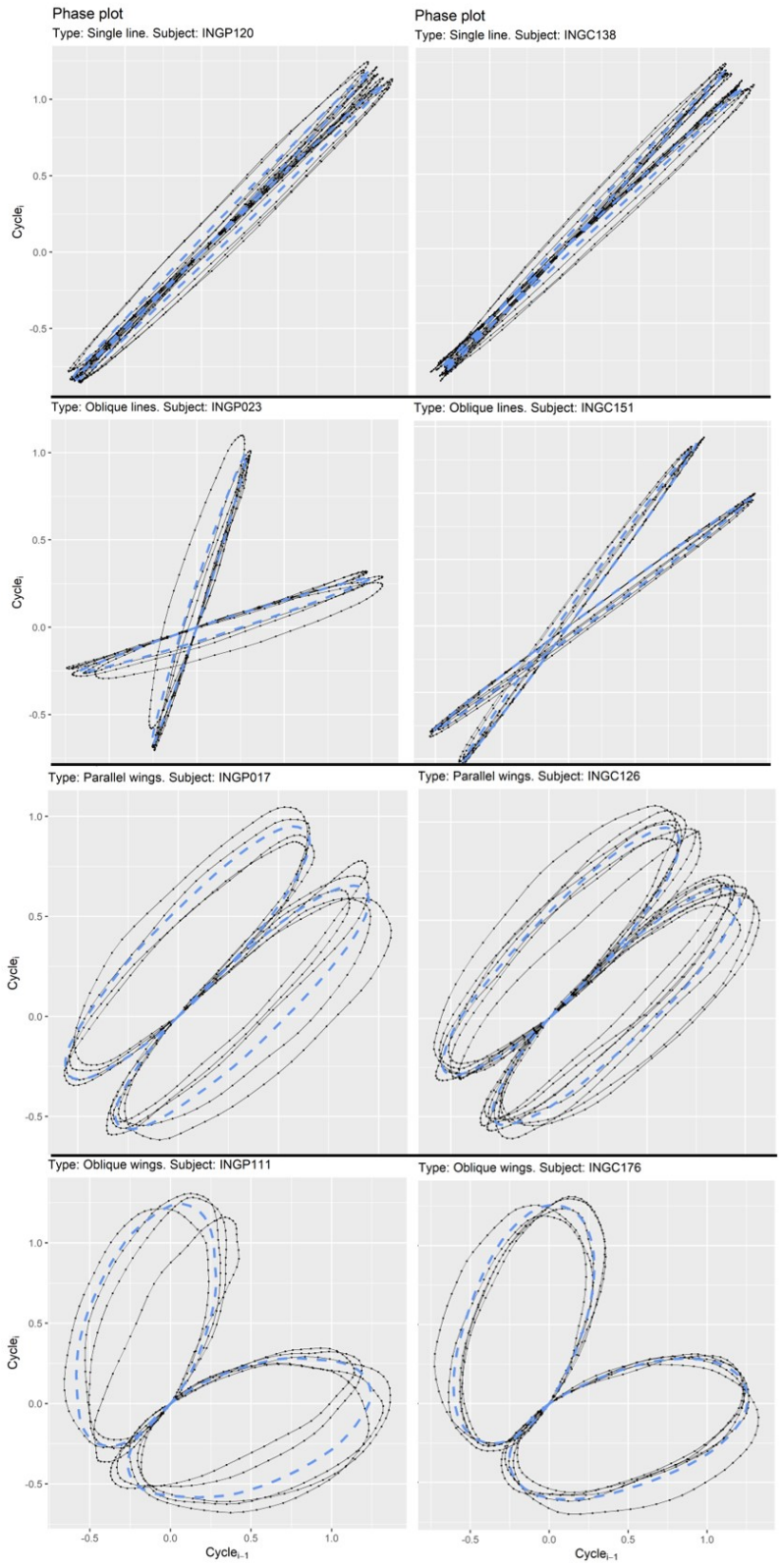

Figure 4.20: Examples of each Phase plot type from PD (left) and Control (Right) subjects. Average orbits shown (blue).

Type / Feature	**SL**	**OL**	**PW**	**OW**	$p^{\dagger}$
Step Length (m)	0.636 ±0.080	0.552 ±0.122	0.721 ±0.026	0.729 ±0.056	SL vs PW **0.021** OL vs PW **0.047**
Step Length Asy (m)	0.028 ±0.023	0.28 ±0.021	0.405 ±0.02	0.597 ±0.01	OL vs OW 0.13 SL vs OW 0.19
Step Time Var (s)	0.18 ±0.005	0.0202 ±0.006	0.0115 ±0.002	0.0149 ±0.004	SL vs PW **0.063** OL vs PW **0.026**
Step Vel (ms^{-2})	0.840 ±0.195	0.974 ±0.249	1.42 ±0.071	1.52 ±0.138	OL vs PW **0.0079** SL vs PW **0.038**
Step Vel Var	0.063 ±0.024	0.074 ±0.022	0.085 ±0.056	0.0701 ±0.017	SL vs OL 0.31 SL vs OW 0.66

Table 4.4: Typical ST domain feature values for PD participants exhibiting each. † Significance was assessed at the $\alpha = 0.05$ level for each transition individually. The top two transistor (most significant) are shown.

walking 3-4 similar bouts on a 10m walkway. Looking at the results shown in table 4.4 it is temping to make inferences on the implications of participants transitioning from one type to another. For example, the exhibiting type PW (parallel wings) appears to be associated with a lower step time variability and greater step velocity (an established biomarker for physical capability). Such a transition is immediately discernible from observing phase plots from the participant in question. Lab-based data alone is unlikely to hold enough variety of gait to reliably test this theory but does serve as a solid and reproducible baseline. The distribution of Phase plot types among the PD and CL cohorts is summarised in table 4.5. The p-values are

	PD	CL	p
n	92	111	-
Asy_θ	18.9 ± 12.1	8.9 ± 11.4	-
γ	0.937 ± 0.0083	0.945 ± 0.011	-
d	0.847 ± 1.16	0.45 ± 0.41	-
	Counts		
SL	48	96	$<$ **0.001**
OL	24	5	$<$ **0.001**
PW	14	8	**0.145**
OW	6	2	0.305

Table 4.5: Predominant Phase plot type by group.

calculated using Fishers' exact test. The distribution of Types among both cohorts' phase plots is also significantly different. CL subject generally produce single line (SL) type plots (86%). The approach illustrated in Figure 4.19 is based on subjective interpretations but is sufficient in distinguishing the four emergent Phase Plot types for the purposes of subsequent analyses. Alternative methods such as those applied in handwritten digit classification may perform well here and should be explored in future analysis that aims to build on this particular avenue of Phase Plot analysis.

It is not uncommon for a given subject in either the PD or control cohort to exhibit more than one Phase plot type distribution at different timepoints. However, there is evidence even given the controlled lab-based environment that participants can be attributed a particular Phase plot type and that they are significantly more likely to reproduce this type at subsequent timepoints. Despite the presence of within-subject variation, the overall distribution of Phase plot types is very consistent across all timepoints in the case of lab-based data (see Figure 4.21). These properties of Phase plot Type will also be analysed in greater detail in chapter 6 to see how we might expect PD Phase plot types to evolve with disease progression (PD group) or with ageing in general (control group). In chapter 5 we will analyse in detail how the added variety of free-living impacts the type of Phase plot

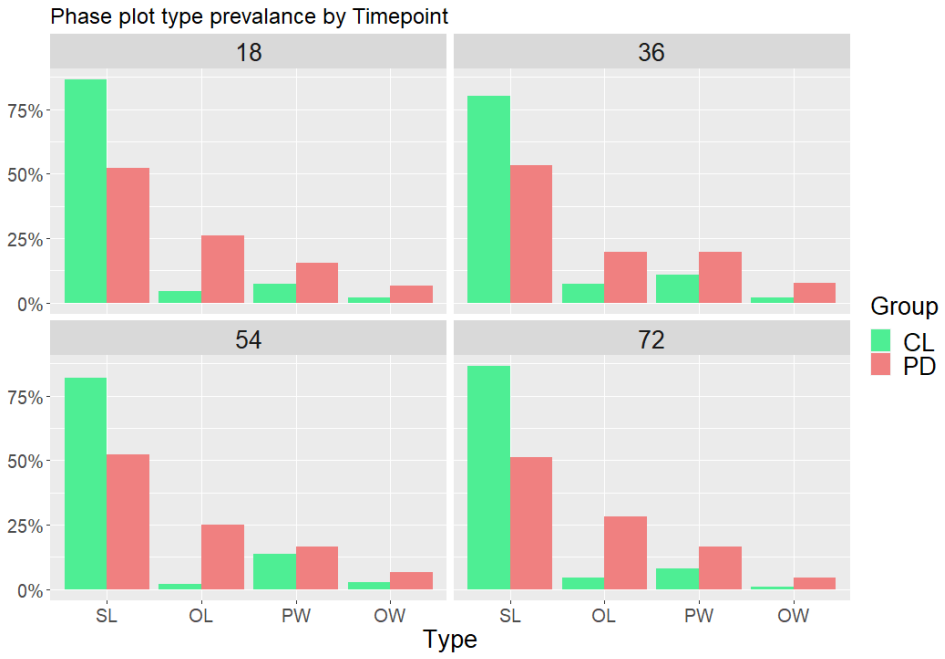

Figure 4.21: Consistent distribution of Phase plot types across timepoints for lab-based gait

produced by participants in both groups and also how increased ADL impacts this classification system for Phase plots.

Type-transitions To validate the fingerprint interpretation of gait there are several properties we aim to demonstrate. One of these is within-subject type-consistency i.e. can we say that each participant predominantly exhibits one specific phase plot type? Let us assume that the overall proportion of each types is fixed for each group. then we define

$$T_{PD} = (p_{SL}, p_{OL}, p_{PW}, p_{OW}) \text{ and } T_{CL} = (c_{SL}, c_{OL}, c_{PW}, c_{OW})$$

as the respective prevalences of each Phase plot type in the PD and CL group with

$$\sum_{i=1}^{4} T_{PD_i} = \sum_{i=1}^{4} T_{CL_i} = 1.$$

These values can be estimated by normalising the values given in 4.5. Let g_{iX} be the probability that subject i within group g exhibits phase plots of type X.

$$\begin{aligned} H_0 &: p_{iX} = g_X \text{ for all } i \text{ and } g = PD \text{ or } CL. \\ H_1 &: p_{iX} = g_{iX} \text{ for } g = PD \text{ or } CL. \end{aligned} \tag{4.3}$$

Say we have a population of size n, four possible Types (states) and four timepoints between which participants may feasibly transition between Phase plot types. A given subject has the prevalence vector $T_g = (g_{SL}, g_{OL}, g_{PW}, g_{OW})$ where g is p or c depending on the subjects group. Given that $\sum T_g = 1$ we can write $g_{OW} = 1 - g_{SL} + g_{OL} + g_{PW}$ to reduce the number of parameters. Under H_0 the probability of this subject exhibiting Type X at timepoint t is g_X. Therefore, the probability of this same subject exhibiting type $Y \neq X$ at time *t+1* is

$$\sum_{T \neq X} g_T = 1 - g_X$$

For each group we have the prevalences $T_g = (g_{SL}, g_{OL}, g_{PW}, g_{OW})$ and if we take these as the initial distribution of types at time t then the probability of a given subject exhibiting a different type at time *t+1* is

$$\tau_g = \sum g_T(1 - g_T).$$

It then follows (under H_0) that the expected number of transitions in a population of size n_g across l_g timepoints is

$$\tau_g n_g l_g$$

	τ_g	E[Tr] under H_0	Actual Tr	p
PD	0.632	175	79	**<0.001**
CL	0.244	81	52	**<0.001**

Table 4.6: Phase plot type transitions for lab-based gait

For the lab-based dataset, we can calculate the corresponding values for the PD and CL groups and this is given in Table 4.6. Under H_0 the number of transitions observed in each group, TR_g is distributed as

$$TR_g \sim Bin(n_g l_g, \tau_g)$$

we can calculate p-values associated with the test detailed in Equation 4.3. From the p-values reported in Table 4.6 we can safely conclude that Phase plot types are not randomly distributed among participants based on a simple group-specific proportion. Rather, there are subject-specific factors which lead to individuals consistently producing the same Phase plot type.

4.3.4 The clinical Utility of Phase Plots: Estimation of the MDS-UPDRS (III) score using Mixed Effects Models

Mixed-effects models, sometimes referred to as mixed models, are statistical models which incorporate both fixed and random effects and are particularly useful in longitudinal studies which include repeated measures. In our dataset random effects may be included at the level of the individual. There are many factors related to lifestyle and other comorbidities which are not observed in our dataset but which likely impact an individual's gait and performance at each visit to the lab. Including a random effect for participant ID allows for this between-subject variation. Features within the Phase and ST domains will be treated as fixed effects along with

other available subject data such as Age, MDS-UPDRS score, and bout index (index of 3-4 bouts completed at each visit).

To assess the clinical utility of Phase plots we can fit several different mixed effects models. There are two dependant variables of interest that we aim to model. Firstly, the group of a subject i.e. can we reliably classify a PD or CL subject? And secondly, the MDS-UPDRS score. To interpret these mixed effects models we will be relying on estimated standard errors of fitted parameters as well as associated effect sizes and confidence intervals. In the case of modelling the disease group we can also rely on the odd-ratios associated with specific feature effects to see how Principal components or individual features impact the estimated probability of belonging to the PD group.

Firstly, we model MDS-UPDRS with the first four principal components of the ST domain all as fixed effects and Phase plot type as a random effect. Secondly, to also allow us to compare relative performance of feature domains, we model MDS-UPDRS with the corresponding principal components of the Phase domain as fixed effects and with Phase plot type as a random effect as before. As part of the random effects, an intercept is estimated for each Phase plot type.

All reported fixed effect sizes found in Table 4.7 are statistically significant based on their respective 95% confidence intervals (reported in appendix Table 8.2) constructed from their estimated standard errors. It is promising to see large proportions of variance being explained by the inclusion of phase plot type in these mixed models, but free-living data analysis is need to fully validate these results as well as the usefulness of classifying phase plot types in this way.

Fixed effect	effect size	Random effect	effect size
	ST domain		
PC1	0.12 (±0.039)	OL	-1.23
PC2	0.15 (±0.061)	OW	2.36
PC3	-0.33 (±0.010)	PW	-1.84
PC4	-0.53 (±0.012)	SL	0.70
	Phase domain		
PC1	-0.14 (±0.042)	OL	-1.02
PC2	0.43 (±0.04)	OW	2.28
PC3	0.43 (±0.07)	PW	-1.88
PC4	0.22 (±0.10)	SL	0.62
	All features		
PC1	0.18 (±0.036)	OL	-1.14
PC2	-0.11 (±0.038)	OW	2.43
PC3	-0.072 (±0.051)	PW	-1.98
PC4	0.24 (±0.063)	SL	0.69

Table 4.7: Fixed effect sizes - Modelling MDS-UPDRS on principal components of Phase and ST domain.

4.3.5 Mixed Effects Logistic Regression

We follow a similar protocol for modelling Group based on lab data- assessing the fit when using ST only followed by Phase only. Here we fit the following logistic mixed effects model:

$$P(PD_i = 1) = S(\mathbf{X_i}\underline{\beta} + \mathbf{Z_i}\underline{b_i} + \underline{\epsilon_i}) \tag{4.4}$$

where S is the sigmoid function (4.2). PD_i is an indicator variable equal to 1 when participant i has a diagnosis of Parkinson's disease and 0 otherwise. $\mathbf{X_i}$ is the design matrix for the fixed effects, the first four principal components in this case, and similarly $\mathbf{Z_i}$ contains the random effects which in this case represents the predominant Phase plot type exhibited by subject i.

When interpreting these models it is important to bear in mind the context of

Accuracy	Specificity	Sensitivity
	ST domain	
69.2%	68.4%	70.5%
	Phase domain	
70.8%	70.3%	69.4%

Table 4.8: Predicting disease group using logistic mixed effects models (4.4)

the gait from which features from both domains are derived. The highly controlled environment within the lab is necessarily masking a huge amount of variation otherwise caused by variation in ADL. These mixed effects models should therefore be treated sceptically, however they are very useful in terms of steering our further analysis of free-living data. Establishing a valid baseline (in this case, lab-based gait features) is important as it allows us to assess the impact of environment on our novel feature domain as well as quantify the so-called white lab coat effect [62] in terms of gait patterns. In later chapters investigating longitudinal trends we will include an effect for timepoint. In general successive timepoints are treated as fixed effects and the elapsed time between timepoints is assumed equal for all participants in the study so it stands to reason that the specific effect of going from one timepoint to the next is approximately equal across all participants. In cases where time is treated effectively as continuous then it cannot be included as a random effect as these must be categorical. In our case, we have very distinct timepoints separated by 18 months. We must acknowledge that not all PD participants have an equally well-managed diseases. Variation in the disease management and medication regime discipline could feasibly result in varying impacts associated with each 18-month interval. This potential justification for timepoint as a random effect is explored more in chapter 6.

4.4 Conclusions

Phase plot analysis satisfies several key requirements for wide-scale deployment and clinical assessment within gait analysis:

- Features of the phase domain are derivable from a single discreetly worn device.
- Very small demand on time and data volume. A very brief bout of steady state ambulation is sufficient to determine an individual's phase plot type - a robust and reproducible signature of their gait. This will be validated further in Chapter 5.
- Results are objective.

The high within-subject consistency of phase plots types means that these features may be used to represent a compact and comprehensive overview (a snapshot) of a person's gait. This leads us to adopt the signature or "fingerprint" interpretation of phase plots to reflect their specificity not just to a given subject, but to the state of their condition (PD in this case) at the time of recording. Strong relationships between features of phase plots and ST features of gait were found. We identified several potential transitions of phase plot types which correspond to significant changes in specific ST characteristics. This helps with interpretation of these novel phase plot features by linking them to well-known traditional gait characteristics.

Significant effect sizes were found for ST domain features in modelling of MDS-UPDRS and promising performance measures were shown when predicting disease group. This domain of traditional features is well-validated in the literature so we should expect this good performance. Phase domain features appear to perform similarly well compared to these traditional features both in terms of modelling MDS-UPDRS, a proxy of disease progression, and detecting the presence of PD itself. Classification performance measures around 70% are very promising given

that all of the gait features so far are derived in a single constrained test environment which is generally understood to mask the disease manifestation in gait. In chapter 6 we will build on this mixed effects modelling to include time point and participant age as effects.

These lab-based analyses shed light on several characteristics of particular features in each domain. Asymmetry and variability features in the ST domain are prone to skew, likely due to lack of variability in lab-based straight line gait and limitations relating to human physiology. Features of the Phase domain were similarly prone to skew and strict bounds but these are often traceable back to the mathematical geometric definition of these features e.g. ellipse eccentricity is necessarily bounded above by 1 due to the definition of an elliptic conic section. Interestingly step time seems relatively similar across PD and controls, at least when compared to other spatio-temporal features. It appears that overall, PD participants' average step lengths are reduced compared to their healthy counter parts. But due to similar reductions in step velocity, the overall step time of PD participants' remains relatively constant

The highly controlled environment associated with this data brings with it several benefits and detriments from an analysis point of view. Firstly, the fact that this data are fully annotated removes the requirement for any gait detection algorithms to identify the time spans in which bouts of gait were occurring. The same walkway being used for all participants removes any variability that would otherwise be introduced by environmental factors such as uneven walking surfaces or adverse weather conditions. However, while 10m is far enough for sufficiently stable gait to be recorded, this upper limit on bout length means we cannot analyse the impact on gait, if any, of prolonged walking or indeed the relationship between gait features and walking duration. The participants' awareness of the highly controlled environ-

ment can itself introduce a bias in the data. There is evidence in the literature to suggest that simply being aware of their being observed can impact their gait [63]. This psychological phenomenon is often referred to as the "white (lab) coat effect". This specific environment-related impact will be quantified in chapter 5 following analysis of real-world accelerometer data of the same subjects.

The reported classification performance associated with both Phase and ST domain features were slightly lower than values reported in a similar study by Rehman et al [41], however they made use of continuous bouts of walking including right-hand turning.

Higher frequency sensors may mitigate the small error on IC (initial contact) estimates which would allow Phase plots to be constructed on gait cycles segmented by GEs (gait events). This would potentially improve interpretability as each phase plot orbit would then represent a gait cycle as defined in the model shown in Figure 4.1.

Our exploratory analysis of ST and Phase feature densities highlighted some interesting and notable characteristic distributions potentially due to constraints of physiological factors or of their respective mathematical definitions. It is unclear from these lab-based analyses to what degree these distributions are also characteristic of the recording environment. This will be investigated as part of the assessment of the impact of environment on gait characteristics in Chapter 5.

For lab-based gait we have shown that:

- These novel phase domain features can distinguish between PD and CL patients based solely on the accelerometry with performance comparable to that of traditional features.

- Phase plots are consistent and reproducible within subjects from both PD and CL groups. This supports their use as a reliable signature of PD subjects' gait

and hence disease state.

- In general, a combination of ST and Phase features slightly outperforms either domain alone. The improvement is not very large however, so this relative performance will also be assessed in real world setting.

- Analysis of multicollinearity within and between feature domains supported the hypothesis that the features of this novel domain do indeed carry gait-related information not explained by ST features alone.

We have successfully demonstrated the effectiveness and practicality of the novel methodology and feature domain introduced in chapter 2 through its application to PD gait accelerometry. Lab-based data may represent an unrealistic and non-representative subset of an individual's real world gait, however these analyses are an excellent proof of concept for Phase Plots and the new Phase domain of features showing that they can match and potentially exceed the performance of ST gait characteristics in detecting PD. The results of this chapter form a solid foundation and justification for extending to real-world and longitudinal analysis.

Chapter 5

Real World Gait Analysis

5.1 Introduction

Real-world gait monitoring and analysis is superior to lab-based and scripted tasks in that the gait data are representative of individuals' ADL rather than their performance of a single constrained task [64–67, 26, 1, 2, 68]. There are, however, significant challenges and drawbacks associated with real-world monitoring. In particular, contextual information was not present as data were only collected with accelerometers. A reliable gait detection algorithm is required. Patterns of gait may differ greatly between subjects, so extended periods of recording are required to ensure sufficient gait is present. The protocol, detailed in chapter 3, included seven-day recording sessions throughout which wearable accelerometers continuously recorded triaxial acceleration at 100Hz.

5.1.1 Challenges

When working with the real-world portion of the ICICLE dataset we encounter a different source of missingness due to the unscripted nature of real-world walking.

Whichever way we segment the seven days of data we have no guarantee of there being valid gait in any given time span. Even if a participant has perfect attendance and is present at all timepoints, there are many unknowns which may impact their activity levels and hence the amount of gait accelerometry available for them in each day/hour etc. It is understood that PD patients have reduced physical capability and mobility, and seeing as disease group is an observed variable, we can regard the mechanism of this missingness as at least partially MNAR. To address this missingness we can take advantage of the recording protocol which involved seven full days of continuous monitoring. Moreover, when discretizing daily gait characteristics by hour, we can aggregate features across the seven days. This increases the validity of hourly measures by increasing the expected total duration of gait occurring in each hour. We will also quantify activity levels and factor these into to our analyses to investigate the relationship between gait characteristics and the total duration of gait completed per hour. Where we conduct complete-case analysis on real world data (after aggregating seven days) we must interpret results in the context of parallel analysis on activity levels. Lab-based gait and the associated gait features are a measure of capacity of the subject i.e., the highly controlled uniform walking environment provides an ideal, if unrealistic, setting to record an individual's healthy gait where any PD symptoms may be partially masked. This contrasts with real world data which is recorded continuously with no scripted activities. For this reason, rather than a measure of capacity, real world gait data is regarded as a more valid measure of performance based on ADL [23]. Given this distinction between lab-based and real-world, we must be cautious not to include in our analyses any assumptions of equivalence between the gait associated to each data sources.

5.2 Aims

5.2.1 Exploratory

An initial exploratory analysis will be conducted and compared against that of the lab-based gait characteristics. It may not be immediately obvious what the source of any differences are e.g., a more relaxed environment, increased variety of ADL, etc. This initial analysis will serve to highlight any potential differences and similarities which warrant further scrutiny and analysis. Both similarities and differences between lab and real-world gait characteristics will be interesting subjects of analysis. We will also see what real-world phase plots look like and provide a subjective interpretation at this exploratory stage.

Many ST and Phase domain features have recognisable and characteristic distributions when derived from lab-based data. We will use the real-world derived gait characteristics to compare and contrast with their corresponding distributions from real world gait. This will shed light on whether these distributions are the result of purely physiological constraints, their mathematical definition, or the controlled circumstances of lab-based gait.

5.2.2 Real World Daily Trends

A major advantage of real-world gait accelerometry is that we are able to analyse daily patterns and trends in gait characteristics as opposed to a short and potentially unrepresentative snapshot of an individual's gait. We will assess how gait characteristics from each feature domain evolve over the course of the day. As previously mentioned, we will make use of the repeated measures in this real-world portion of the experiment design by aggregating seven days of hourly segmented data into one "average" daily pattern. Reliably monitoring and predicting daily trends such as

these is of clinical interest and may be used to inform decision support tools [44]. Any results from analysis of these daily patterns will be interpreted in terms of the associated activity levels.

5.2.3 Signature of Gait in Real World Settings

Phase plots and the associated novel feature domain have now been validated as a reproducible signature of an individual's gait which hold individual information relating to PD patients' gait and physical capability. However, this has been validated only in the case of lab-based data. There are downsides to lab-based gait analysis e.g., we rely on an individual having sufficient availability and mobility to attend appointments, which can introduce bias in the associated datasets, especially when subjects are from elderly or less-mobile demographics which is the case here. For these and other reasons, it is preferable to have methods which are deployable in real world settings. We will investigate the utility of Phase plot features and the validity of this signature of gait in real world scenarios. The increased diversity of ADL in real world settings leads to several questions regarding the novel Phase domain and signature of gait.

- Do subjects have a well-defined phase plot type (see Figure 4.20) throughout their real-world recording? And is it the same as their respective lab-based Phase plot type?
- If so, how much real-world gait is required to discern this type? What is the minimum amount of real-world gait needed to predict an individual's Phase plot type with high certainty? We know 10m walks are sufficient in lab conditions.
- If not, what are the factors determining a phase plot type? e.g., bout length,

activity levels, pathology etc.

- Are Phase plot types distributed among PD and CL subjects in the same proportion as was observed in lab settings (see Table 4.5)?
- Do type-transitions occur at the same rate as in lab-based settings and what, if any, additional clinically relevant information can be extracted from these transitions in a real-world setting?

Each of these questions will be approached separately for PD and CL subjects as we have previously seen that Phase plot features do not manifest themselves similarly across disease groups.

5.2.4 PD and Relationship with Clinical Scales and Disease Status

Like our lab-based analyses we can take MDS-UPDRS scores as a reliable proxy for disease state and progression. We now have a vastly increased volume of data per subject and can answer more specific and nuanced questions regarding the modelling of disease progression by gait characteristics. For example, which features in the ST and Phase domain are best for predicting disease progression and is the performance of these models dependent on time of day? PD patients may be more likely to exhibit off-state gait in the morning before their first medication has taken effect. PD participants in a clinically defined "OFF" state generally do not have their symptoms under control and so gait recording during this state may provide more insight into their current level of disease progression.

5.2.5 Lab versus Real World: The Impact of Environment

We will assess the relative performance of lab and real-world gait characteristics from the ST and Phase domain. Each setting has its benefits and deficits from an experiment design point of view. For example, real world gait is recorded during unscripted ADL and is likely far more representative of an individual's actual daily gait, but it can be difficult to annotate a full dataset and detect all valid gait. In lab-based gait we can reliably classify and segment all gait cycles with a high degree of certainty at the expense of natural variety of bouts. In the case of the novel Phase domain is not immediately clear whether the added variety of ADL in real world gait will improve the performance of phase plots by making them more representative of individuals' gait or if it will significantly reduce their interpretability due to the unknown context during the associated gait recording.

We can quantify the impact of increased variety ADL - by comparing all lab-derived gait characteristics with those from real-world setting. We can also quantify the specific impact of environment by comparing ≈10m Lab walks with short real-world bouts of walking. Although unknown sources of variation will still occur due to unscripted ADL, this will help quantify the size of the "white lab coat effect" in the context of short walking bouts.

5.2.6 Questions

Exploratory

- Which gait characteristics are sensitive to the change in recording setting and how is this reflected in their distributions across PD and CL subjects?
- What, if any, are the main visual differences between phase plots constructed from lab-based gait and those constructed from real-world gait?

Real world

- Is seven days of continuous accelerometry sufficient for a reproducible daily pattern (hourly) of gait characteristics?
- Are intermittent lab-based walking bouts equivalent to real world bouts in terms of disease classification?
- How do real-world bouts of walking relate to clinical scales (e.g. MDS-UPDRS-III) and disease state?
- Can we treat lab-based gait as a subset of an individual's real-world gait or is it fundamentally different?
- Are short real-world bouts similar to the short walking bouts recorded in lab settings and, If so, is this consistent across disease Group and feature domain?
- How do overall activity levels and bout lengths relate to gait characteristics?
- How do the daily patterns of gait characteristics vary between and PD and CL subjects?
- How much real-world gait is required to ascertain an individual's gait signature? If it requires more than a short bout such as those recorded in the lab setting, then this would be an example of lab-data outperforming real world. Unscripted real-world monitoring necessarily result in a large volume of relevant gait data so it will be helpful in future research to know which bouts hold the most clinically relevant information.

5.3 Methods for Real-World Gait Analysis

To allow for valid cross-environment comparisons, we will present similar summary tables of PD vs CL gait characteristics highlighting significant differences, following appropriate Bonferroni corrections. As part of our exploratory analysis of real-world data we will perform a PCA for parallel comparison with Lab-data. It may be the case that significantly different loadings are observed for the Phase domain depending on the environment.

5.3.1 Daily Trends

Statistical parametric mapping (SPM) is used for assessing between-group variations in daily patterns of gait characteristics. In these analyses, "between-group" may be taken to mean disease group (PD and CL) or between any two subsets of Phase plot types (SL, OL, PW, OW). SPM was initially developed for neuroimaging but has more recently appeared in the biomechanics literature [69]. SPM is ideal for region of interest (ROI)-related hypothesis testing because it is valid for arbitrary 1D geometries such as those produced by gait characteristics over the course of a day [70], [71]. One such daily pattern is shown for the secondary Type 1 feature Asy_{Area_m} in Figure 5.1. As well as these smoothed path plots, polar plots are helpful in providing a quick overview of a feature's progression over the course of a day (see Figure 5.2). SPM will be used for identifying ROIs in daily patterns of gait features i.e., times in the day (between 06:00 and 23:00) during which we may expect to see increased discrepancy between PD and CL subjects. This is closely linked to the detection of OFF-state gait which during which a PD subjects' symptoms are not being sufficiently controlled by their medication. SPM was implemented using the open source spm1d code (v.M0.1, www.spm1d.org) in MATLAB® (R2015). Plots such as those shown in Figures 5.1 and 5.2 are produced

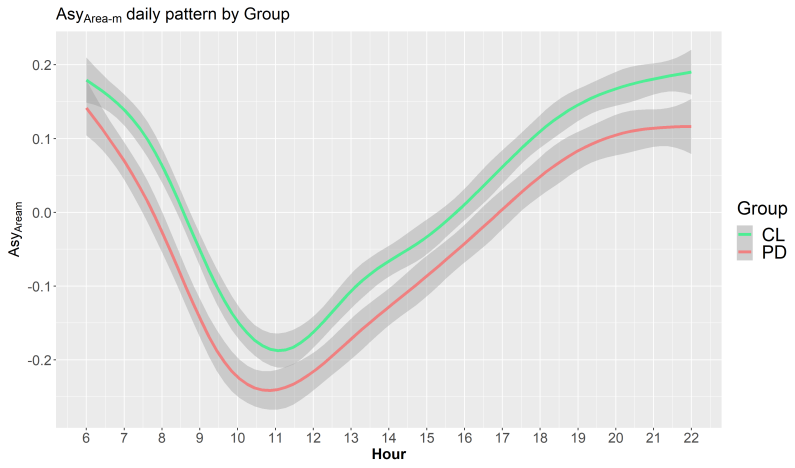

Figure 5.1: Smoothed progression of the Type-1 Secondary feature, Asy_{Area-m} by group.

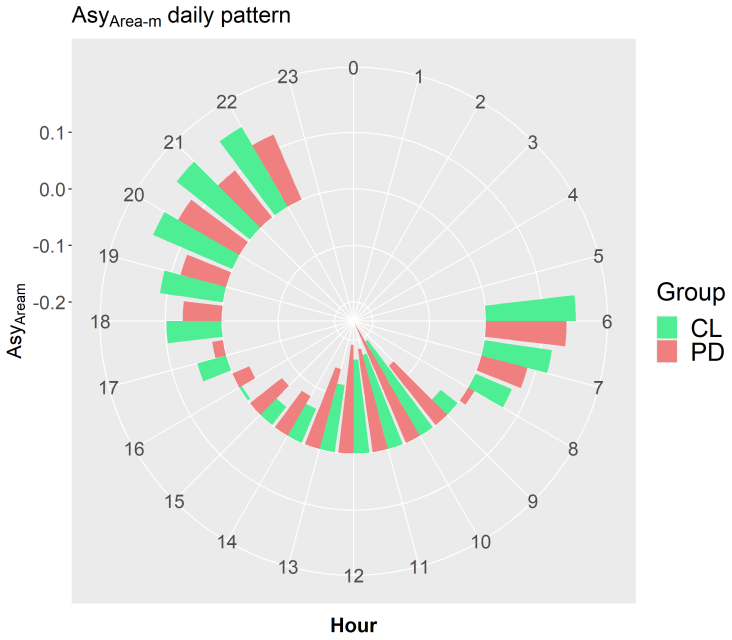

Figure 5.2: Polar plot of Asy_{Area-m} by group.

by aggregating all feature values by hour and group in real-world settings. Polar plots in particular can be helpful in depicting daily patterns.

In the case of 1D data, which is what we have when regarding gait characteristics over the course of a day, SPM first computes a test statistic continuum (usually the t-statistic) from a set of experimentally measured 1D signals. This step is

similar to 1-dimensional mean and standard deviation continuum computation. The technique then involves conducting statistical inference at a Type I error rate of α which is usually equal to 0.05 but subject to multiple-comparison correction, by calculating the critical test statistic value above which a randomly generated test statistic continua (generated by smooth Gaussian process) would not exceed in (1 - 100α)% of cases. The assumption of Gaussian process is not uncommon in gait-related studies and has been shown to within the relevant literature [72–74]. If the experimentally observed continuum exceeds that critical value the null hypothesis is rejected. This general approach to classical hypothesis testing has been validated extensively in 1D univariate and multivariate data [70]. In the cases where the null hypothesis is rejected, this methodology is very intuitive in identifying the time frames associated with the test statistic exceeding the critical value.

Functional Principal components analysis (FPCA). PCA was used in 4 and applied to each feature domain to reduce the number of features used and hence simplify the related models. In this chapter looking at real-world gait analysis we will, again, explore the utility of PCA in dimension reduction but will also expand to use Function Principal Components Analysis (FPCA). FPCA is a statistical technique used for identifying and investigating the main modes of variation in waveforms (see Figure 5.3 for an example).

There are several reasons we may expect to see daily variation in gait characteristics, for example, morning akinesia (impairment of voluntary movement) is a motor symptom in PD which is attributed to a delayed effectiveness of the subjects' first medication dose of the day. Tabbasco et al [75] estimated that 60% of subjects receiving treatment for PD were exhibiting morning akinesia. When implementing FPCA we will pay close attention to the early morning hours in both PD and CL groups to assess whether there is a morning effect observable in the extracted gait

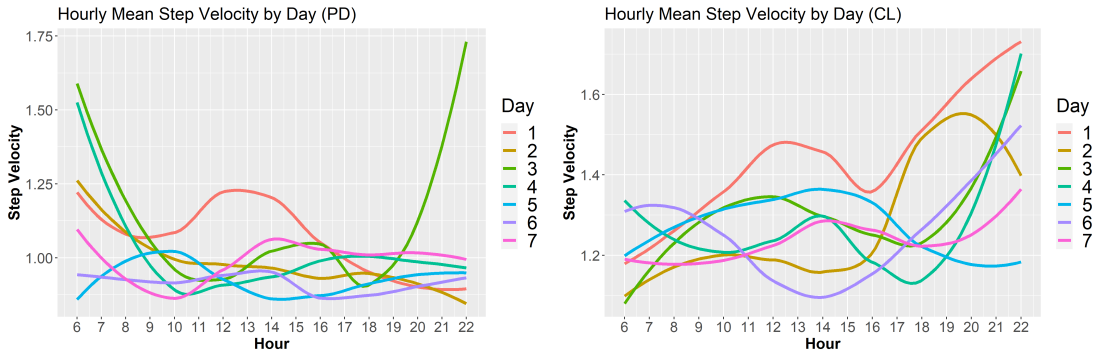

Figure 5.3: Daily Step Velocity trends for a typical PD (left) and CL (right) subject demonstrating significant within subject variation.

characteristics. Any conclusions drawn from FPCA must be scrutinised carefully with regards to activity levels among the PD and CL groups- several features such as step length variability are likely to be skewed in the case of reduced levels of valid gait or variability in bout length. We can see why a method such as FPCA is required, in addition to SPM which looks at overall trends, by plotting the separate daily trends of features for individual subjects. Spaghetti plots are a standard approach for this with examples shown in Figure 5.3.

We will also assess how the main modes of variation from 6am to 10pm differ (if at all) between PD and CL subjects. In addition, the function principal components will also be assessed to see how they differ depending on subject's predominant Phase plot type. We can then quantify the degrees to which an individual's disease group (PD or CL) and Phase plot type (SL, OL, PW, or OW) each impact their daily gait characteristic patterns.

Different methods are available for FPCA depending on the sparsity of the data [76]. While attrition and attendance lead to discrete drop-out in the data (see Chapter 3), daily gait patterns generally present as smooth time series, see Figure 5.3, as long as some gait is recorded each hour. Briefly, FPCA is conducted on daily gait patterns by:

1. For a given feature X e.g., Asy_{γ_m} or Step length variability, let $X(t) = [X_1(t), ..., X_n(t)]$ be the collection of zero-mean curves defined by every available daily time series for X.

2. The first FPC $\phi_1(t)$ is the function which maximises $Var(s_1)$ where $s_1 = (s_{1,1}, ..., s_{1,i})$ and
$$s_{1i} = \int \phi_1(t) X_i(t) \, \mathrm{d}t$$
subject to the constraint $||\phi_1(t)||^2 = \int \phi_1^2(t) \mathrm{d}t = 1$.

3. Similarly for $\phi_2(t)$, we aim to maximise $Var(s_2)$ subject to the constraints:
$$||\phi_2(t)||^2 = \int \phi_2^2(t) \, \mathrm{d}t = 1$$
and
$$\langle \phi_1, \phi_2 \rangle = \int \phi_1(t)\phi_2(t) \, \mathrm{d}t = 0.$$

4. ϕ_1 represents the main mode of variation in the data. This algorithm continues similarly for $i = 1, 2, 3, ...$

5.3.2 Disease Progression and Classification

Mixed effects models (MEMs) are a useful tool for assessing how real-world gait characteristics can model proxy measures for disease progression such as the MDS-UPDRS score referenced in Chapters 3 and 4. MEMs can also be used to assess multicollinearity among gait features which is a likely given the number of gait characteristics extracted (16 Phase and 15 traditional).

Non-linear Mixed effects models (NLMEMs), in this case based on the logistic transformation, will be used for assessing how well real-world gait features can be used to classify PD-CL subjects. As before, the respective activity levels, time of

day etc. provide important context for this classification. If a particular subset of the cohorts were completing very little valid gait then this would potentially reduce the performance of the classification through lack of feature data.

5.3.3 Signature of Gait

We have too few follow-up timepoints (18, 36, 54, and 72-months post diagnosis) to justify chain analysis on participant phase plot type across follow-up dates. However, using real world data we are able to extract each participant's predominant phase plot type on an hourly basis and regard the resulting daily sequences as a discrete-time Markov Chain (DTMC), $(X_n, n \in 1, ..., 17)$ where X_n is one of the four Phase plot types: SL, OL, PW, OW. We have no reason to assume this Markov chain is not strongly connected. There is a directed path between any two states. i.e., the transition probability, $p_{ij} > 0 \; \forall \; i, j \in \{SL, OL, PW, OW\}$

In the first instance we will aim to answer the questions: are the associated transition matrices significantly different from the identity matrix I_4? [77] [78]. And what significance (if any) is contained in the propensity of subjects, from either PD or CL group, to transition between the four Phase plot types? The lab-based analysis in chapter 4 highlighted the clinical relevance of phase plot transitions, where a participant exhibits a different phase plot type to what was observed at previous timepoint(s). The real-world recordings provide a much richer and varied dataset to validate these hypotheses and explore the implications of these transitions. It is very clear that Phase plot types are not distributed similarly across PD and CL subjects, indeed the vast majority of CL subjects predominantly exhibit Single Line (SL) type phase plots. We will examine these distributions of Phase plot types in real world settings and will extend our analysis to see how an individual's Phase plot type may evolve over the course of the day.

5.4 Results

5.4.1 Exploratory Analysis

To remove variation caused by gait initiation or gait termination, the first and last 3 steps in all detected bouts were disregarded prior to calculation of ST and Phase domain features. The vast majority of features in Table 5.1 are highly significant, even following Bonferroni multiple comparisons correction. It is important to bear in mind however, that statistical significance does not necessary translate to better performance in disease classification or modelling of disease progression. For these purposes, we should also pay attention to the effect sizes which in Table 5.1 are expressed as percentage differences (calculated as CL - PD). We can see, for example, that across all timepoints, days, and Phase plot types, having a diagnosis of PD appears to correspond to a 15% reduction in step length and step velocity. Step time, however, is only slightly reduced ($\approx 2\%$). This same phenomenon was found in lab-based analysis in chapter 4, where both step velocity and length both reduced in a manner than preserved a consistent step time (duration).

Figure 5.4 shows the impact of regarding lab-based gait as a subset of real-world gait. The smaller peak visible in the lower left of each plot is a result of gait recording completed in the lab- the bias associated with recording environment is clear. Upon visual inspection, the empirical densities of the ST and Phase domain features in real world settings are noticeably different to their corresponding densities derived from lab gait data (see Figure 5.5). These differences, however, are not consistent across features. For example, ST features relating to variability of gait have much greater spread, likely a result of increased ADL compared to uniform scripted walking in the lab.

This impact of environment is investigated fully in section 5.4.7 but for now it

Feature	CL	PD	Mean difference, %	p
Phase Domain				
		Primary features		
Area	0.35082	0.28982	-17.39	**<0.01**
γ	0.94103	0.93182	-0.9785	**<0.01**
Asy_{θ}	6.837	8.8683	29.71	**<0.01**
Asy_{Area}	12.758	9.1264	-28.47	**<0.01**
GoF	14.641	14.479	-1.107	0.309
SD_{r_1}	0.10571	0.069374	-34.37	**<0.01**
SD_{r_2}	0.46739	0.33822	-27.64	**<0.01**
		Secondary features		
Asy_{γ_m}	0.042078	0.065419	55.47	**<0.01**
Asy_{γ_M}	0.055168	0.061321	11.15	**<0.01**
Asy_{θ_m}	9.8124	11.579	18	**<0.01**
Asy_{θ_M}	6.8344	7.3897	8.125	**<0.01**
Asy_{Area_m}	36.495	35.11	-3.795	0.301
Asy_{Area_M}	34.59	30.866	-10.76	0.0301
GoF_m	68.646	68.761	0.1679	0.723
GoF_M	123.56	107.33	-13.13	**0.005**
SD_{GoF}	35.938	35.198	-2.058	0.349
Spatio-temporal Domain				
		Mean characteristics		
Step time	0.75784	0.746	-1.562	**<0.01**
Stance time	0.90952	0.89495	-1.602	**<0.01**
Swing time	0.59941	0.58711	-2.053	**<0.01**
Step length	0.7803	0.66344	-14.98	**<0.01**
Step velocity	1.1842	1.0059	-15.06	**<0.01**
		Variability (var) characteristics		
Step time var	0.49141	0.44873	-8.685	**<0.01**
Stance time var	0.48865	0.45469	-6.95	**<0.01**
Swing time var	0.4527	0.41224	-8.938	**<0.01**
Step length var	0.33839	0.27388	-19.06	**<0.01**
Step velocity var	0.48539	0.40079	-17.43	**<0.01**
		Asymmetry (asy) characteristics		
Step time asy	0.2129	0.19958	-6.258	**<0.01**
Stance time asy	0.20785	0.19801	-4.736	**<0.01**
Swing time asy	0.19983	0.1877	-6.068	**<0.01**
Step length asy	0.11503	0.09794	-14.86	**<0.01**
Step velocity asy	0.18779	0.15418	-17.89	**<0.01**

Table 5.1: Real world feature values (at 18 months post diagnosis) from the spatio-temporal and phase domains.

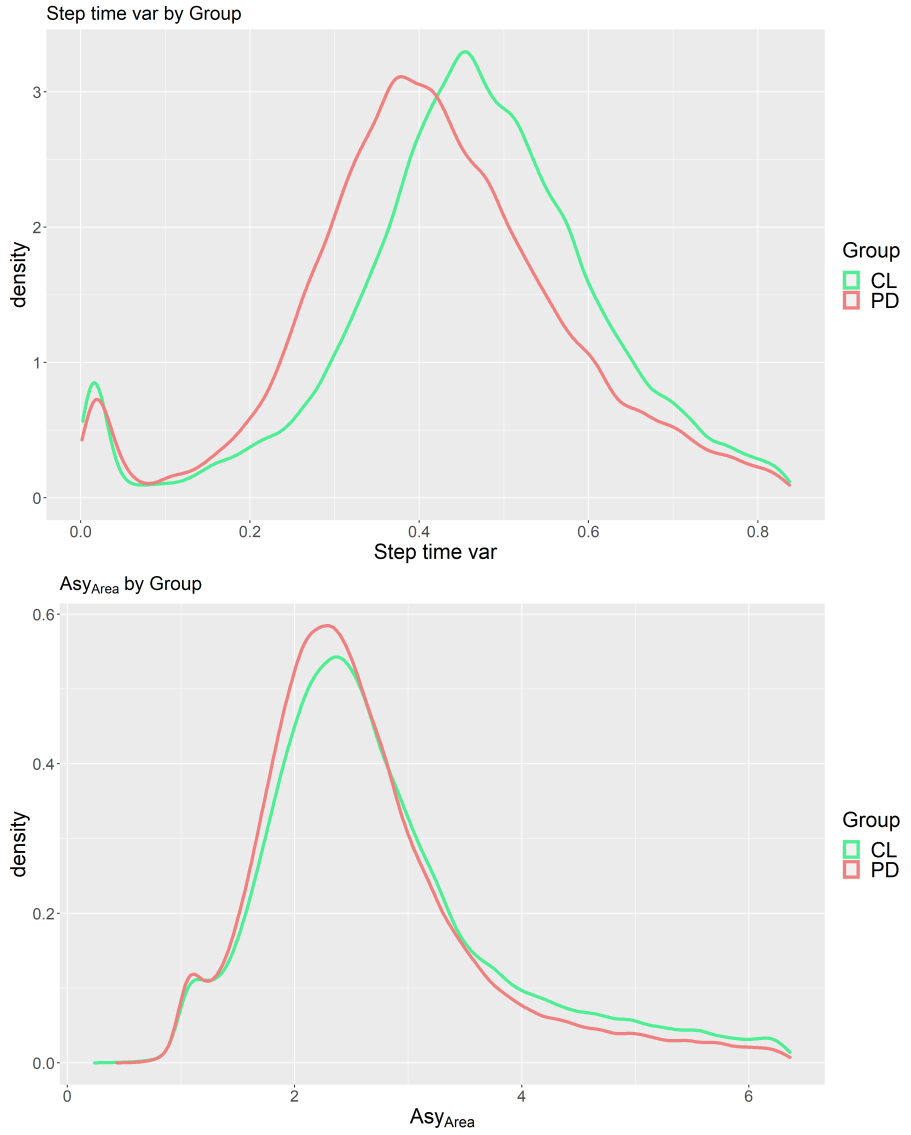

Figure 5.4: Bimodal distributions in the empirical densities of Step time variability (top) and the Phase feature Asy_{Area} (bottom) as a result of combining lab-based and real-world data.

is sufficient to show why we must not treat lab-based and real world as equivalent.

Empirical densities for all features within the Phase and ST domains across environment and disease group can be found in the Appendix (8.1).

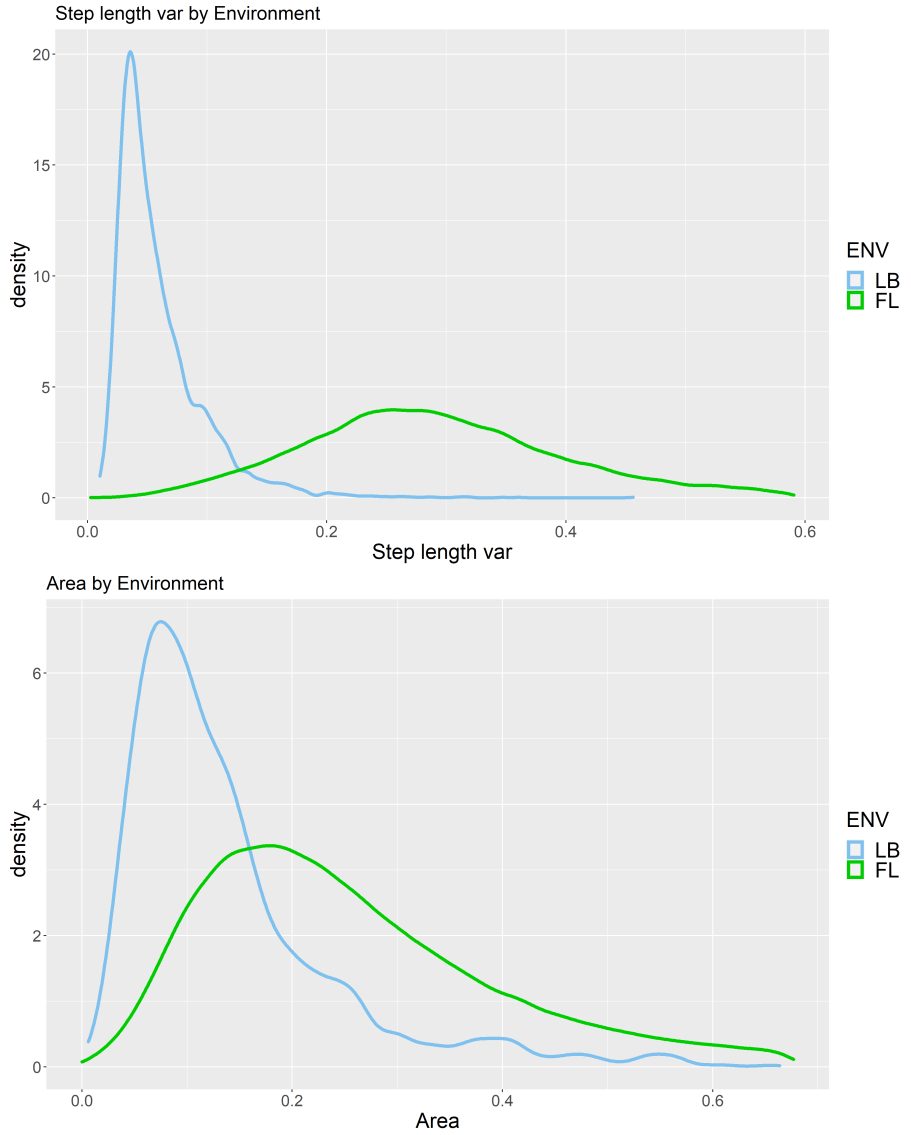

Figure 5.5: An example ST (upper) and Phase domain (lower) feature showing significantly increased spread due to ADL of real-world setting.

5.4.2 Principal Components Analysis

As in chapter 4 we can conduct a Principal Components Analysis (PCA) of the features extracted under real-world conditions as well as on each domain separately.

In both feature domains we observed that, in general compared to lab-based data, the top n PCs accounted for a greater percentage of variance in the feature space. For example, in lab-based settings, 5 PCs of the Phase and ST domains explained

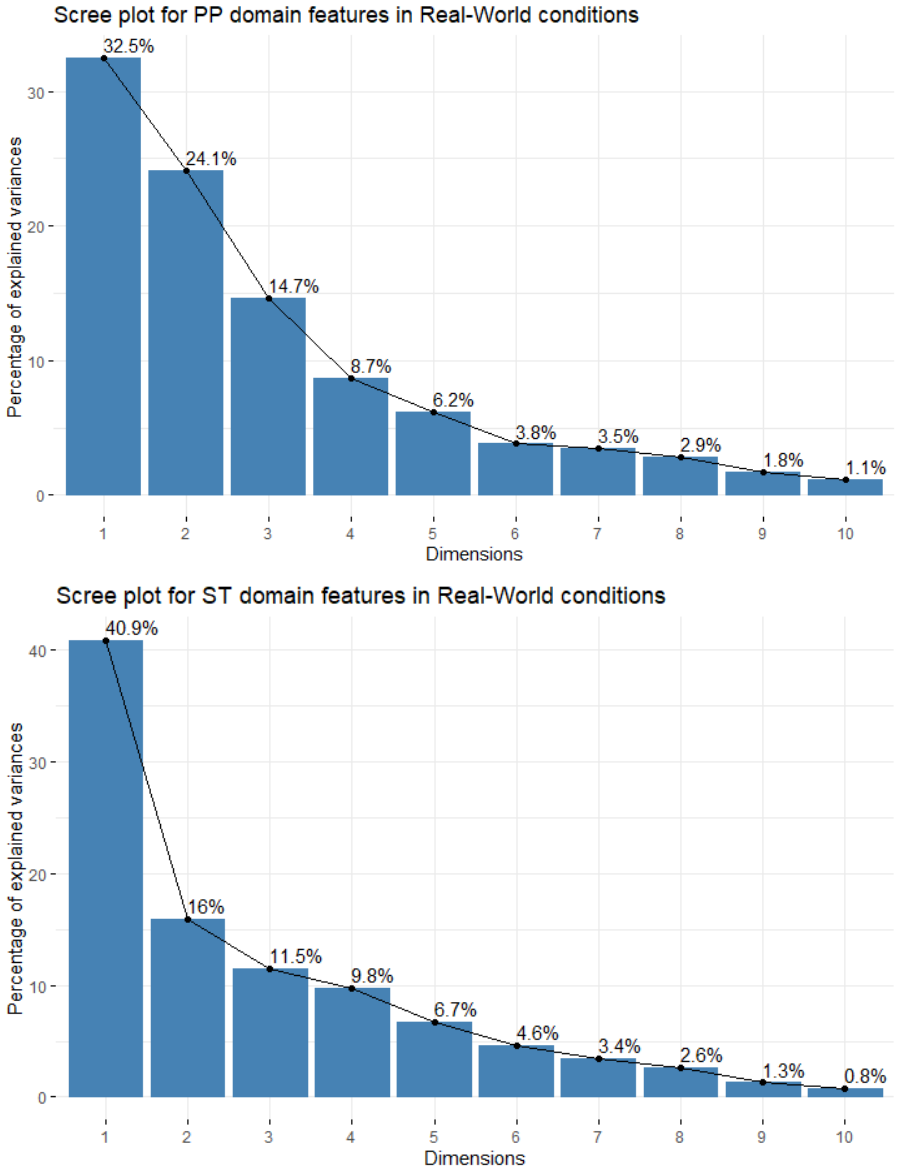

Figure 5.6: Scree plots showing the variance accounted for by each of the first 10 Principal Components (PCs) with each feature domain.

62% and 79% of their respective variances. PCA in real-world settings yielded 86% and 84.9% for Phase and ST domains respectively (see Figure 5.6). To find an explanation for this increase in explained variance we can look at the weightings, or *loadings*, of each PC to assess the relative importance of the domain's constituent features. We can visualise the top 5 PCs of the ST domain by plotting their loadings

for each feature (see Figure 5.7 for Real-world loadings). From this we can see that all five of the PCs shown include a noticeable peak in their loadings for a feature related to either asymmetry or variation e.g., PC1 and PC2 both largely depend on step length asymmetry. The added variety of ADL in real-world recording appears to be highlighting gait abnormalities in terms of asymmetries. As in Chapter 4, the first four PCs of each feature domain will be assessed via their performance as part of Mixed Effects Models.

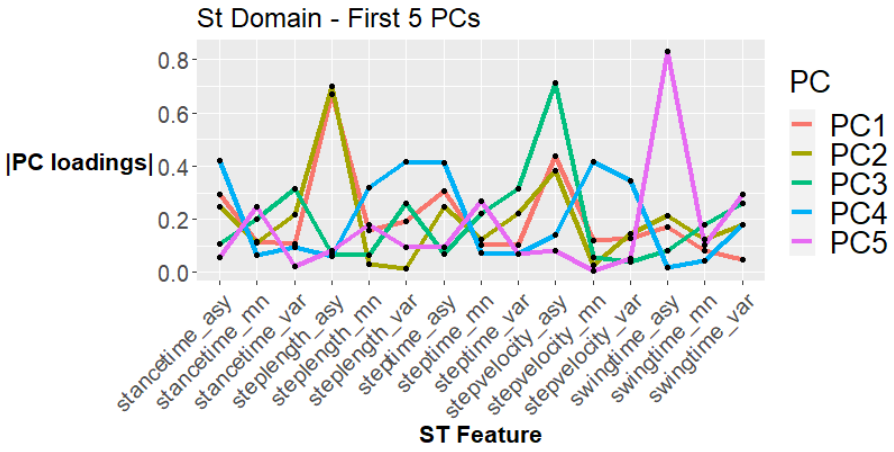

Figure 5.7: Feature PCA loadings for the Spatio-temporal domain.

5.4.3 Activity Levels

Both PD and CL exhibit similar activity levels in terms of absolute quantity of gait per hour and both have a modal value of about 1 minute 44 seconds. This is right skewed towards greater values in both groups and it is more clinically relevant to report on mean activity levels. Both groups spent about 12% of each day performing a walking activity. While activity levels are useful for contextualising the results of analysis and scrutinising their validity, Figure 5.8 is taken from data aggregated over all timepoints and days so does not communicate other sources of variability, for example, between different phase plot types.

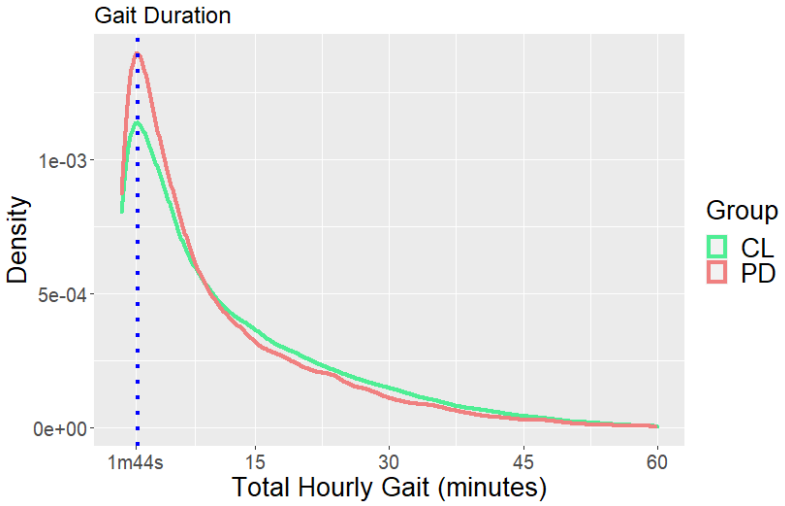

Figure 5.8: The distribution of hourly gait duration recorded under real world conditions

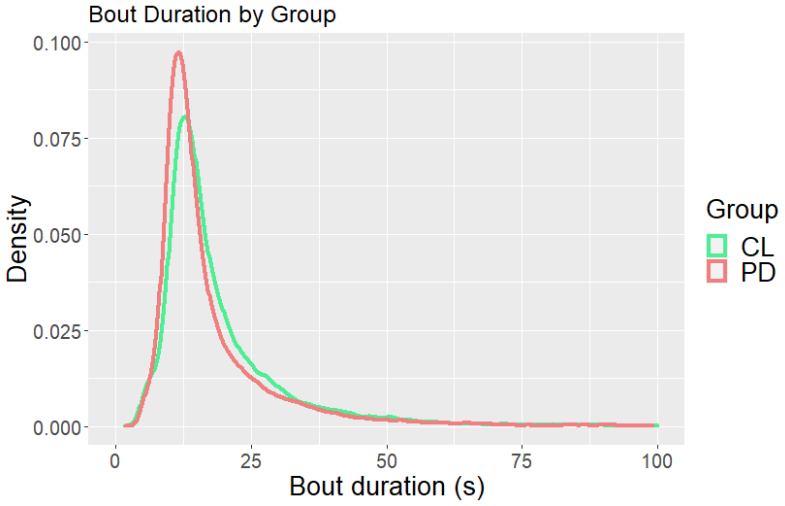

Figure 5.9: Distribution of bout durations across all subjects by disease Group

Figure 5.8 and 5.9 show macro level gait features which are assessed in more detail by Del Din et al [1].

In general, PD subjects carried out $\approx$ 14% more bouts than their age-matched control counterparts, however, these PD bouts where on average 12% shorter in duration than those of the control group (see Figure 5.9). This resulted in a relatively comparable average gait duration overall. This difference in overall gait duration

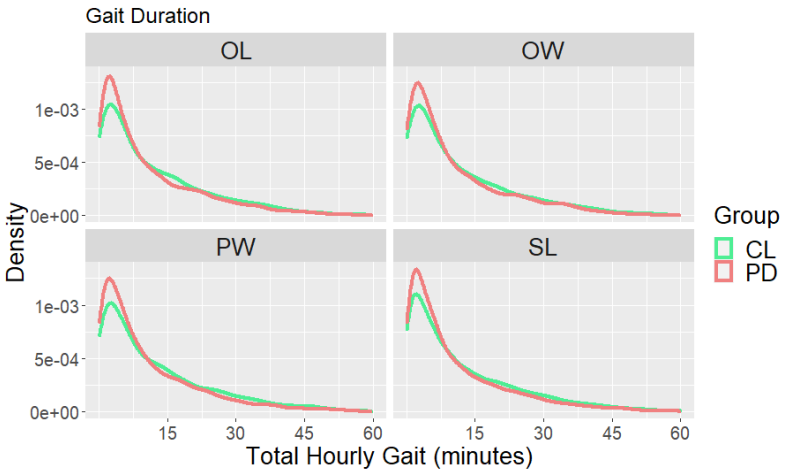

Figure 5.10: Hourly activity levels by Phase plot Type - showing consistent distribution across types.

is consistent across the course of the day but is most pronounced around 10:00 to 13:00 with percentage difference reducing somewhat towards the late afternoon (see Figure 5.11). The overall distribution shown for activity levels (assessed by total hourly gait) in Figure 5.11 is similar to the distribution of bout lengths (an alternate means of assessing activity) presented by Del Din et [1].

This approach to assessing the pattern or distribution of (bouts of) gait is found in the literature and is relevant to studies concerning the fractal properties of gait [79]. Other measures are available such as the α measure which which describes the distribution of bout lengths [80, 81]. Activity level was distributed similarly across all Phase plot Types (see Figure 5.10).

To investigate how traditional and Phase domain features are related to activity levels, the 20% quantiles of hourly gait duration where calculated (see Figure 5.12) find 5 sub-intervals of an hour each of which correspond to approximately equal hourly activity levels. The resulting intervals (expressed in seconds) are: (0-126), (127-313), (314, 620), (620-1188), and (1189 - 3600). Interestingly, this means that approximately equal number of hours comprise over 20 minutes of gait (fourth in-

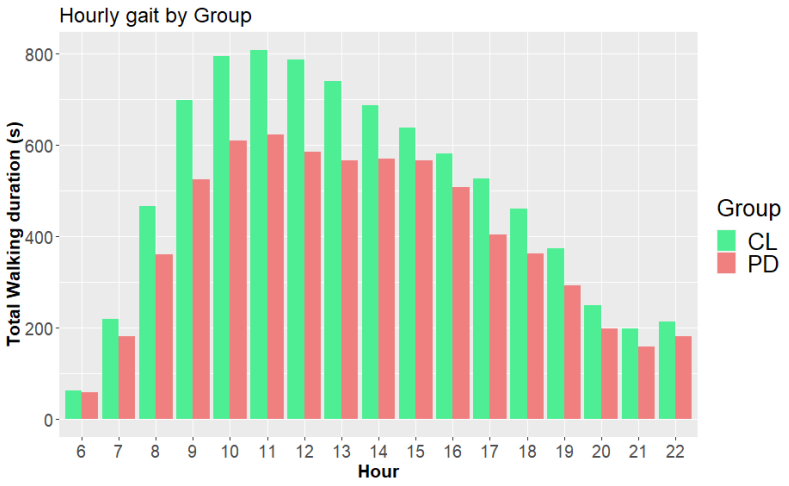

Figure 5.11: Mean hourly activity levels.

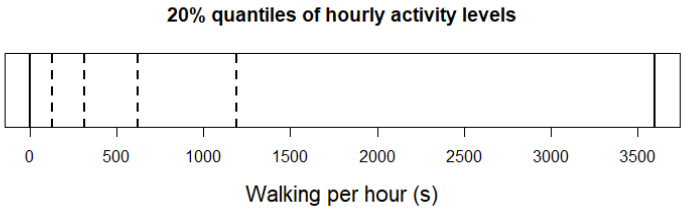

Figure 5.12

terval) as comprise under 2 minutes (first interval). This is not too surprising given the heavily right-skewed distribution shown in Figure 5.8. These quantiles were averaged across all subjects (PD and Control).

This discretisation of activity levels provides a clear framework for assessing the relationship (if any) between time spent walking and feature values. An impact of environment is clear to see in Figure 5.13 however, the contribution of each activity quantile is not constant (see Figure 5.14), indeed higher levels of activity appear to be associated with a reduced asymmetry in step velocity. In addition, in Figure 5.15 we can see a consistent location shift associated with disease group. We employ two-way Analysis of Variance (ANOVA) to quantify and substantiate the impact of activity on these features and will include an interaction term for disease Group.

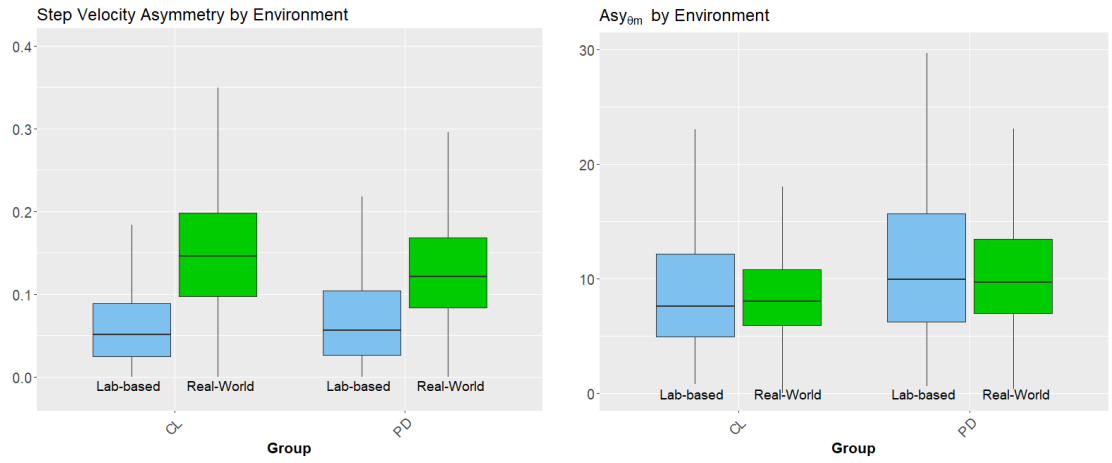

Figure 5.13: Two features (one Spatio-temporal and one Phase domain) demonstrating different apparent impacts of environment.

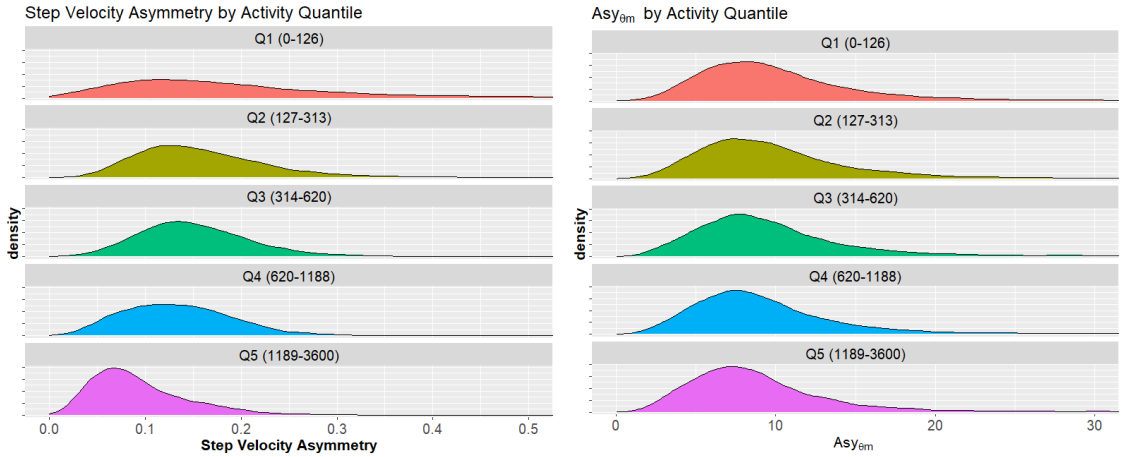

Figure 5.14: Two features (as in Figure 5.13), split by activity quantiles defined in 5.12.

This will allow us to disentangle the respective impacts of activity and PD. Boxplots for all features split by environment and group can be found in the Appendix (8.1).

All features from the ST domain are highly significant with respect to both Activity Quantile and Group and also yielded significant interaction terms. The associated effect sizes are particularly large for asymmetry-related features (see Table 5.2). The majority of Phase domain features show significant differences across activity quantiles, however very few exhibit a significant *Activity:Group* interaction.

Feature	Activity	Group (PD)	Activity:Group
Phase Domain			
	Primary features		
Area	-	-17.6 %	0.084
γ	2.6%	-1.0%	0.74
Asy_{θ}	-16.2%	29.6%	0.124
Asy_{Area}	-	-28.0%	0.532
GoF	-	-	0.11
SD_{r_1}	-	-33.4	0.257
SD_{r_2}	-10.0%	-28%	0.14
	Secondary features		
Asy_{γ_m}	-26.9%	55.4%	0.075
Asy_{γ_M}	-19.2%	11.2%	0.94
Asy_{θ_m}	-10.97%	18.0%	0.279
Asy_{θ_M}	-9.29%	8.13%	$<$ **0.001**
Asy_{Area_m}	7.57%	-	0.280
Asy_{Area_M}	-	-10.76%	0.193
GoF_m	8.70%	0.16%	**0.044**
GoF_M	16.03%	-13.13%	**0.0024**
Spatio-temporal Domain			
	Mean characteristics		
Step time	-3.54%	-1.56%	$<$ **0.001**
Stance time	-2.82%	-1.60%	$<$ **0.001**
Swing time	-3.49%	-2.05%	$<$ **0.001**
Step length	-9.87%	-14.9%	$<$ **0.001**
Step velocity	-5.44%	-15.1%	$<$ **0.001**
	Variability (var) characteristics		
Step time var	12.5%	-8.69%	$<$ **0.001**
Stance time var	13.5%	-6.95%	$<$ **0.001**
Swing time var	21.4%	-8.94%	$<$ **0.001**
Step length var	-11.49%	-19.1%	$<$ **0.001**
Step velocity var	-11.4%	-17.4%	$<$ **0.001**
	Asymmetry (asy) characteristics		
Step time asy	-43.3%	-6.26%	$<$ **0.001**
Stance time asy	-42.7%	-4.74%	$<$ **0.001**
Swing time asy	-39.2%	-6.06%	$<$ **0.001**
Step length asy	-50.9%	-14.86%	$<$ **0.001**
Step velocity asy	-52.7%	-17.89%	$<$ **0.001**

Table 5.2: ANOVA results of Phase and ST domain features. Activity and Group effect sizes are omitted where $p > 0.05$. Effect sizes have been converted to relative percentage differences from quantile 1 (0-216s) to quantile 5 (1189-3600s). For the interaction term, only the associated p-values are reported.

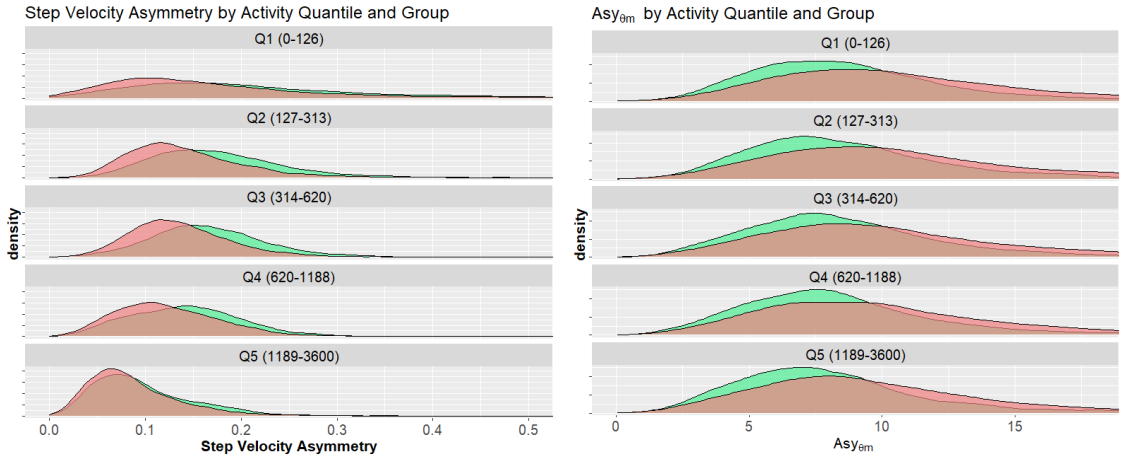

Figure 5.15: Two features (as in Figure 5.13), split by activity quantile (see Figure 5.12) disease group: PD (red) and CL (green).

These interactions are best visualised in interaction plots such as Figure 5.16. The differing gradients between successive activity quantiles (x-axis) are evidence of the interaction between disease group and activity quantile. It is clear from this analysis that the Phase domain and ST domain of features differ greatly in terms of their relation to activity levels. In fact, several Phase domain features (for example: Asy_{Area} and SD_{r1}), appear to be invariant with respect to activity quantiles. On the other hand, the feature Asy_{Area_m} appears to be invariant with respect to disease group once we account for the activity levels, although this is only observed in a single feature. Phase plots' invariance under differing activity levels may be beneficial in the monitoring of PD progression as it seems to imply that valid Phase domain features can be extracted from subjects regardless of their activity levels or physical capability.

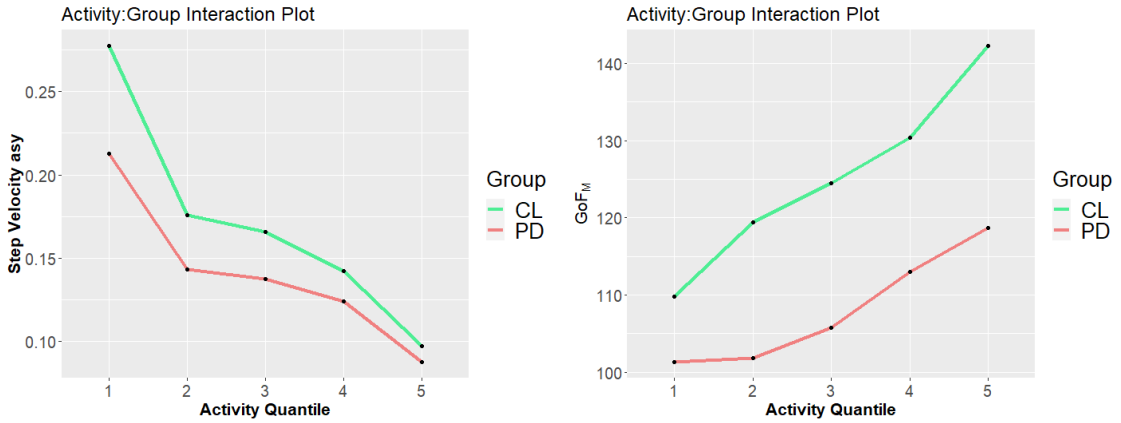

Figure 5.16: GoF_M (Phase domain) and step velocity asymmetry (ST domain) interaction plots.

5.4.4 Daily Trends

Statistical Parametric Mapping

We apply Statistical Parametric Mapping (SPM) to ST and Phase domain features' time series to identify fluctuations in daily gait across PD and CL subjects. SPM offers a robust means of assessing differences in gait features between PD patients and healthy controls on a per hour basis. SPM has been applied in a similar manner to Alzheimer's patients' gait by Buckley et al [82], who proposed that applying SPM in this way may contribute to personalised care by helping identify when impairments occur.

Feature	Threshold cluster intervals
Phase Domain	
	Primary features
Area	06-23 ($p < 0.001$)
γ	06-23 ($p < 0.001$)
Asy_{θ}	06-23 ($p < 0.001$)
Asy_{Area}	06-23 ($p < 0.001$)
GoF	No RoI
SD_{r_1}	08-14 ($p = 0.007$), 15-22 ($p = 0.003$)
SD_{r_2}	No RoI
	Secondary features
Asy_{γ_m}	06-23 ($p < 0.001$)
Asy_{γ_M}	06-23 ($p < 0.001$)
Asy_{θ_m}	06-23 ($p < 0.001$)
Asy_{θ_M}	06-23 ($p < 0.001$)
Asy_{Area_m}	No RoI
Asy_{Area_M}	No RoI
GoF_m	No RoI
GoF_M	No RoI
SD_{GoF}	No RoI
ST Domain	
	Mean characteristics
Step time	06-08 ($p = 0.007$), 21-23 ($p = 0.046$)
Stance time	06-08 ($p = 0.010$), 21-23 ($p = 0.046$)
Swing time	07-09 ($p = 0.015$), 20-21 ($p = 0.05$), 22-23 ($p = 0.046$)
Step length	06-23 ($p < 0.001$)
Step velocity	06-23 ($p < 0.001$)
	Variability (var) characteristics
Step time var	06-10 ($p < 0.001$), 15-23 ($p < 0.001$)
Stance time var	06-10 ($p < 0.001$), 11-12 ($p = 0.036$), 15-23 ($p < 0.001$)
Swing time var	07-13 ($p < 0.001$), 15-23 ($p < 0.001$)
Step length var	06-23 ($p < 0.001$)
Step velocity var	06-23 ($p < 0.001$)
	Asymmetry (asy) characteristics
Step time asy	06-08 ($p = 0.032$), 19-20 ($p = 0.042$), 22-23 ($p = 0.044$)
Stance time asy	08-09 ($p = 0.048$), 22-23 ($p = 0.047$)
Swing time asy	15-16 ($p = 0.047$), 21-22 ($p = 0.05$)
Step length asy	06-08 ($p = 0.006$), 14-17 ($p = 0.05$)
Step velocity asy	06-09 ($p = 0.002$), 12-17 ($p < 0.001$), 19-23 ($p < 0.001$)

Table 5.3: Regions of Interest (RoI) identified by applying SPM to all features for PD and CL groups. All reported regions yielded $p < 0.05$. 06-23 represents the full timeseries.

When conducting SPM on a particular feature basis to compare daily time series for PD and CL subjects there are three possible outcomes:

- Case 1: No regions of interest (RoI) are identified by the analysis for the feature in question (Figure 5.17).
- Case 2: One or more RoIs are identified for the feature (Figure 5.18).
- Case 3: The entire timeseries (all 17 hours) are identified as a single RoI (Figure 5.19).

Table 5.3 shows the intervals (hour-to-hour) of all RoIs for both Phase and ST feature domains. There are several noticeable differences between the feature domains. Firstly, all 15 ST features have at least one RoI associated with them compared to only 10 of the 16 Phase domain features. Secondly, all but one of the Phase domain features exhibit either Case 1 or Case 3 listed above. It is possible for features to appear not significant in terms of SPM analysis but still represent an overall difference between PD and CL. This is because each point in the parametric map, $SPM(t)$ is calculated based on feature data associated with a single hour.

SPM has potential to be an excellent means of extracting value from large real-world datasets such as those resulting from the ICICLE-GAIT study as it takes advantage of 7-days of continuous recording and could be used to identify fluctuations in gait features associated to particular medication in-take times.

Functional Principal Components Analysis

SPM was performed and demonstrates promise for identifying times of day when PD symptoms may not be sufficiently masked by medication i.e., OFF-State gait. However, this methodology works partly by aggregating each subject's 7-days of gait data without considering the underlying modes of variation. For example, there may

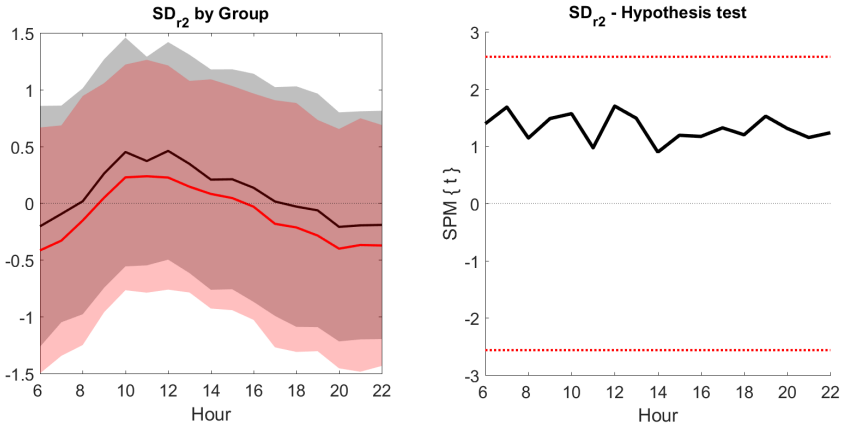

Figure 5.17: The Phase domain feature, SD_{r2} showing no RoIs identified by SPM.

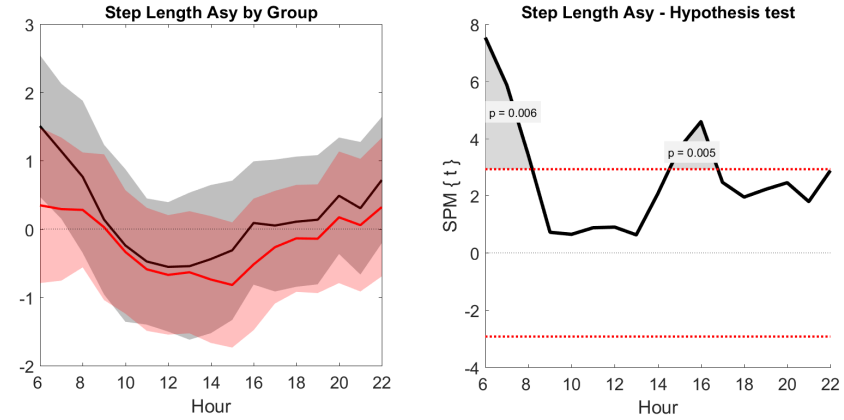

Figure 5.18: The ST feature, Step length asymmetry showing two RoIs identified by SPM.

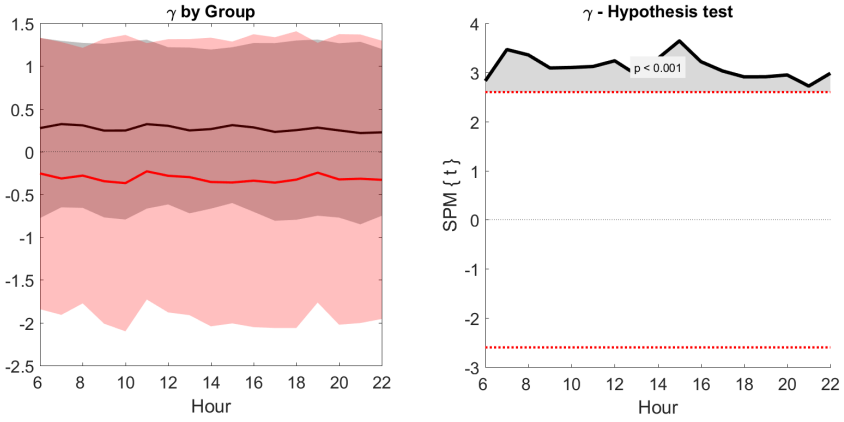

Figure 5.19: The Phase domain feature, γ (ellipse eccentricity) showing a single RoI extending across the full timeseries.

be subsets of the PD or CL cohorts who, for a given feature, exhibit characteristic peaks in their respective daily timeseries (see Figure 5.18 for example) while others remain fairly constant across the day. Functional Principal Components Analysis (FPCA) is an ideal method for identifying these modes of variation.

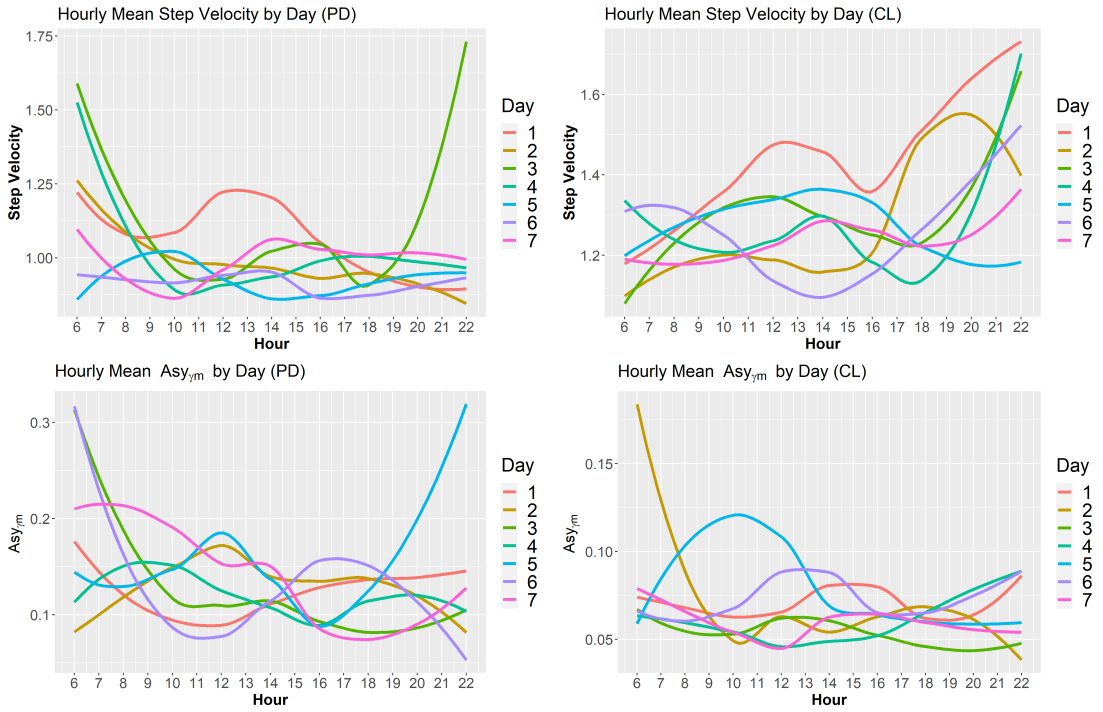

Figure 5.20: Daily Step Velocity trends for a typical PD (left) and CL (right) subject demonstrating significant within subject variation.

Given the variety of ADL present in real-world data, it may be helpful to scrutinise the eigenfunctions associated to each FPC (functional principal component) following FPCA. Together with their respective fractions of explained variance, these can help identify any recurring modes of variation or daily gait patterns within the PD and CL groups. FPCs extracted for each of the seven days of the real-world recording period are shown in Figure 5.20 for Asy_{γ_m} and step velocity. The first eigenfunction (that is the eigenfunction associated with the first fPC) represents the main mode of variation in the daily patterns of the feature in question. The first Eigenfunction for the majority of features is a relatively flat timeseries with no obvious trend compared to subsequent FPCs.

For almost all features of both domains, the main fPC exhibiting a relatively flat daily signal with a slight trend if any and with little difference between PD and CL participants. Subsequent fPCs showed more feature-specific characteristic waveforms with some features showing clear PD-CL divergence. However, these are not

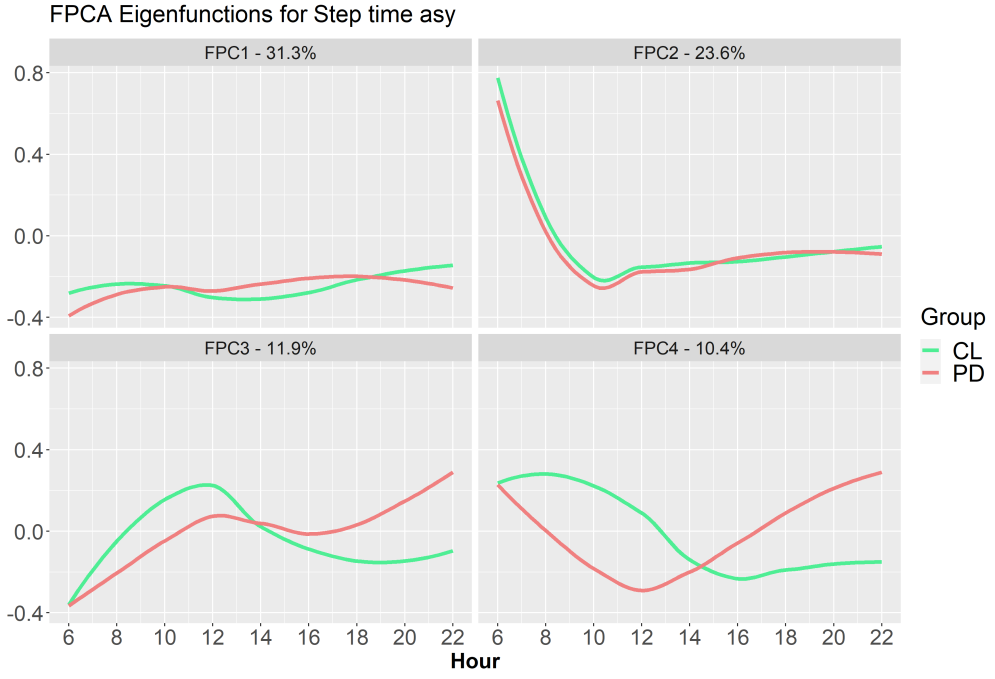

Figure 5.21: Top four FPCs for Step time asymmetry by group.

Figure 5.22: Top four FPCs for Step length asymmetry by group.

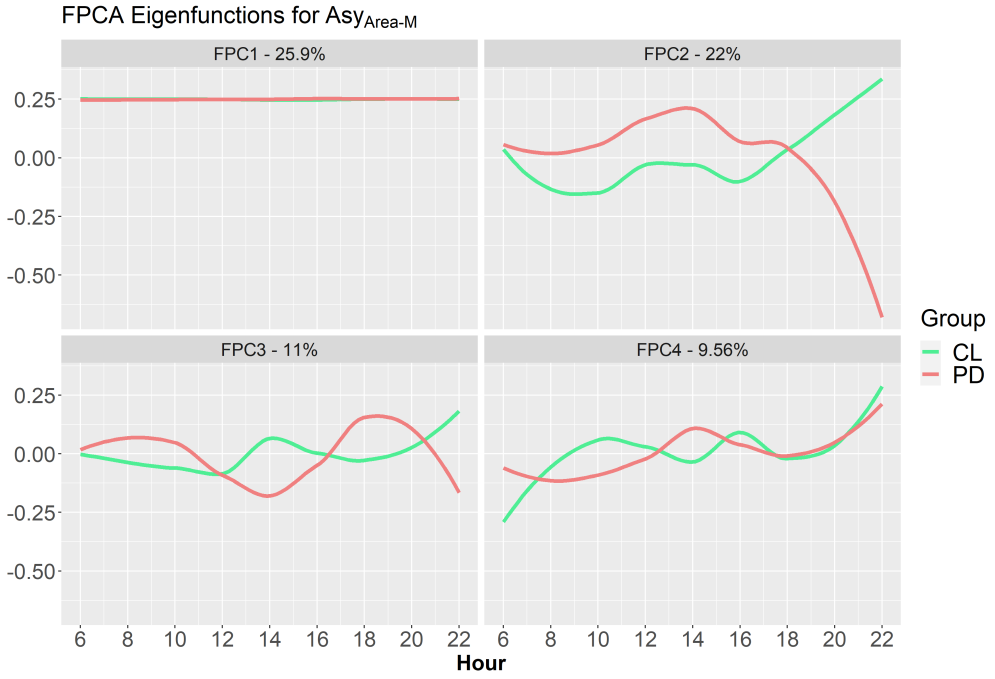

Figure 5.23: Top four FPCs for Asy_{AreaM} by group.

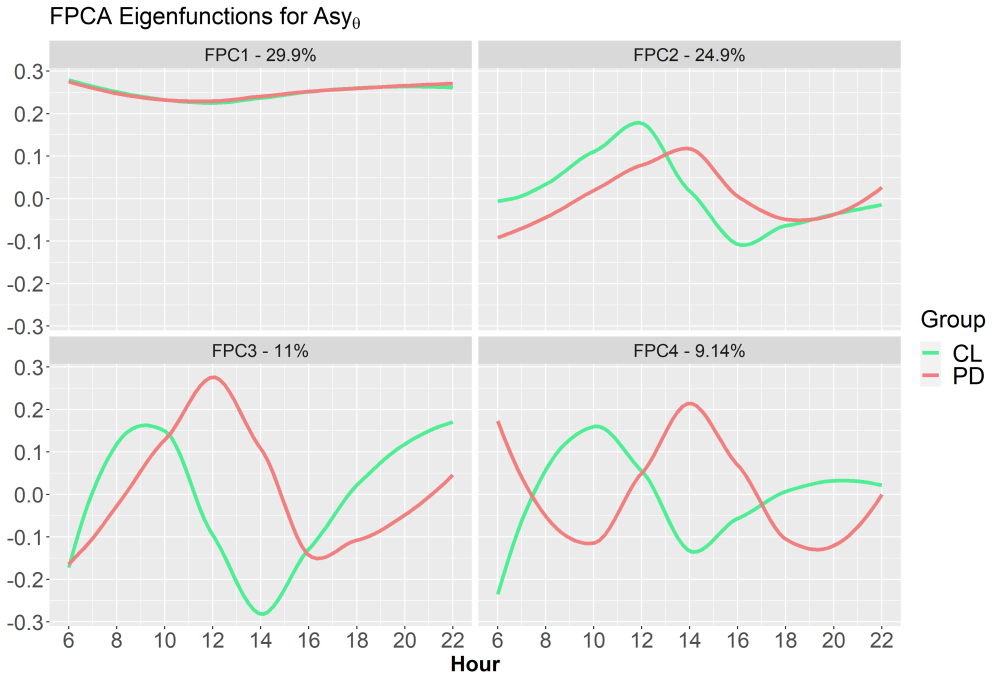

Figure 5.24: Top four FPCs for Asy_θ by group.

interpreted in detail due to the low fraction of explained variance associated with the second, third and fourth fPC etc. Given the low variance associated with these fPCs there is a risk of over-analysing and drawing invalid conclusion. In summary, there is generally commonality in the daily patterns of features for both disease groups' main fPC. Differences only appearing in the subsequent fPCs associated with much smaller fractions of variance.

5.4.5 Signature of Gait in Real-world Settings

The Phase plots shown in Figure 5.25 are taken from bouts of the same participants as those shown in the similar Figure 4.20 from lab-based gait. The real-world bouts corresponding to these Phase plots comprised of approximately 25 gait cycles and where not taken from any particular time of day or timepoint. The most obvious difference appears to be the much denser clusters of ellipses in each plotted Phase plot. While the overall Phase plot types are still easily distinguishable, the added

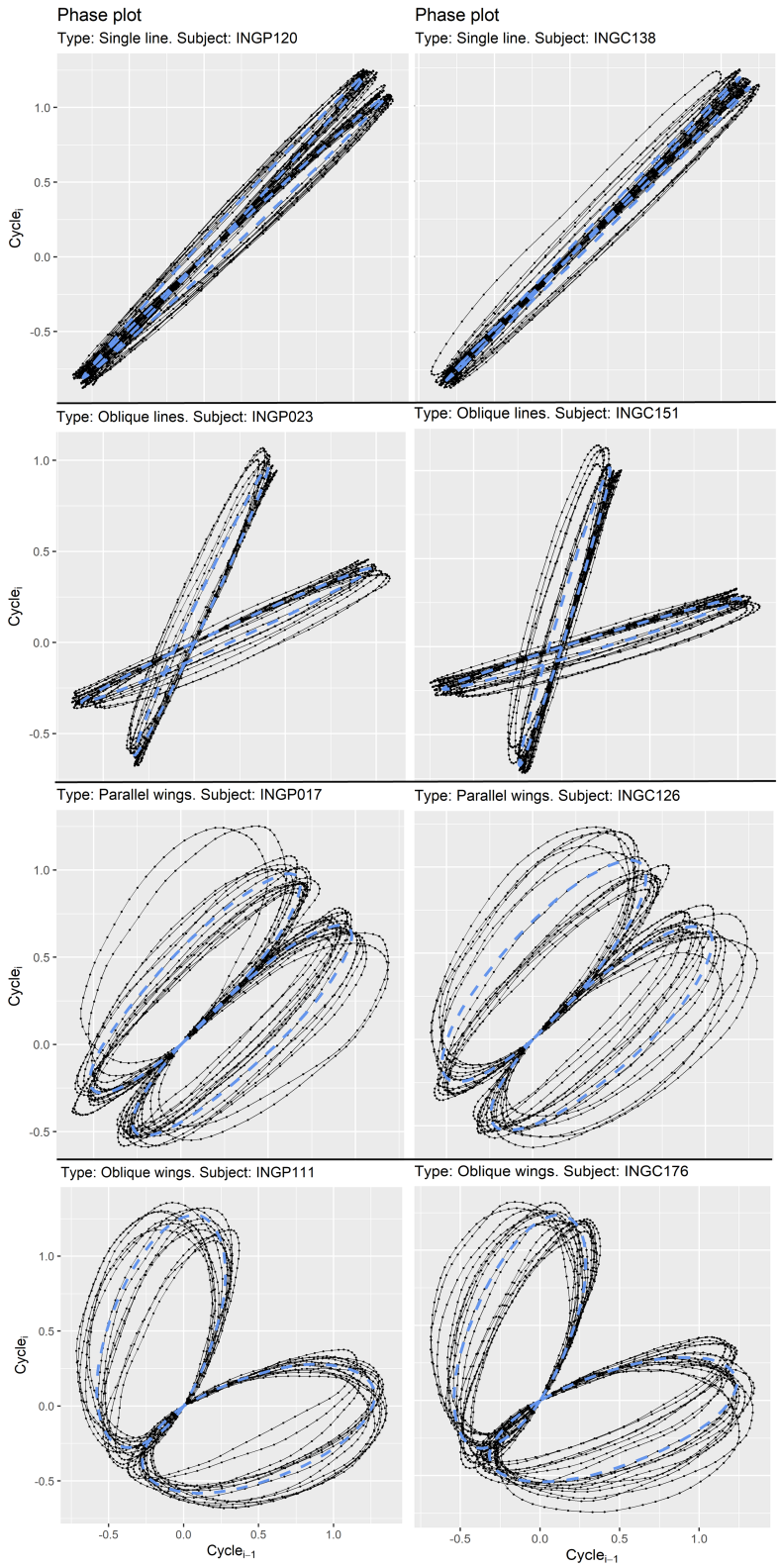

Figure 5.25: Examples of each Phase plot type from PD (left) and Control (Right) subjects in real world gait. Average orbits shown (blue).

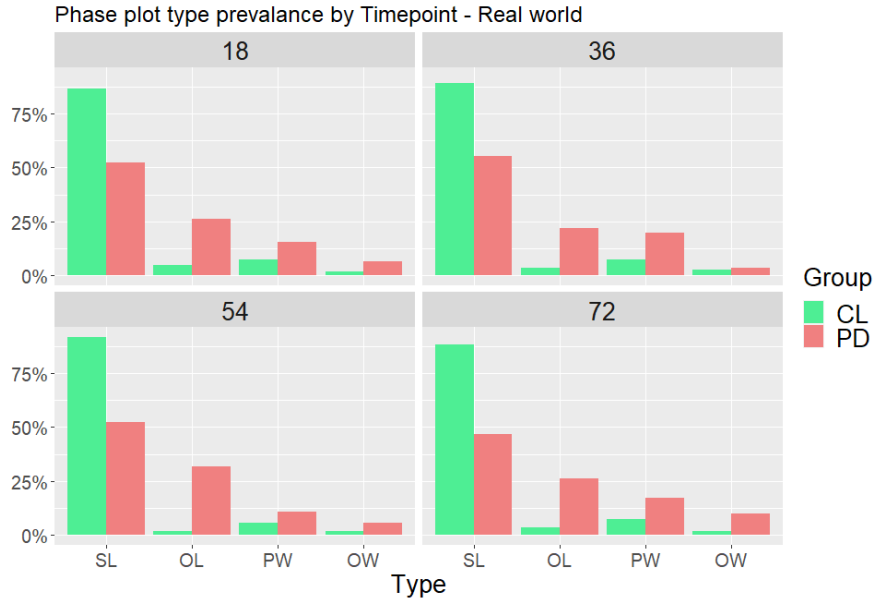

Figure 5.26: Distribution of predominant types in real world setting. Modal Phase plot across all seven days as each Timepoint.

	PD	CL	p
n	92	111	-
Asy_θ	16.3 ± 6.28	13.2 ± 8.18	-
γ	0.928 ± 0.061	0.942 ± 0.029	-
d	0.898 ± 1.23	0.47 ± 0.41	-
	Counts		
SL	44	91	$<$ **0.001**
OL	25	7	$<$ **0.001**
PW	17	9	**0.0348**
OW	6	3	0.305

Table 5.4: Predominant Phase plot type across all timepoints by group.

variability of ADL is leading to occasional disparities in among orbits of an individual Phase plot. This is particularly apparent in the case of OW and OL type Phase plots.

When looking at predominant Phase plot Type over all 7 days of real-world recording (Figure 5.26), the distribution closely resembles the Type distribution seen in lab-based settings 4.21. In lab-based settings each participant had a well-defined

predominant Phase plot type- at a given time point, their predominant type was simply the type which was produced from their relatively small amount of steady-state gait. In real world conditions we have a far larger and more unpredictable data set. In the case of real-world data, we the define a participant's predominant Phase plot type as the modal value among the sequence of hourly fitted types across their respective seven-day recording period. Using this definition produces the familiar distribution seen in Figure 5.26 but masks a lot of the finer scale variability in Phase plot type e.g., over the course of the day.

Table 5.4 shows the count data for predominant Phase plot type for all participants. The between-group proportions show similar patterns to the corresponding count data for lab-based gait in Chapter 4 with Controls being far more likely to exhibit a predominantly SL (single line) type Phase plot compared to the PD subjects. A chi-square test of independence showed that there was a highly significant association between Group and predominant Phase plot Type, $\chi^2(2, N = 202) = 28.6, p < 0.001$. PD subjects have a significantly higher propensity to exhibit to type OL (Oblique lines) and PW (Parallel wings). The values associated with Phase plot type OW (Oblique wings) are very low, accounting for only about 4% of the total sample size. Given the relatively small counts associated with OW Phase plots, it may seem rational to omit these cases from future analysis to avoid introducing potential bias, however, the count data in Table 5.4 is based solely on predominant Phase plot types exhibited across all real world data available which totals up to 500 hours for each participant[1]. The low count values reported in Table 5.4 simply reflect that it is unlikely for participants of either the PD or Control group to predominantly exhibit OW type Phase plots in favour of SL, OL, or PW. The OW type is not necessarily under-represented in the dataset as a whole.

[1]This calculation is based on the assumption of 7 days of recording at 4 separate timepoints and comprising the hours 06:00 to 23:00 (17 hours per day).

Type / Feature	**SL**	**OL**	**PW**	**OW**	$p^{\dagger}$
Step Length (m)	0.741 ±0.119	0.714 ±0.186	0.709 ±0.108	0.691 ±0.127	**SL vs PW** **< 0.001** **OL vs PW** **< 0.001**
Step Length Asy (m)	0.110 ±0.108	0.107 ±0.090	0.101 ±0.086	0.100 ±0.105	OL vs OW 0.091 SL vs OW 0.067
Step Time Var (s)	0.478 ±0.181	0.464 ±0.174	0.462 ±0.171	0.461 ±0.185	**SL vs PW** **< 0.001** **OL vs PW** **< 0.001**
Step Vel (ms^{-2})	1.12 ±0.272	1.07 ±0.259	1.08 ±0.261	1.04 ±0.267	**OL vs PW** **< 0.001** **SL vs PW** **< 0.001**
Step Vel Var	0.457 ±0.169	0.431 ±0.156	0.436 ±0.156	0.423 ±0.154	**SL vs OL** **0.0022** SL vs OW 0.421

Table 5.5: Between-Timepoint type-transitions. ST domain feature values for PD participants exhibiting each Phase plot Type. Type-to-Type contrasts shown in the right-most column correspond to those presented in Chapter 4 for valid comparisons.

Phase Plot Type Transitions

In Chapter 4 we were able to observe and investigate type-to-type transitions between follow-up timepoints. This analysis highlighted the potential significance of such transitions in terms of traditional features and implications for physical capability. For example, based on the lab data we may hypothesise that a transition from PW to OL corresponds to a significant reduction in gait velocity and reduced physical capability (see Table 4.4).

Table 5.5 shows the results of a similar analysis being applied to real-world gait data. There are 6 possible Type-to-Type transitions. All transitions that showed

statistical significance in lab-based settings also showed significance in real-world settings. Transitions involving the Phase plot Type OW were generally not significant, likely due to it being under-represented among the subjects' predominant types. Despite this, a transition of SL to OW or OL to OW is approaching significance in terms of the feature step length asymmetry. This analysis substantiates the conclusions drawn in Chapter 4 regarding Type transitions and shows that their apparent clinical relevance is not just an artefact of lab-based gait but is also present and observable in real-world data.

Hour-Hour transitions Correspond to much smaller scale fluctuations - related to medication state rather than overall disease decline. So far we have only investigated Phase plot Type transitions on timescales of over a year. This has been dictated by the experimental design and follow up dates separated by 18-month gaps. We have achieved this by determining each subject's predominant Type at each timepoint, meaning that the transitions we have observed are more likely the results of changes in disease state or physical capability over time. To assess the relevance of type transitions to daily disease fluctuations we must reduce the timescale considerably. To do this, we instead determine each subject's predominant Phase plot type on a per hour basis. Since are only looking at the hours of 06:00 to 23:00 this technique results in a discrete-time sequence of Types with length $n = 17$. One such sequence is available per subject per day.

Figure 5.27 shows the daily sequence produced by a typical PD patient at timepoint of 36 months and on day 4 of recording. A representative Phase plot is shown for each hour. This subject has predominant Phase plot type, OL.

It is fairly common for several hours in day to go without sufficient gait data to discern a Phase plot type. The 7-day recording protocol, however, ensure that in the vast majority of cases we have several bouts of gait per hour per subject which

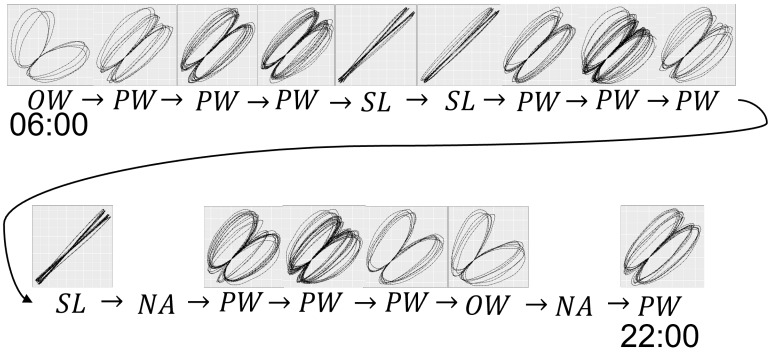

Figure 5.27: A PD subject's Phase plot Type sequence over a single day. During the hours 17:00-18:00 and 21:00-22:00 insufficient gait was recorded to produce valid Phase plots.

allows us to build up a general daily trend or sequence i.e., it is generally unlikely for a subject to consistently produce no data across particular hours for all 7 days at a given timepoint.

There are several benefits to regarding subjects' hourly Phase plot type sequences rather than their respective predominant type. For example, we can investigate the previously underrepresented OW type. We can also now contextualise Phase plot Types in terms of fluctuations on much smaller timescales, a few hours rather than years.

Hourly Phase plot Type sequences, such the example shown in Figure 5.27, can be extracted for every participant for each of the seven days for all timepoints at which they were present. Treating this sequence as a DTMC allows us to quantify and investigate the nature of between-Type transitions.

Once we have estimated the 4 by 4 transition matrix, $\mathbf{P}$, associated to a predominant Type and group (PD or CL) we can calculate the respective stationary distribution π, a non-negative vector of length 4 whose entries sum to 1 and which satisfies

$$\pi\mathbf{P} = \pi.$$

We can observe quite easily that all states (Types) in this Markov chain can be reached regardless of initial state. We can therefore conclude that the underlying Markov chain is irreducible and is aperiodic. This condition is sufficient to conclude that there will be a single unique stationary distribution.

The stationary distribution of a Markov Chain describes the proportion of time spent in each state assuming a sufficiently long run to remove any dependence on the initial state. In our case, it describes the proportion of time spent exhibiting each Phase plot type conditional on their respective predominant type at that timepoint.

In Figure 5.28 we can see that for each predominant type, unsurprisingly more time is spent in that type than any other. However, the specific stationary distributions have some notable differences.

For both disease groups, those with predominant type OW exhibit much more diffusion in their stationary distribution when compared with the other three types (see the smaller peaks in the top-right panel of Figure 5.28). This can be interpreted as showing that Type OW is more likely to be a temporary state that subjects have an increased tendency to transition out of. This is consistent with findings of chapter 4 regarding the under-representation of OW among predominant Types ($< 4\%$). Upon further inspection, we can see that this diffusion is particularly expressed in the CL group. In fact, across all predominant Types except SL, CL subjects yield notably more diffuse stationary distributions, this can be seen by observing highest green (CL) peak in OL, OW, and PW panels of Figure 5.28 and noting its reduced value compared to the equivalent values for the PD group. This trend reverses in the case of Type, SL in which case controls spend an estimated 79.1% of their time in their predominant SL state compared to 67.7% for PD subjects.

It is very clear certain type transitions are more feasible than others depending on the predominant Type. Moreover, for a given predominant Phase plot Type, there

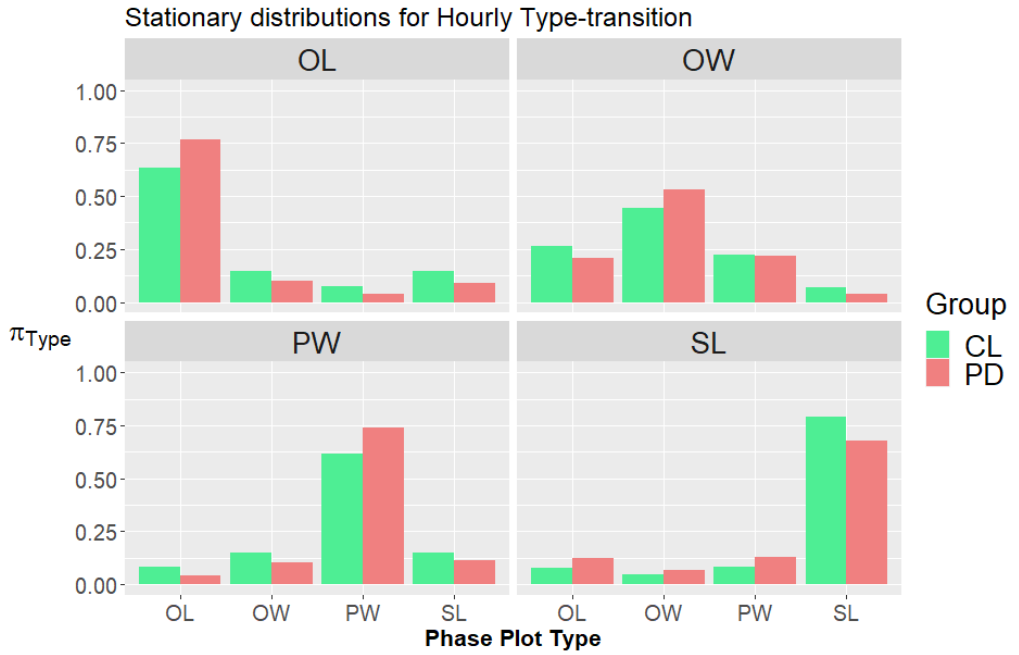

Figure 5.28: The stationary distributions π_{Type} of subjects' hour-to-hour sequences. These distributions, π_{Type} are estimated separately for subjects with each predominant type.

are consistently two other types which are more likely to occur than the remaining fourth. This is clearest in the case of Type OW in the top-right panel of 5.28 where the Types OL and PW share far more stationary distribution weight than Type SL. A similar distribution can be seen when conditioning on any of the other three Types (OL, PW, and SL), where two other Types each represent approximately twice the weight of their respective stationary distribution when compared to the fourth remaining Type. This property of π_{Type} is consistent across both PD and CL groups and is more easily visualised by the diagram in Figure 5.29.

An alternative interpretation of this property within the π_{Type} is that for each of the four possible predominant Types, there is a corresponding Type to which transitions are far less common than from any other Type. For those subjects of predominant Type OW, the corresponding type is SL which accounts for only 4.5% of the respective subject's Types across all timepoints.

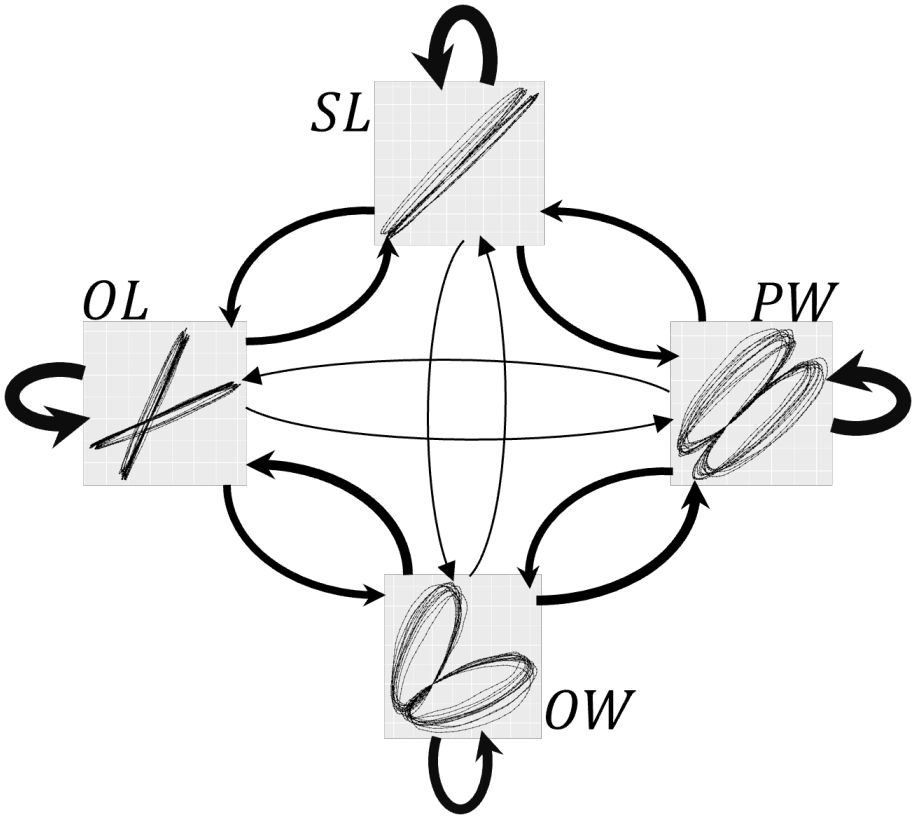

Figure 5.29: Feasible transitions of Phase plot Type. Transition probabilities conditional on starting in the predominant state (Type). Relative probabilities shown by line width. Probabilities have been normalised across PD and CL.

Table 5.6 shows, for each feature the, two most substantial Phase plot Type transitions based on percentage change in the respective feature. Given four Phase plot Types there are 12 possible directed hour-to-hour transitions i.e., the transition $SL - OL$ is considered separately to $OL - SL$. However, after treating mirrored transitions as separate, it becomes clear that these mirrored pairings consistently yielded approximately equal and opposite effects on the ST features. Due to this symmetry, we introduce the convention that we report transitions in their *positive* direction, defined as the direction in which the respective feature tends to increase.

Looking at the top Type transitions across all ST features shows that the majority (12 out of 15) involve a transition to or from OW and/or SL Type Phase plots. Interestingly, SL-to-OW (or OW-to-SL) is the rarest Type transition observed across

Type / ST Feature	**Top transition**	**Second transition**
Mean characteristics		
Step time	PW-OL 1.6%	OW-OL 1.2%
Stance time	PW-OL 1.6%	OW-OL 1.3%
Swing time	PW-OL 1.5%	PW-SL 1.3%
Step length	OW-SL 7.2%	PW-SL 4.7%
Step velocity	OW-SL 7.2%	OL-SL 4.9%
Variability (var) characteristics		
Step time var	OW-SL 3.6%	PW-SL 3.0%
Stance time var	OW-SL 2.9%	OL-SL 2.6%
Swing time var	OL-SL 3.2%	OW-SL 3.1%
Step length var	OW-SL 9.3%	OL-SL 6.1%
Step velocity var	OW-SL 8.0%	OL-SL 6.1%
Asymmetry (asy) characteristics		
Step time asy	OW-SL 5.4%	OW-OL 4.5%
Stance time asy	OW-SL 5.2%	OW-OL 4.7%
Swing time asy	OW-SL 4.7%	OW-OL 4.0%
Step length asy	OW-SL 10.1%	PW-SL 8.1%
Step velocity asy	OW-SL 10.9%	PW-SL 7.0%

Table 5.6: Hour-to-hour type-transitions. Transitions with the largest and second largest significant effect sizes shown.

all real-world gait data (see Figure 5.26 and 5.29). Due to experiment design and practical limitations of gait data we must accept a degree of error in estimating a participant's Type each hour, in particular if they have not recorded sufficient gait activity. This is an indirect effect of the unpredictable nature of real world gait during ADL and may be addressed in future studies if more detailed annotations of ADL are made.

5.4.6 PD Classification in Real-world Settings

To assess the clinical utility of Phase plots we can fit several different mixed effects models. There are two dependant variables of interest that we aim to model. Firstly, the disease group of a subject i.e., can we reliably classify a PD or CL subject using

generalised mixed effects models and secondly, the MDS-UPDRS score which is taken as a proxy for PD-progression. To interpret these mixed effects models, we will be relying on estimated standard errors of fitted parameters as well as associated effect sizes and confidence intervals. In the case of modelling disease group, we can also rely on the odds-ratios associated with specific feature effects to see how Principal components or individual features impact the estimated probability of belonging to the PD group. Including a random effect for participant ID allows for this between-subject variation. Features within the Phase and ST domains will be treated as fixed effects.

Firstly, we model MDS-UPDRS with the first four principal components of the ST domain as fixed effects and Phase plot type as a random effect. Secondly, to also allow us to compare relative performance of feature domains, we model MDS-UPDRS with the corresponding principal components of the Phase domain as fixed effects and with Phase plot type as a random effect as before. As part of the random effects, an intercept is estimated for each Phase plot type.

Similarly to the results of the MDS-UPDRS modelling conducted in Chapter 4, all fixed effects associated with the first four PCs of each feature domain (as well as for all features) were significant at the 5% level. Compared to the Lab-based analysis, the majority the random effects sizes have increased in magnitude. I.e., the impact of Phase plot Type on MDS-UPDRS appears more pronounced in Real-world settings during ADL. To contextualise the effect sizes in Table 5.7, the mean MDS-UPDRS value for PD subjects is 32.7 ± 10.2 (see Table 3.1).

Classification performance (Table 5.8) in Real-World settings has increased across all feature domains and by all three metrics (accuracy, sensitivity, and specificity) compared with the corresponding results in Chapter 4 (see Table 4.8). Interestingly, specificity has increased by a greater proportion than sensitivity, suggesting that

Fixed effect	effect size	Random effect	effect size
	ST domain		
PC1	1.22 (±0.063)	OL	-1.73
PC2	0.58 (±0.12)	OW	2.57
PC3	0.80 (±0.13)	PW	-1.02
PC4	0.23 (±0.015)	SL	0.18
	Phase domain		
PC1	1.2 (±0.13)	OL	-1.47
PC2	-1.14 (±0.026)	OW	2.21
PC3	1.30 (±0.032)	PW	-1.01
PC4	0.73 (±0.046)	SL	0.27
	All features		
PC1	1.16 (±0.013)	OL	-1.47
PC2	1.14 (±0.025)	OW	2.21
PC3	1.3 (±0.032)	PW	-1.01
PC4	-0.72 (±0.046)	SL	0.27

Table 5.7: Effect sizes - Modelling MDS-UPDRS on principal components of Phase and ST domain.

Accuracy	Specificity	Sensitivity
	ST domain	
72.6%	75.7%	71.5%
	Phase domain	
71.5%	72.0%	71.2%
	All features	
74.3%	78.4%	73.4%

Table 5.8: Predicting disease group using logistic mixed effects models (4.4)

Real-World gait data offers a lower false positive rate. ROC curves and their respective AUC (Area Under the Curve) values are a well-known measure of binary classifier performance. Figure 5.30 shows the ROC curves for classification of PD via NLMEMs (see equation 5.1) with S representing to the sigmoid function (equation 4.2)

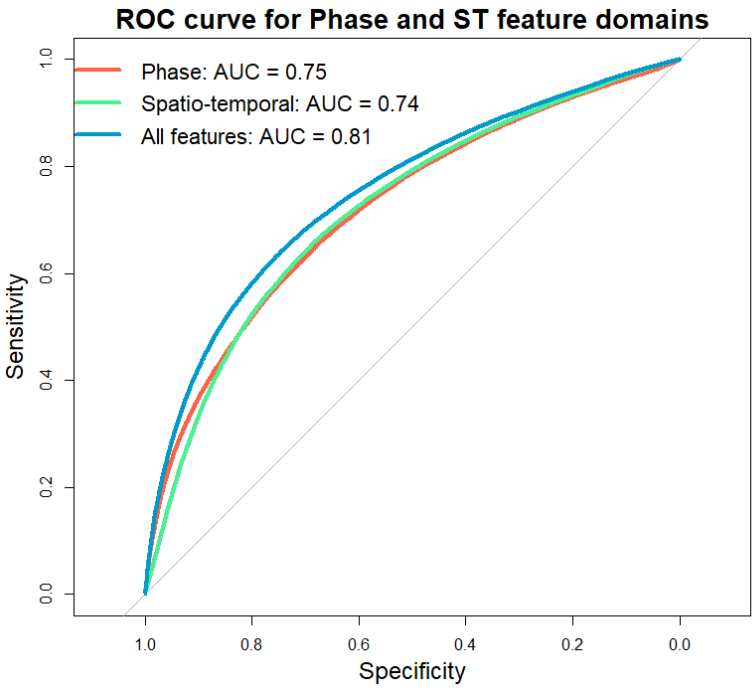

Figure 5.30: ROC curves for the classification of PD using Phase and ST domain features in Real-World settings.

$$P(PD_i = 1) = S(\mathbf{X_i}\underline{\beta} + \mathbf{Z_i}\underline{b_i} + \underline{\epsilon_i}) \tag{5.1}$$

As in previous analyses, PD_i is an indicator variable equal to 1 when participant i has a diagnosis of Parkinson's disease and 0 otherwise. $\mathbf{X_i}$ is the design matrix for the fixed effects, the first four principal components in this case, and $\mathbf{Z_i}$ contains the random effects which in this case represents the predominant Phase plot type exhibited by subject i.

5.4.7 Lab vs Real-World: The Impact of Environment

In the lab-based portion of the ICICLE-GAIT study, participants were asked to perform four intermittent straight line walking trials over a 10 m walkway at their preferred speed [83] [14]. People with PD were tested approximately one hour after

their medication intake. The Real-world portion of the data collection took place at the end of the lab-based testing session. Participants wore the accelerometer for one week. Schooten et al [84] showed that just 5 days of continuous accelerometer data was sufficient for reliable estimation, although their study concerned a trunk-work sensor. Measuring gait in real life reflects habitual gait performance and is not confounded by heightened attention or altered by the observer effect found during lab-based assessment. Wearable accelerometers also allow movement to be captured continuously over longer periods of time, which is not practical in a laboratory or clinical setting.

In terms of total recorded data, the approximate ratio of lab-based to real-world data is 1:20,000. This is based on a single participant accruing ≈ 30 seconds of lab-based gait followed by 7 continuous days real-world recording. Including only the hours from 06:00 to 22:00 reduces this to 1:14,000 and finally, only considering times during which actual ambulation is occurring brings the final ratio to 1:1200 (lab : real world). Any analyses aiming to assess the impact of recording environment must be conducted carefully to minimise the bias towards the particular recording protocol for lab-based gait e.g., fixed length of the 10m walkway. For this reason, when directly comparing lab and real-world gait we include only comparably short bouts from real-world settings i.e., those bouts with duration under 25 seconds. Even at this duration, the variety in real-world settings and ADL has a clear impact on the empirical distribution of both ST and Phase domain features (see Figures 5.31 5.32).

Comparable bouts were extracted on a per subject basis. Here, bouts are considered comparable if they are similar in duration. In lab-based settings, this may vary between subjects due to variations in step velocity / lengths etc. Finding comparable bouts in this way still allows for several conflating factors in addition to recording

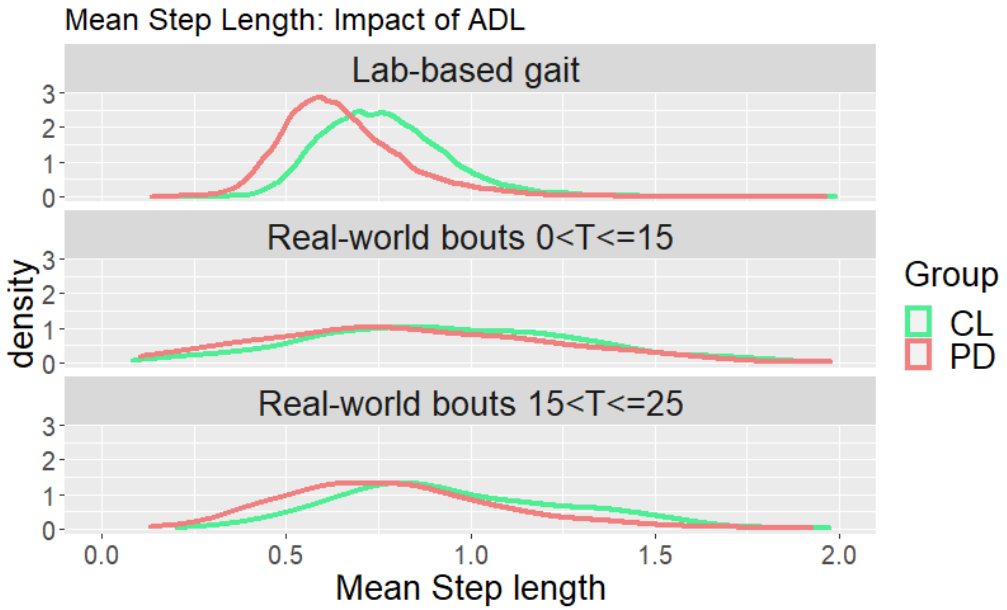

Figure 5.31: Mean step length in lab-based settings and in Real-World conditions for two short bout durations intervals

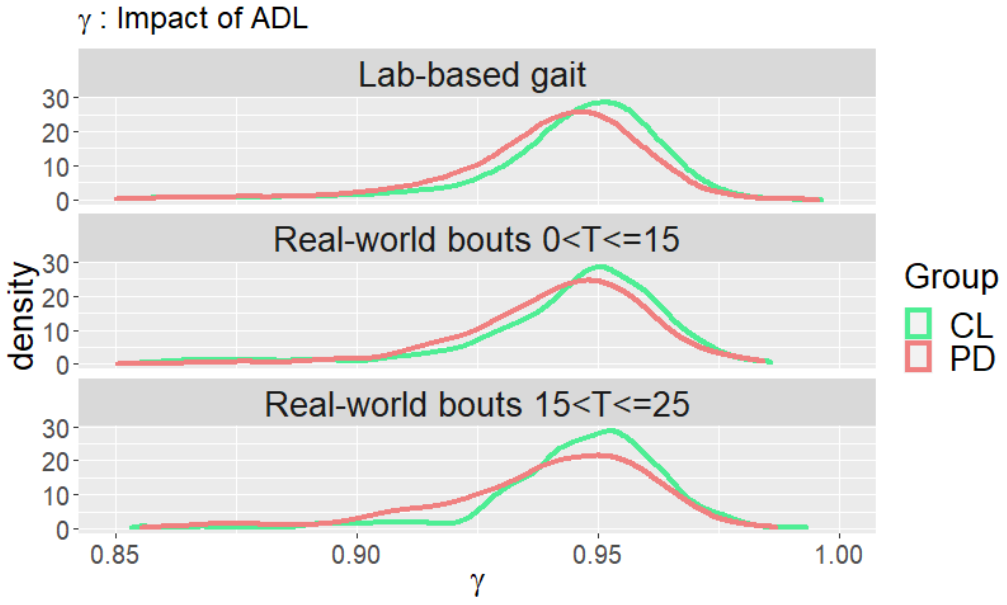

Figure 5.32: γ (mean ellipse eccentricity) in lab-based settings and in Real-World conditions for two short bout durations intervals

Feature	Lab-based	Real-World $0 < T \leq 15$	Real-World $15 < T \leq 25$
Phase Domain			
	Primary features		
Area	0.113	+109%	+93.7%
γ	0.948	-0.214%	-0.319%
Asy_{θ}	5.58	+19.5%	+13.9%
Asy_{Area}	1.17	+132%	+125%
GoF	6.44	+115%	+112%
SD_{r_1}	0.022	+122%	+121%
SD_{r_2}	0.054	+167%	+163%
	Secondary features		
Asy_{γ_m}	0.0128	+130%	+131%
Asy_{γ_M}	0.0129	+152%	+147%
Asy_{θ_m}	8.49	+8.77%	+9.13%
Asy_{θ_M}	4.2	+49.9%	+47.5%
Asy_{Area_m}	3.13	+134%	+124%
Asy_{Area_M}	4.45	+147%	+143%
GoF_m	26.2	+114%	+111%
GoF_M	35.3	+122%	+98%
SD_{GoF}	29.2	-10.3%	-11.9%
Spatio-temporal Domain			
	Mean characteristics		
Step time	0.543	+19.5%	+21.8%
Stance time	0.703	+15.3 %	+15.1%
Swing time	0.389	+21.0%	+26.5%
Step length	0.554	+20.2%	+23.9%
Step velocity	1.03	+9.3	+10.9
	Variability (var) characteristics		
Step time var	0.017	+1020%	+1490%
Stance time var	0.0413	+390%	+472%
Swing time var	0.0295	+275%	+580%
Step length var	0.0485	+248%	+241%
Step velocity var	0.0927	+152%	+238%
	Asymmetry (asy) characteristics		
Step time asy	0.00994	+1890%	+1630%
Stance time asy	0.0256	+570%	+457%
Swing time asy	0.0218	+262%	+462%
Step length asy	0.031	+293%	+146%
Step velocity asy	0.0532	+223%	+158%

Table 5.9: Lab-based and Real-World features values from the spatio-temporal and Phase domains. Features derived from Lab-gait and comparably short bouts (< 25s) in real-world settings.

environment e.g., medication state. In lab-based gait, participants completed their respective bouts approximately one hour after medication intake which removes to some degree the effect of medication from subsequent analyses. It is difficult to remove this complication from real-world gait data without additional information on specific medication intake times for PD subjects. By extracting many comparable real-world bouts however, it is reasonable to assume that we may capture both medication ON and OFF state gait i.e., some bouts recorded when the patient's PD symptoms were being masked by medication and some not. Table 5.9 shows the results of these comparisons. Significance was assessed using the Mann-Whitney U test. All features' location shifts (from lab to both duration categories) were significant at the 1% level. This shows that in real-world conditions, even during comparable short bouts, both ST and Phase domain features are significantly effected by the unrestricted environment. The impact of environment and increased ADL is most clearly apparent in features related to asymmetry and variability with some features such as Step time asymmetry increasing by a factor of 10 or more. The general trends observed here when comparing Lab bouts and Real-world bouts of various length are in line with similar analyses conducted by Del Din et al [1].

As an aside, many of the ST features in the table also exhibit significant increases across the two bout duration categories shown. This is consistent with the results of section 5.4.3 where ST gait features showed an increased sensitivity to varying activity levels compared to Phase domain features. As a general rule, gait recorded in highly controlled settings represents a participant's best possible gait or their *capacity*. This contrasts with Real-world gait data which reflects the participant's actual performance [23].

5.5 Discussion

The majority of all features showed highly significant differences between PD and CL with a range of percentage differences; sufficing to say that not all features are similarly affected by disease group (PD / CL). Visual inspection of the empirical densities of a given feature from Lab-based bouts and those recorded during ADL in Real-World conditions shows the substantial impact of recording environment and experiment protocol. In real-world data the first few PCs all showed high loadings associated with features related to asymmetry or variability of gait. This relative importance of variability and asymmetry became a recurring theme in these Real-World analyses. Segmenting activity levels by 20% quantiles offered a framework to assess dependence of features on duration of gait carried out by participants. Phase domain features are generally invariant across all activity quantiles. This may improve their versatility as a clinical tool particularly applied to frail or less mobile cohorts, as participants need not be required to carry out long durations of gait to produce a valid set of Phase domain features and associated signature of gait. Analysis of variance (ANOVA) testing showed that all ST features were sensitive to activity quantile and that the degree of this sensitivity significantly interacted with disease group. Overall, in the real-world portion of this experiment, PD and CL tended to complete similar amounts of gait (in terms of total duration) however this was distributed differently between groups. PD participants tended to accrue their total gait duration through 14% more individual bouts than members of the CL group. The decreased average duration of these bouts, however, largely cancelled out any difference. SPM analysis demonstrated multiple regions of interest across daily timeseries for ST domain features whereas features from the Phase domain tended to either produce a single highly significant region of interest or none at all. This may demonstrate that, as with activity quantiles, Phase domain features are

also less sensitive to daily fluctuations than the more traditional ST features. This strengthens the interpretation of Phase plots as an objective signature of gait but may also suggest that Phase features are not best suited for detecting OFF-state gait over very short timescales. The assumption Gaussian Processes has been used previously in the context gait patterns and kinematics however, assessing the precise suitability of this assumption in Phase plot is recommended as a future research task. Statistical non-Parametric Mapping (SnPM) should also be explored as an alternative as it relies on fewer assumptions for the distribution of the data and may be more appropriate in this context. Expanding the lab-based analysis has validated the proposed Phase plot-based signature of gait in real-world settings. For Real-world gait we have still observed the same four Phase plot types (SL, OL, PW, OW) and validated that individuals' predominant lab-based Type is preserved in their corresponding Real-world gait. Both PD and CL may temporarily transition out of their predominant Phase plot type on multiple occasions throughout the day. DTMC analyses of participants' sequence of daily types highlighted interesting details about the relative stationary distributions associated to participants with each predominant type- particularly those associated with Type OW. Following the modelling of MDS-UPDRS scores and disease group via mixed effects models, it appears that the increased ADL has helped express between-group differences related to disease group or rather the highly controlled Lab-based environment had been masking them to some degree. PD classification is more accurate in Real-World settings and also produces lower false positive/negative rates. As before, combining both ST and Phase domain features produces notably better performance than either feature domain alone. Throughout this chapter it is plain to see that Lab and Real-World recorded gait data are fundamentally different. The impact of recording environment is expressed more clearly in ST features related to variability and asymmetry.

The majority of Phase domain features are also clearly affected by environment with many features more than doubling their respective lab-based means. The average increase seen in ST features was considerably larger with one feature increasing 18-fold. This is not surprising given that Real-World gait necessarily included an increased variety of ADL and turning compared with straight line lab-based bouts. These results are in line with previous literature in which Real-world gait is superior to lab-based in the context of classifying PD and identifying risk.

Chapter 6

Longitudinal Analysis

6.1 Introduction

Analysing ST and Phase domain feature over longer periods gives insight into how PD may impact on gait performance beyond that which can be expected as a result of healthy ageing. In this chapter we look at the progression of gait features up to 6 years following PD diagnosis. The age-matched control group allows us to disentangle the simultaneous impacts of pathology and ageing. It is possible for a given feature to be sensitive to neither, both, or just one of these effects as shown by Wilson et al [85]. Understanding the PD-specific impact on gait features is necessary for targeted and individualised medication tailoring as well as general disease tracking. I.e. it is important to know the relative extent to which gait disturbances are *acceptable* effects of ageing. The ICICLE-GAIT dataset also allows us to incorporate the impact of recording environment into these analyses and see if there are significant advantages of one setting over the other e.g. the highly controlled Lab-based gait sessions may mask the impact of ageing.

In previous chapters we have already taken several Longitudinal approaches. We validated the Phase plot based Signature of gait partly by analysing timepoint-

timepoint Phase plot Type transitions and substantiated Lab-based Phase plot Type transitions by showing their consistency with their corresponding Real-World transitions. We have also looked in detail at the series of Type-transitions recorded by participants in Real-World conditions on a daily basis, demonstrating the significance of Type-transitions on the small hour-to-hour timescale.

What remains is to:

- Analyse the progression of Phase domain features across all available timepoints. As before, we keep traditional ST features as an established reference.
- Quantify the (interacting) effects of age, group (PD vs CL), and environment (Lab vs Real-World) on the progression of these features.

6.2 Aims and Hypotheses

Initially, we can form subjective hypotheses based on exploratory analysis. Spaghetti plots are an accessible means of showing all participants' trends at each follow-up timepoint (18, 36, 54, and 72 months) for a given feature. For each aspect of longitudinal trend analysis, we can additionally check for any dependence on environment e.g. Lab masks ST feature more than it masks some Phase domain features.
For any trends in ST or Phase domain features, or impacts of ageing, we can investigate how these trends or impacts are masked or preserved in each recording environment.

In general we form the following hypotheses related to each gait feature:
H_0 : The observed progression of feature i is equal in Lab and RW settings.
H_1 : Either the Lab or RW recording environment exhibits a greater progression in either PD or Control participants. Similarly we form the following hypotheses related to each gait feature:

H_0 : The observed effect of ageing on feature i is equal in CL and PD participants.
H_1 : Either the CL or PD participants exhibit greater sensitivity to ageing (in either recording environment).

6.3 Methods for Longitudinal Analysis in PD

6.3.1 Feature Progression by Group and Environment

Linear mixed effects models (LMEMs) are used to model the progression of both ST and Phase domain features. Follow-up timepoints (18, 36, 54, 72 months) are included as fixed effects along with a random intercept for each participant to account for individual variability. We also include in these models indicator variables for Environment and Group to allow us to compare feature progression between PD and CL participants. Finally, each participant's age at baseline is also included in the model to control for the impact of ageing. I.e. the value of feature y for participant i and timepoint t is modelled as

$$y_{it} = \beta_{0i} + \beta_1 t + \beta_2 I(PD_i) + \beta_3 I(RW_i) + \beta_4 I(PD_i)t + \beta_5 I(RW_i)t + \beta_6 age_i + \epsilon_{it} \quad (6.1)$$

where $I(PD_i)$ and $I(RW_i)$ are indicator variables representing participant Group and current recording environment, and age_i is their baseline age. β_{0i} is the random intercept for participant i. Finally ϵ_{it} is the residual error for participant i at time t.

6.3.2 Impact of Ageing

Within any analysis related to PD the impact ageing is an unavoidable factor due to the demographics of those with a diagnosis- typically those over 60 years of age.

Figure 6.1: PD participant age distribution.

The particular age distribution for the PD participants included in these analyses is shown in Figure 6.1.

In addition to controlling for the impact of ageing in models of feature progression, we can focus in on this effect to better understand how each feature progresses per year, for example, rather than solely in terms of time since diagnosis. The overall trend in mean step length associated with age shown in Figure 6.6. As previously discussed in Chapter 5, Lab and Real-world recorded gait are fundamentally different measures, for this reason we also separate the plot by environment. Two-way Analyses of Covariance (ANCOVAs) were performed to assess how the ST and Phase domain features can be expected to progress as a result of ageing in both PD and CL subjects. ANCOVA is a useful method for assessing the interaction effect (if any is present) of two independent variables, in this case, participant age (treated as continuous) and group (PD or CL).

This particular interaction effect of Age and Group is important as it will help contextualise the overall progression of gait features in both PD and CL groups by shedding light on the separate impacts of ageing and pathology on gait. Throughout these analyses we assume that feature progression observed in the control group is

the result of the ongoing effect of ageing. Given the demographic and age range of the participants, it is unrealistic to assume that progression observed even in control participants is purely the result of healthy ageing. As in the PD group, there is potential for additional unobserved comorbidities to factor into the observed progression in gait characteristics. As with previous analyses in this thesis we will compare and contrast how this effect of ageing is expressed in lab-based and real-world recording settings.

6.4 Results

6.4.1 Feature Progression (Follow-Up) by Group

Tables 6.1 and 6.2 show the results of LMEMs to assess the progression of ST and Phase domain features across all available timepoints.

In the first instance we can establish a baseline feature progression from the age-matched controls and subsequently quantify any additional progression associated with PD. Seven of the 15 ST domain features significantly progressed in CL subjects and, to a greater extent, in PD subjects. Six features showed significant progression in PD only and 2 features did not appear to progress in either group. These results based on feature progression up to 6 years post-diagnosis are consistent with a recent longitudinal analyses of a similar subset of ST features [85]. We see a similar picture within the Phase domain, in that 8 of the 16 Phase domain features progressed significantly for both Controls and PD. In addition, 3 features appeared to progress only in PD subjects. There does not appear to be any preference for Primary or Secondary Phase plot features.

Significance in the column for PD (†) is assessed in terms of progression relative to Controls i.e. $p < 0.05$ implies significant deviation from the progression observed

in the Control group. Conversely, $p > 0.05$ does not imply no progression with respect to timepoint, rather that there is not a significant deviation from the trend (if any) present in CL subjects.

	Control		PD		PD:Timepoint interaction		RW:Timepoint interaction	
Feature	yearly Δ	p	yearly $\Delta^{\dagger}$	$p^{\dagger}$	β	p	β	p
Primary features								
Area	2.89%	0.079	0.687%	0.915	-0.0016	0.172	-0.00163	$<$ **0.001**
γ	-0.236%	**0.003**	0.0543%	$<$ **0.001**	0.000189	$<$ **0.001**	5.82e-05	$<$ **0.001**
Asy_{θ}	0.91%	**0.001**	2.35%	$<$ **0.001**	0.00129	0.91	0.00857	**0.008**
Asy_{Area}	-5.42%	0.146	-11.6%	**0.043**	-0.0277	0.446	-0.103	$<$ **0.001**
GoF	-0.888%	0.526	-0.568%	0.499	0.00257	0.697	-0.102	$<$ **0.001**
SD_{r_1}	-0.214%	$<$ **0.001**	2.18%	0.133	-0.0036	$<$ **0.001**	-0.00326	$<$ **0.001**
SD_{r_2}	1.6%	0.195	1.03%	**0.025**	-7.75e-05	0.637	-0.00071	$<$ **0.001**
Secondary features								
Asy_{γ_m}	2.25%	**0.016**	1.44%	$<$ **0.001**	4.97e-05	0.512	-0.000389	$<$ **0.001**
Asy_{γ_M}	4.15%	**0.001**	-0.0452%	**0.005**	-0.000195	**0.025**	-0.000415	$<$ **0.001**
Asy_{θ_m}	2.69%	**0.006**	1.47%	**0.001**	0.0028	0.79	0.0024	0.427
Asy_{θ_M}	2.52%	**0.024**	-0.972%	**0.001**	-0.0155	0.058	-0.014	$<$ **0.001**
Asy_{Area_m}	12.9%	**0.001**	10.2%	0.415	-0.265	0.155	-0.248	$<$ **0.001**
Asy_{Area_M}	-2.95%	0.728	-2.92%	0.93	-3.33	0.709	3.48	0.175
GoF_m	0.713%	0.302	-2.39%	0.03	-0.135	**0.018**	-0.504	$<$ **0.001**
GoF_M	-0.992%	0.945	0.0665%	0.073	0.0524	0.703	-0.858	$<$ **0.001**
SD_{GoF}	1.35%	0.238	0.376%	0.628	0.012	0.778	0.0338	**0.042**

Table 6.1: Phase domain feature progression (real-world) from diagnosis date. † significance assessed in terms of relative progression relative to Controls. Percentages are calculated from 18-month values.

Feature	Control		PD		PD:Timepoint interaction		RW:Timepoint interaction	
	yearly Δ	p	yearly $\Delta^{\dagger}$	$p^{\dagger}$	β	p	β	p
Spatio-temporal Domain								
Mean characteristics								
Step time	0.0125%	0.812	-1.54%	$<$ **0.001**	-0.000677	$<$ **0.001**	-0.00263	$<$ **0.001**
Stance time	-0.00705%	0.478	-1.43%	$<$ **0.001**	-0.000725	$<$ **0.001**	-0.00248	$<$ **0.001**
Swing time	0.0918%	0.647	-1.66%	$<$ **0.001**	-0.000686	$<$ **0.001**	-0.00249	$<$ **0.001**
Step length	-0.661%	**0.035**	-3.08%	$<$ **0.001**	-0.000408	**0.027**	-0.00213	$<$ **0.001**
Step velocity	-0.761%	**0.003**	-1.65%	$<$ **0.001**	0.000232	0.376	-0.000878	$<$ **0.001**
Variability (var) characteristics								
Step time var	-0.613%	0.281	-1.12%	0.158	-4.73e-05	0.852	-0.00584	$<$ **0.001**
Stance time var	-0.635%	**0.015**	-1.1%	0.65	-0.000107	0.674	-0.00522	$<$ **0.001**
Swing time var	-0.449%	0.412	-0.525%	0.642	-0.000198	0.414	-0.00497	$<$ **0.001**
Step length var	-0.513%	0.136	-2.27%	$<$ **0.001**	-0.000111	0.483	-0.00324	$<$ **0.001**
Step velocity var	-0.276%	0.192	-1.24%	$<$ **0.001**	-8.86e-05	0.675	-0.00436	$<$ **0.001**
Asymmetry (asy) characteristics								
Step time asy	-2.02%	**0.002**	-5.24%	0.799	-0.000127	0.301	-0.00244	$<$ **0.001**
Stance time asy	-2.17%	$<$ **0.001**	-5.46%	0.544	-9.8e-05	0.409	-0.00206	$<$ **0.001**
Swing time asy	-2.12%	**0.002**	-4.51%	0.431	-0.000128	0.264	-0.00204	$<$ **0.001**
Step length asy	-3.39%	**0.005**	-8.21%	0.392	-8.3e-05	0.253	-0.000845	$<$ **0.001**
Step velocity asy	-1.69%	0.078	-4.8%	**0.015**	-1.72e-06	0.987	-0.00131	$<$ **0.001**

Table 6.2: Spatio-temporal domain feature progression (real-world) from diagnosis date. † significance assessed in terms of relative progression relative to Controls. Percentages are calculated from 18-month values.

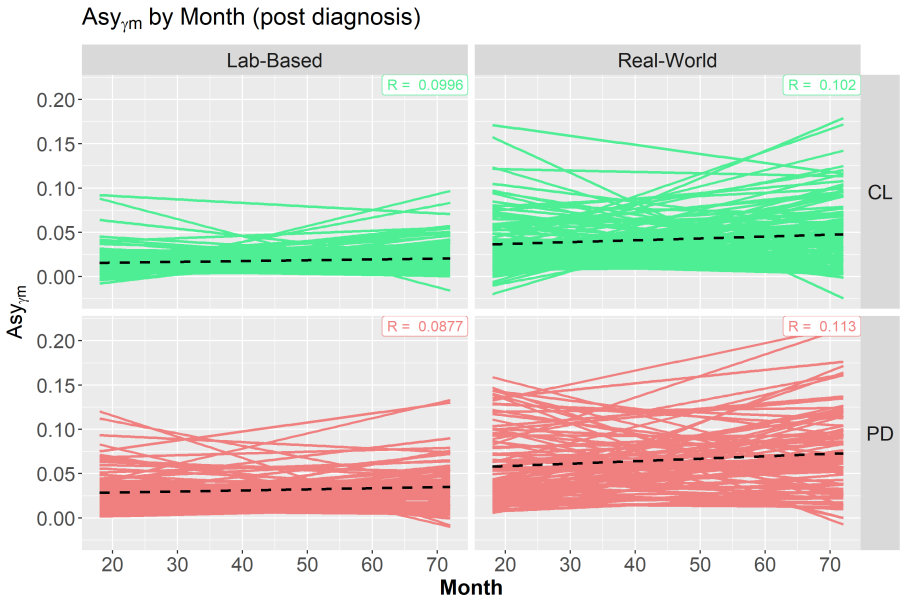

Figure 6.2: Asy_{γ_m} Progression by Group and environment. The impact of environment is progression is clear.

Mean step length is a prime example of Group:Environment interaction. Very strong progression is visible in the PD cohort but only in Real-World settings where

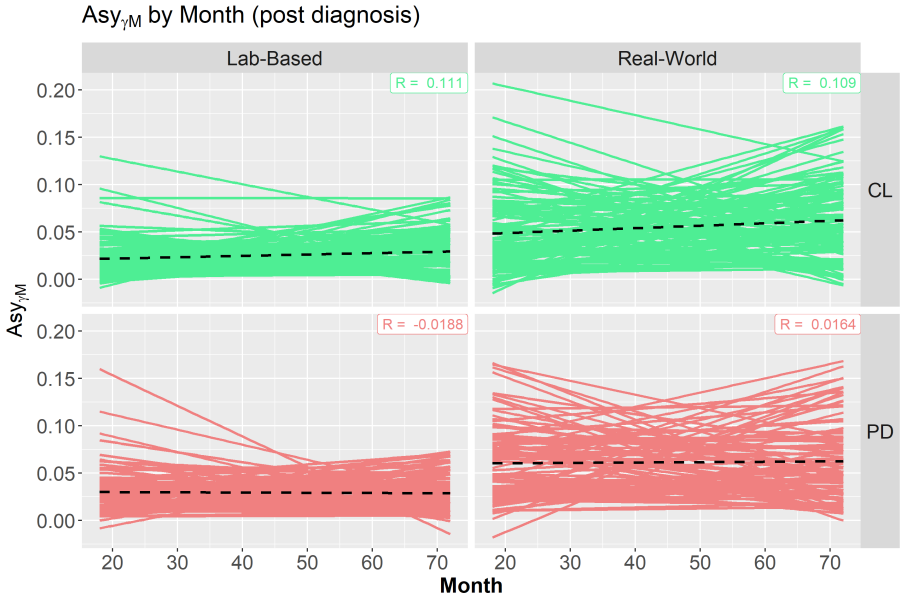

Figure 6.3: Asy_{γ_M} is unlike other features in that it appears to show more progression in the Control group. It is important to note however that the average values is still consistently higher in the PD group.

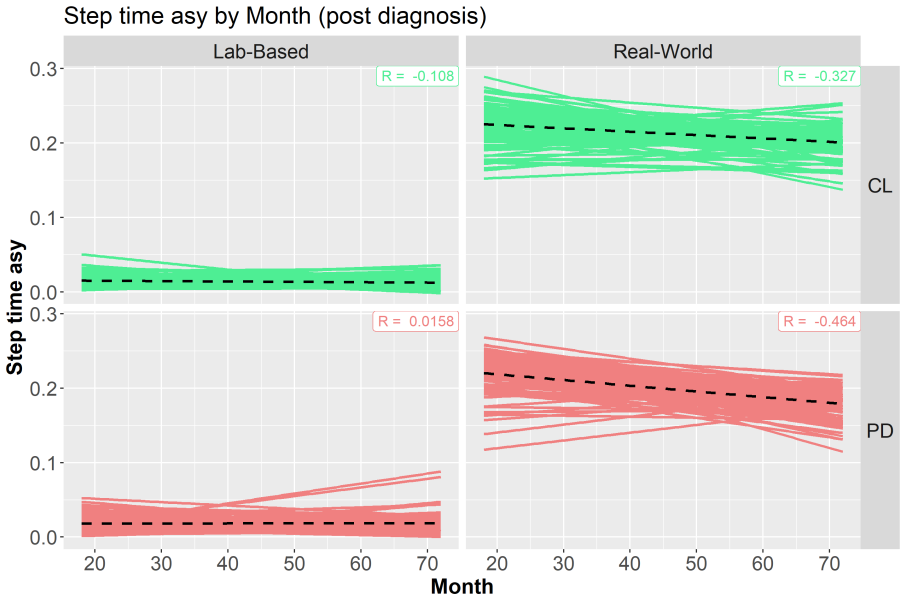

Figure 6.4: Relative progression in many ST features (like step time asymmetry shown here) is quite pronounced relative to Phase domain features. Asymmetry and Variability related features are not surprisingly increased with in the presence of increased ADL.

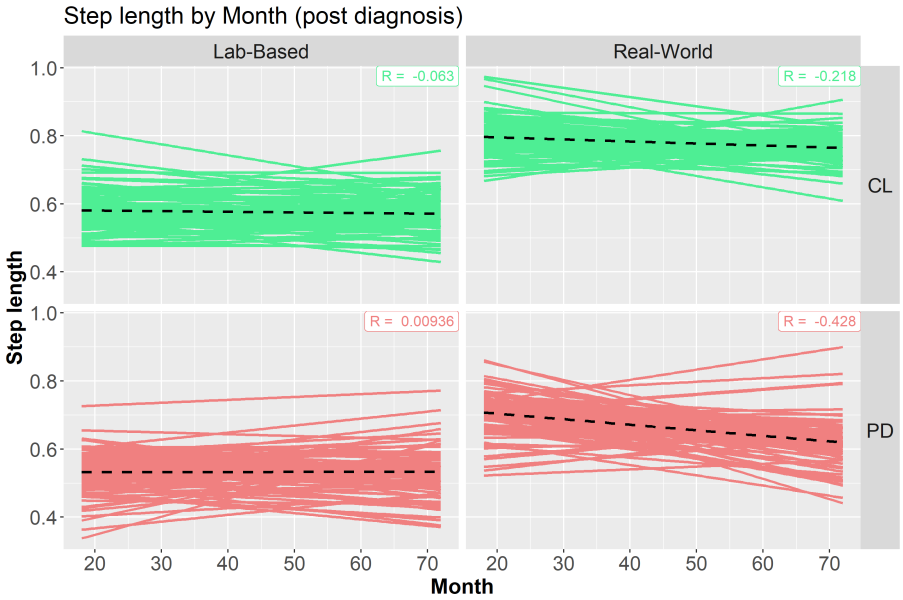

Figure 6.5: The progression of Step length also shows sensitivity to both Group and Environment.

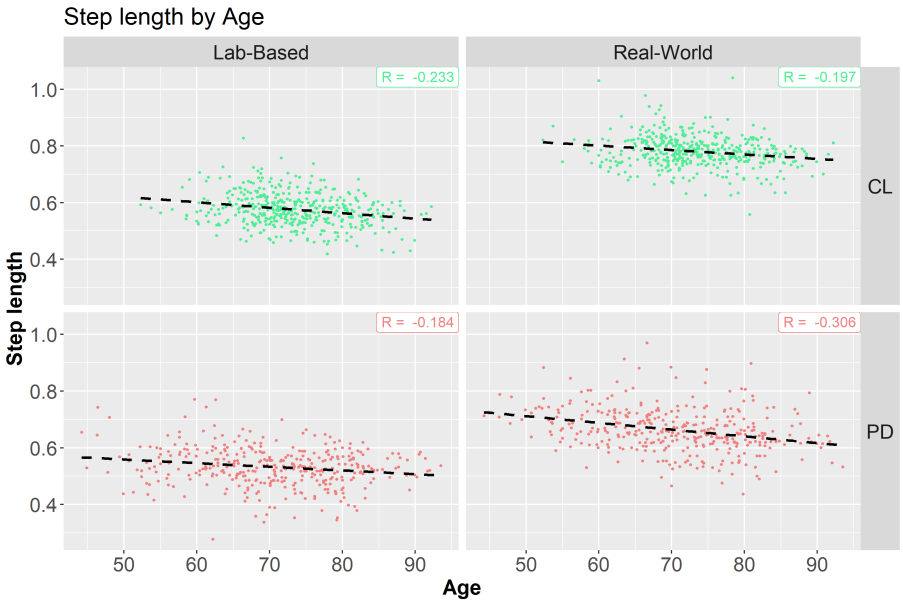

Figure 6.6: Mean step length decreases with age across both disease groups and is not masked by the highly controlled lab-based recording environment.

we see a decline of about 2cm per year in mean step length (see Figure 6.5). Step time asymmetry also shows significant progression in Real-World settings particularly in the case of PD participants (see Figure 6.4). The progression of secondary Phase plot features such as Asy_{gammam} and Asy_{gammaM} shown in Figures 6.2 and 6.3 respectively, also exhibits sensitivity to environment and group.

6.4.2 Impact of Ageing

Table 6.3 summarises the impact of ageing on gait feature differs considerably between feature domains in terms of magnitude, direction and relation to PD. In the case of the ST domain, all mean and variability related features (10 in total) exhibit a significant decline as participants age following diagnosis (see columns 1-2 of Table 6.3). The effect of ageing on four of these ten features interacts with pathology (PD) to accelerate this decline. This added impact of ageing for PD participants appears most apparent in variability-related features. The impact of ageing on length step is

Feature	Age (yearly Δ)		Age:PD interaction	
Phase Domain				
	Primary features			
Area	-7.91e-05	0.172	-0.00182	0.075
γ	-0.000356	0.298	0.000383	**0.043**
Asy_{θ}	0.0219	0.594	-0.0218	0.247
Asy_{Area}	0.0329	0.981	-0.0506	0.577
GoF	-0.00714	0.792	0.017	0.176
SD_{r_1}	0.0088	**0.021**	-0.0107	$<$ **0.001**
SD_{r_2}	0.000787	**0.02**	-0.000493	**0.0129**
	Secondary features			
Asy_{γ_m}	0.000854	**0.006**	-0.000591	**0.012**
Asy_{γ_M}	0.000502	**0.0324**	-0.000492	**0.048**
Asy_{θ_m}	0.063	**0.0166**	-0.0485	0.062
Asy_{θ_M}	0.0234	**0.007**	-0.00474	0.337
Asy_{Area_m}	0.312	0.23	-0.0336	0.298
Asy_{Area_M}	-0.112	0.329	-0.054	0.499
GoF_m	-0.189	0.767	0.242	0.126
GoF_M	-0.0927	0.982	0.145	0.329
SD_{GoF}	-0.0542	0.571	0.169	0.121
Spatio-temporal Domain				
	Mean characteristics			
Step time	-0.000443	$<$ **0.001**	-0.000235	0.1
Stance time	-0.000495	$<$ **0.001**	-0.000288	0.091
Swing time	-0.000419	$<$ **0.001**	-0.000195	0.113
Step length	-0.00134	$<$ **0.001**	-0.00115	0.135
Step velocity	-0.00199	$<$ **0.001**	-0.00125	0.158
	Variability (var) characteristics			
Step time var	-0.000729	$<$ **0.001**	-0.000639	**0.033**
Stance time var	-0.00079	$<$ **0.001**	-0.00056	**0.017**
Swing time var	-0.000771	$<$ **0.001**	-0.000608	0.059
Step length var	-0.000207	$<$ **0.001**	-0.000921	**0.049**
Step velocity var	-0.000264	$<$ **0.001**	-0.00121	**0.006**
	Asymmetry (asy) characteristics			
Step time asy	5.46e-05	0.247	-0.000325	**0.044**
Stance time asy	8.05e-05	0.147	-0.000421	**0.026**
Swing time asy	-0.00011	0.061	-0.00018	0.101
Step length asy	-3.07e-06	0.09	-0.000243	0.253
Step velocity asy	0.000131	0.157	-0.000473	0.015

Table 6.3: ANCOVA results of Phase and ST domain features progression as a function of age and Group.

Figure 6.7: The secondary feature $Asy_{\theta m}$ appears to show sensitivity to participant age but only in the control group.

Figure 6.8: As seen in 6.7 there is no significant trend in $Asy_{\theta m}$ relative to PD participants' age. This figure shows that, regardless of trends, the average PD value in this feature is consistently greater than that of the age-matched controls.

shown in Figure 6.6 and is most pronounced in real-world settings for the PD group.

Within the Phase domain, six features show significant increases with participant age, with five exhibiting interaction with disease group (PD). Interestingly, the nature and interpretation of this interaction is different between Phase and ST features. For example, in the case of ST features such as step time variability, age

and Group (PD) interact in a way which inflates or adds to the overall ageing effect i.e. the interaction is in the same direction as the main effect of ageing. Or more simply, any apparent trend in features with respect to ageing is greater in magnitude in the case of PD participants. This pattern is not reflected in the Phase domain features however. In several Phase domain features, e.g. Asy_{θ_m} their is a clear and significant ageing effect in the control group. The corresponding interaction with PD however, rather than adding to the main ageing effect, reverses it. This is more easily shown graphically Figures 6.7 and 6.8 where we can see the trend for CL subjects, despite a stable average value in PD subjects across the entire age range.

This phenomenon may be explained by the fact that for PD, medication is typically increased to decrease the rate of disease progression. Features such Asy_{θ_m} shown in Figure 6.8 are potentially dopa-sensitive features as their progression appears to be slowed/halted by PD medication [85]. Galna et al investigated the gait dysfunction in PD and the specific impact of medication over 18 months [14] and found that increased (Levodopa equivalent daily dose) was associated with reduced deterioration in several ST features, thus demonstrating their dopa-sensitivity.

The feature Asy_{θ_m}, defined in Equation (2), is related to asymmetries of gait and was shown to correlate negatively with measures of physical capability such as step length, velocity etc. It is therefore reasonable to submit that an increase in this feature is favourable from a clinical perspective. Considering this with the trend shown in Figure 6.7, we might conclude that control subjects' Phase domain features are more sensitive to ageing than PD subjects, which contradicts somewhat the general trend we have seen. However, when overlaying these plots (see Figure 6.8) we can see why this interpretation would be incorrect. While Asy_{θ_m} does significantly increase with age in CL subjects, PD values are consistently higher, or *worse*, at any given age. A more valid interpretation would then be that pathology

of PD subjects has accelerated the ageing effect to the extent that relatively young PD subjects (≈50 years old) have a similar value of Asy_{θ_m} to CL subjects aged 85 and above.

There are several questions which follow naturally from this. The lines of best fit shown in Figure 6.8 appear to meet at the right-most age value (≈ 95 years), suggesting that perhaps the effect of PD is insignificant at this age. Or perhaps that beyond this age CL subjects actually surpass PD subjects in terms of average Asy_{θ_m}, assuming the trend continues and does not simply plateau. These questions are impractical to address with the available data as they concern the upper age bracket present in the ICICLE-GAIT cohort, which introduces significant survivorship bias.

6.4.3 Environment

The vast majority of features from both the ST and Phase domains exhibit significant Environment:Timepoint interactions. This is expressed in Tables 6.1 and 6.2 as the effect of Real-World feature progression relative to Lab-based. This is not surprising as we have previously mentioned the substantial differences caused by recording protocol/environment. These results demonstrate the large degree to which Lab-based gait masks the progression of gait features. Only two features: Asy_{θ_m} and Asy_{Area_M}, do not have this interaction.

6.5 Discussion and Conclusions

Features from both the Phase and ST domain demonstrate significant progression up to 6 years following diagnosis. A subset of feature from each domain show particularly high progression in PD relative to CL. In the ST domain these are: step length (mean and variability), step time (mean), step velocity (mean and variability),

stance time, and swing time. In the Phase domain this subset is: γ (full ellipse eccentricity), Asy_θ (angle subtended by adjacent ellipses), and Asy_{γ_m} (eccentricity asymmetry in Type-II partial ellipses), see Figure 2.16.

For Phase domain features, in addition to sensitivity to ageing, we found evidence of PD accelerating the ageing process as early as 18 months following diagnosis. This increased sensitivity to age was also present to a lesser extent in ST features. Interestingly, features progression with respect to age did not appear to be masked by the highly controlled lab-based conditions. Overall, spatio-temporal features showed more sensitivity to participant age but Phase domain features generally showed a greater Age:PD interaction, i.e. Phase plot features highlight the increased effect of ageing in PD subjects relative to controls. This suggests that Phase domain features may not be *dopa-sensitive* [86] i.e. the progression of these features may be independent from dopamine replacement therapies.

All conclusions drawn from these analyses must be considered in the context of the participants' age range (see Table 3.1).

Unsurprisingly, results from Lab and Real-world gait accelerometry present very differently. The increased ADL associated with Real-World gait clearly reveals more progression in ST and Phase domain features than in Lab settings.

Chapter 7

Overview & Conclusions

7.1 Thesis Contributions

By adapting previously restrictive Phase plot methodology we have introduced a novel Phase domain of gait features. With the procedure outlined in Chapter 2, relatively short bouts of walking ($< 10s$) can reliably yield viable Phase plots. Key features of this procedure are the segmentation of gait accelerometry data via zero-crossing events rather than gait events (e.g. heel strikes), and the fitting of conic sections to all successive cycles, or *orbits*, that make up a given phase plot. Through cross-sectional analyses we have successfully demonstrated Phase plots' clinical relevance in monitoring of Parkinson's Disease (PD) with a single wearable accelerometer.

Longitudinal analysis showed that, similarly to traditional features, Phase domain features predictively evolve following diagnosis. Mixed effects models highlighted and isolated the impact of ageing on Phase domain features, allowing us to quantify the accelerated ageing process associated with PD. Phase plot features are categorised as either primary or secondary, with the latter being further categorised as type I or II (see Chapter 2). There was no apparent preference or advantage

to any of these categories, therefore we suggest that any future application explore alternate structures.

Phase plots proved to be a robust signature of gait reproducible in both lab and real-world recording environments. In addition, Phase plot Types provide a high level classification of gait which can be extracted on a per bout basis. Transitions between Phase plot Types are commonplace in real-world gait recordings, and were shown to be linked to significant changes in spatio-temporal features linked to physical capability.

Established features of the well-known spatio-temporal (ST) domain [15] provided an objective benchmark of against which we assessed the performance of the novel Phase domain and signature of gait. This benchmark supports the conclusion that Phase plots are a very promising tool for accelerometer-based gait analysis in pathological studies.

As expected, the impact of ADL on gait (recorded in real-world conditions) is substantial and clear in both the novel feature domain and traditional features. However, the now validated signature of gait is consistent across lab and real-world gait accelerometry. Between-timepoint transitions observed in lab data are consistently reproduced when analysing corresponding real-world gait data. This is a rare instance in which gait characteristics are not being masked by a highly controlled lab-based environment.

The phase domain of feature is also largely invariant under varying activity levels (total walking time per hour), unlike spatio-temporal features such as step length, velocity etc. This means that future studies need not rely on participants' mobility levels to produce their gait signature. This is particularly beneficial in less mobile cohorts. In terms of disease classification (PD vs Controls) the phase domain of features showed similar performance to traditional features. The best performance

is seen by combining both feature domains.

By including age-matched controls we have accurately quantified the sensitivity of Phase domain features, and their progression, to pathology while controlling for the ageing process. Between the compactness of the Phase plots and the low demand on participant activity, and hence data, the Phase domain and the accompanying signature of gait offer a unique and reliable snapshot of an individual's gait. In several analyses, improved performance was found by combining both traditional features with the novel Phase domain. We may infer from this that not only can the Phase domain perform well in itself, but should also be considered as an additional tool to augment analysis based on more traditional gait features. By modifying and validating this Phase plot methodology we have expanded the clinical application of Phase plots and built on previous work [18, 32], which has previously been almost exclusively limited to ECG analysis. In several of the analyses presented, the added value of the Phase domain was incremental, however, future studies which look to apply the domain in other clinical settings may find more prominent added value e.g. Phase domain features may compliment conventional features to better monitor response to therapy of other clinical interventions.

7.2 Limitations

Drop-out and attrition were unavoidable sources of variation. Although careful consideration was given to the imputation method a degree of survivorship bias was inevitable, especially in the upper age brackets and later follow-up timepoints.

Discretisation of activities levels, by bout length or otherwise, goes some way to addressing the variation caused by unannotated ADL in real-world gait data. However, there is considerable variety in daily activities which we cannot practically label and as such this represents an unobserved source of variation. There are

examples in the literature of ADL being fully annotated [40] by utilising footage from a body worn camera, although this requires considerable manual post-processing as well as the introduction of an addition wearable device. Analyses regarding the specific impacts of ageing and recording settings could be by controlling for patient increases in medication. This is usually done by calculating each patients Levodopa equivalent daily dose (LEDD) [85].

In the field of wearable technology, and moreover within accelerometer-based gait analysis, there is no universal standard practice for sensor location or configuration. Although there are several advantages to the particular protocol and sensor configuration within ICICLE-GAIT (discrete, central on the frontal plan, etc), this is no guarantee the novel methodologies presented here will perform similarly in other sensor configurations.

7.3 Further Research

In the early development stages of this novel Phase plot analysis, decisions were made with the initial objective of establishing a stable Phase plot methodology for continuous signals. Here, "stable" means that we can be confident that a general bout of walking from any participant will yield a Phase plot to which elliptical conics may be fitted to produce Phase domain features. This is not a trivial assumption and required several critical adaptations e.g. segmenting gait cycles via zero-crossing events in place of the more familiar gait events (e.g. heel strikes). The current state of the methodology may be considered a minimal viable product (MVP). Having validated this MVP and the utility of Phase plots, a sensitivity analysis should be conducted to assess the impact of varying these adaptations as well as the following factors:

- Method of smoothing accelerometry data.
- Gait segmentation by zero-crossing instead of IC and how this may be impacted by postural (in)stability.
- Sensor setup and configuration:

  What are the benefits associated with different sampling frequencies?

  Sensor location e.g. wrist, ankle, trunk etc. How well does this Phase plot methodology generalise with respect to sensor location.

  The augmentation of this feature domain with other signals e,g, gyroscopic data.

Honing the procedure for Phase plot construction and subsequent feature derivation is a necessary step in producing a fully generalisable tool applicable to a wide range periodic bio-signals.

Chapter 8

Appendix

8.1 Lab-based addition figures

8.1.1 densities

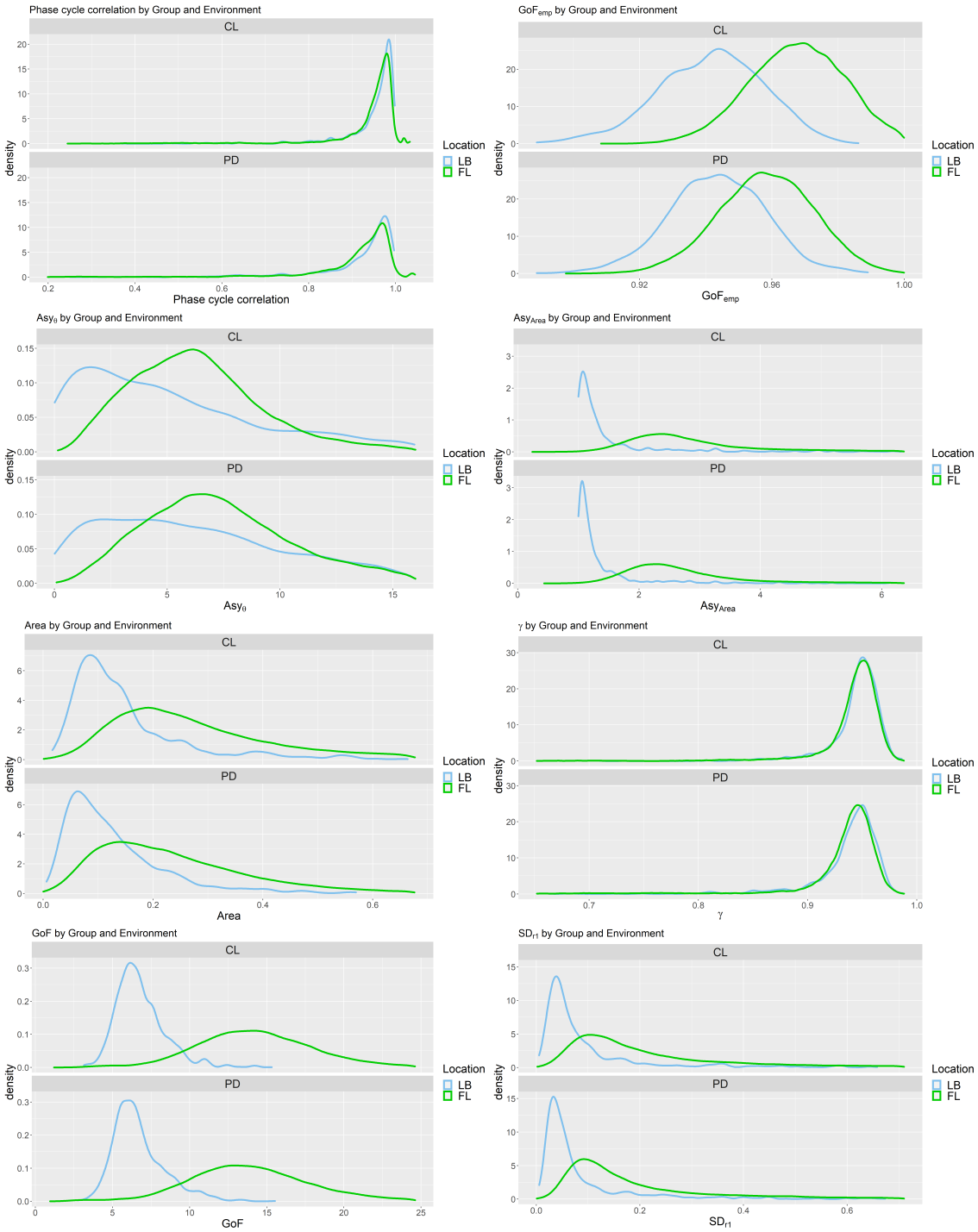

Figure 8.1: All Phase and ST density plots for both disease groups. Lab-based and real world. 1-8 of 36

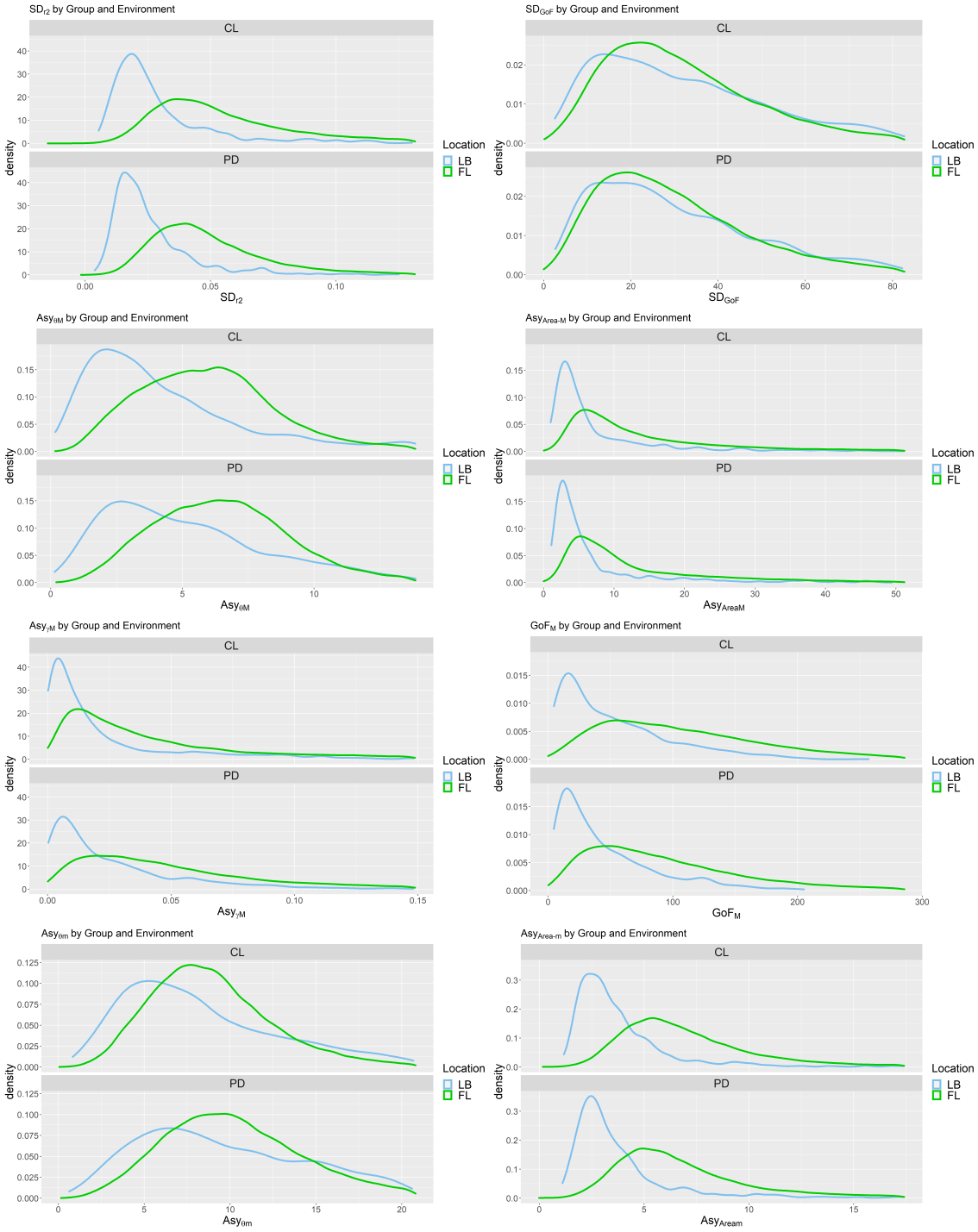

Figure 8.2: All Phase and ST density plots for both disease groups. Lab-based and real world. 9-16 of 36

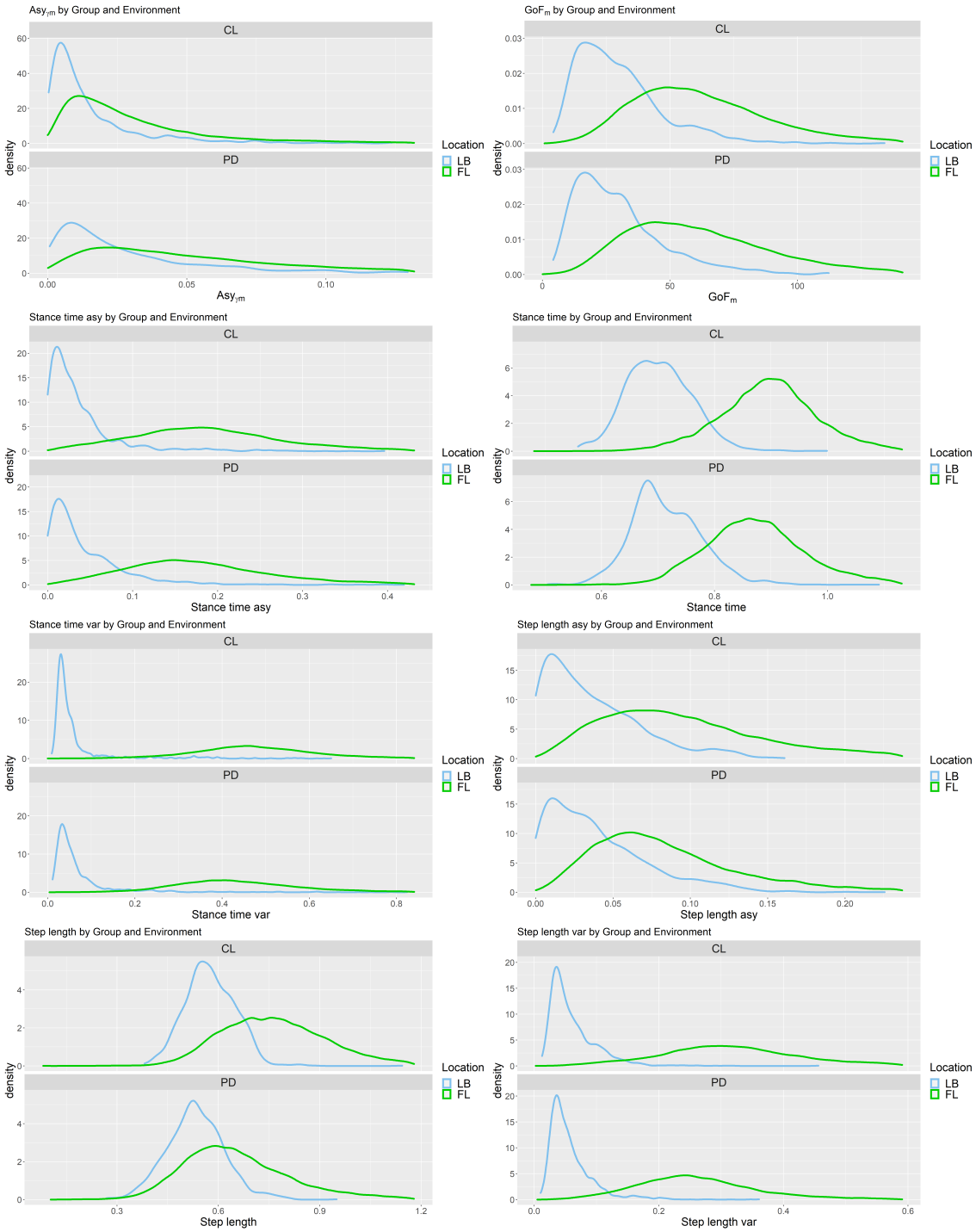

Figure 8.3: All Phase and ST density plots for both disease groups. Lab-based and real world. 17-24 of 36

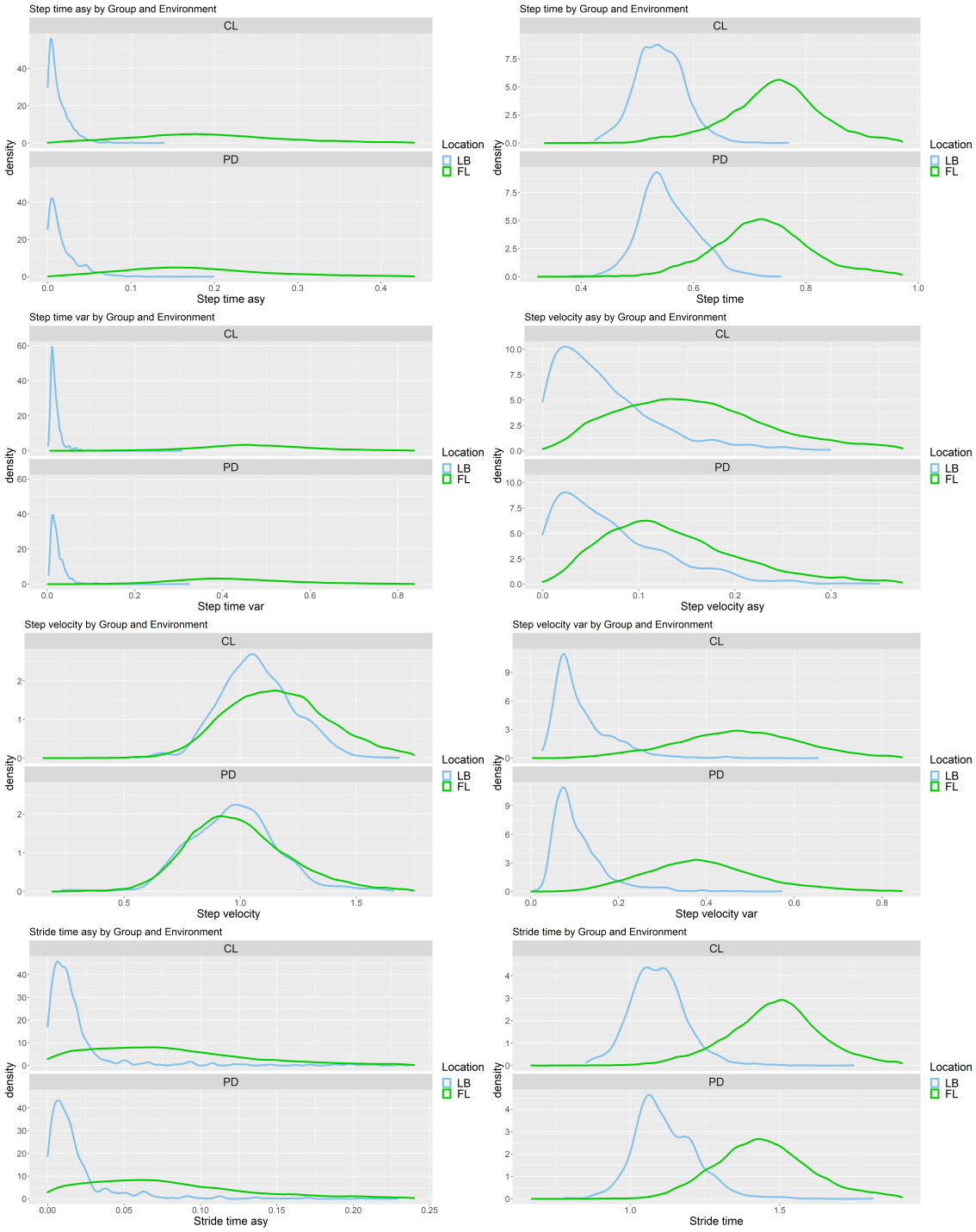

Figure 8.4: All Phase and ST density plots for both disease groups. Lab-based and real world. 25-32 of 36

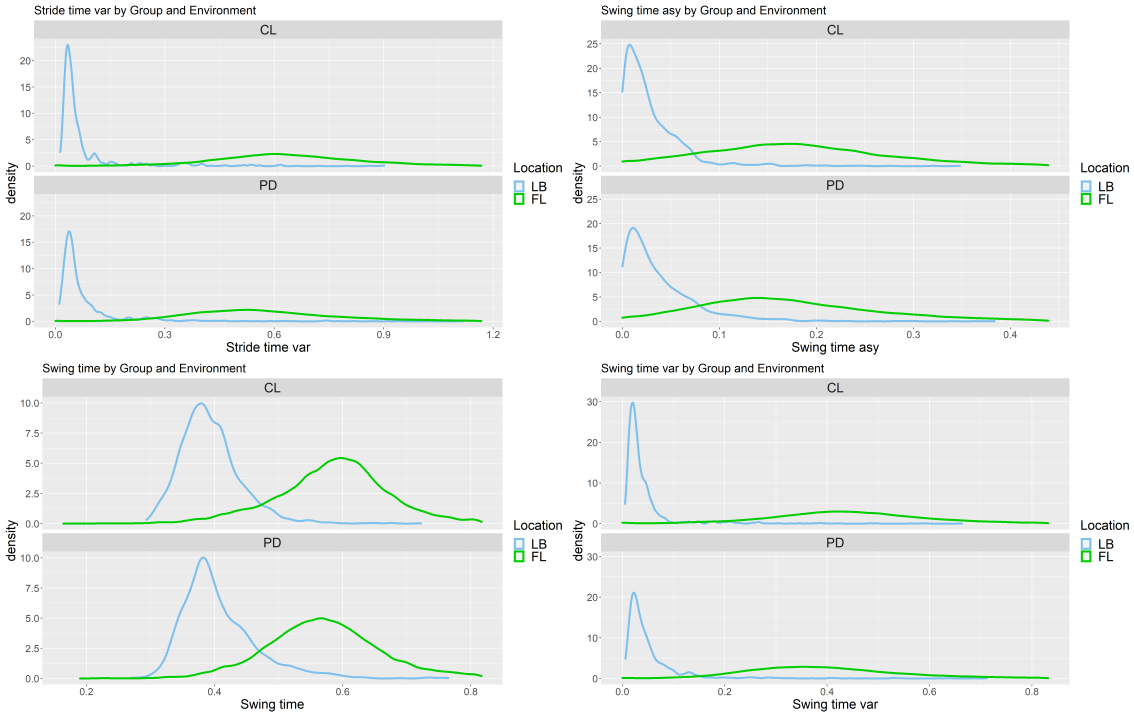

Figure 8.5: All Phase and ST density plots for both disease groups. Lab-based and real world. 33-36 of 36

8.1.2 Box-plots

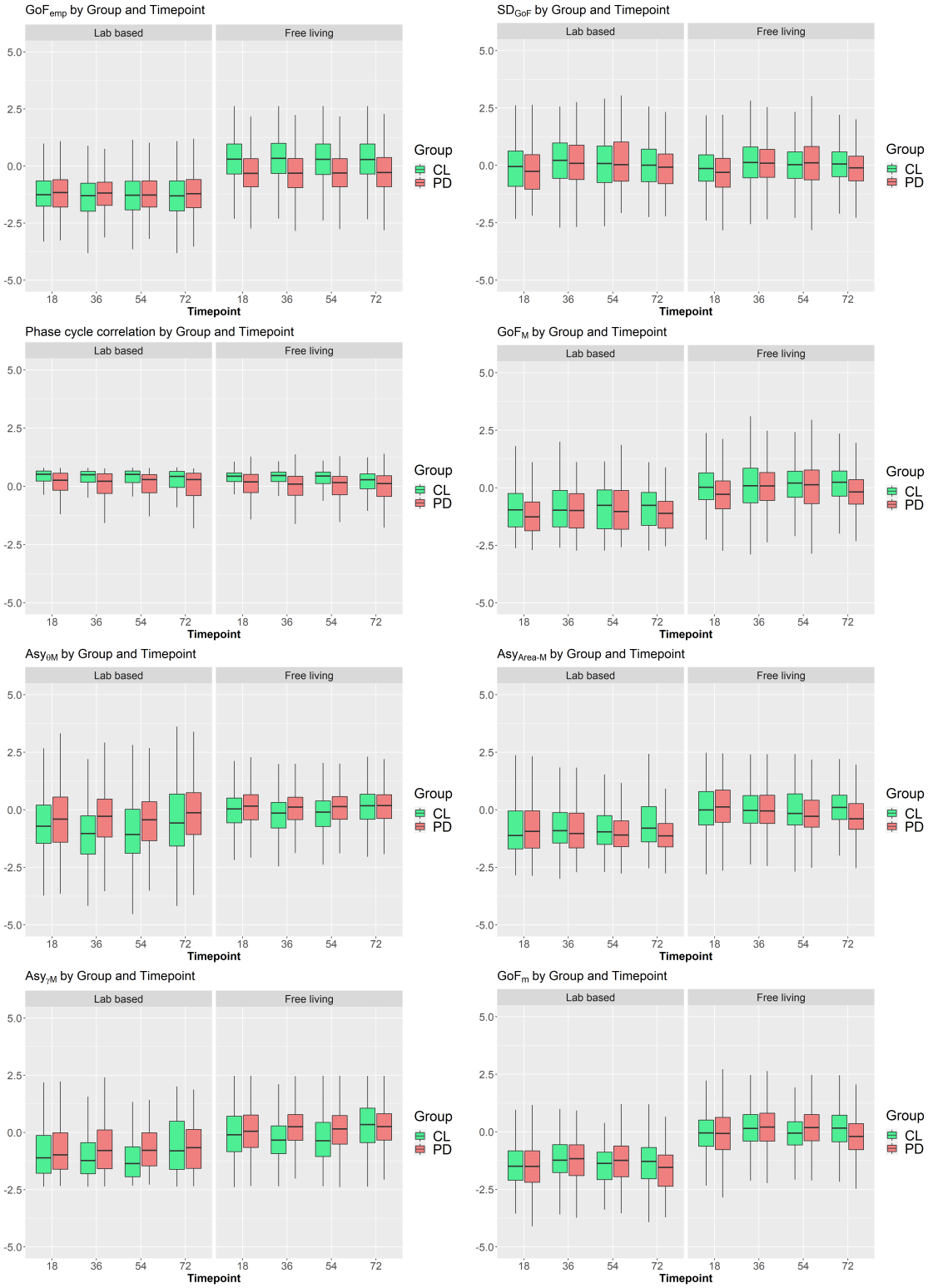

Figure 8.6: All Phase and ST box plots by disease groups. Lab-based and real world. 1-8 of 36

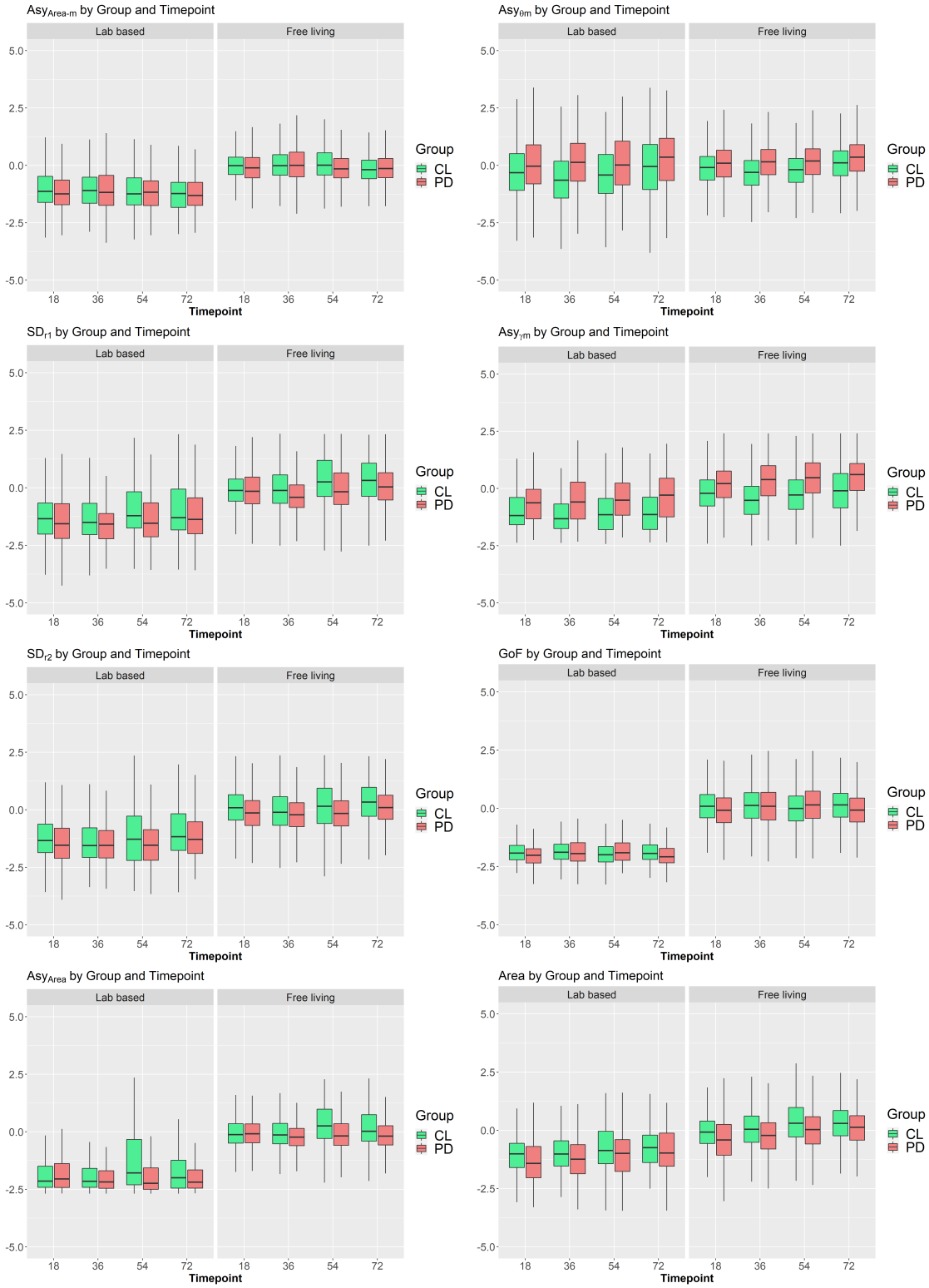

Figure 8.7: All Phase and ST box plots by disease groups. Lab-based and real world. 9-16 of 36

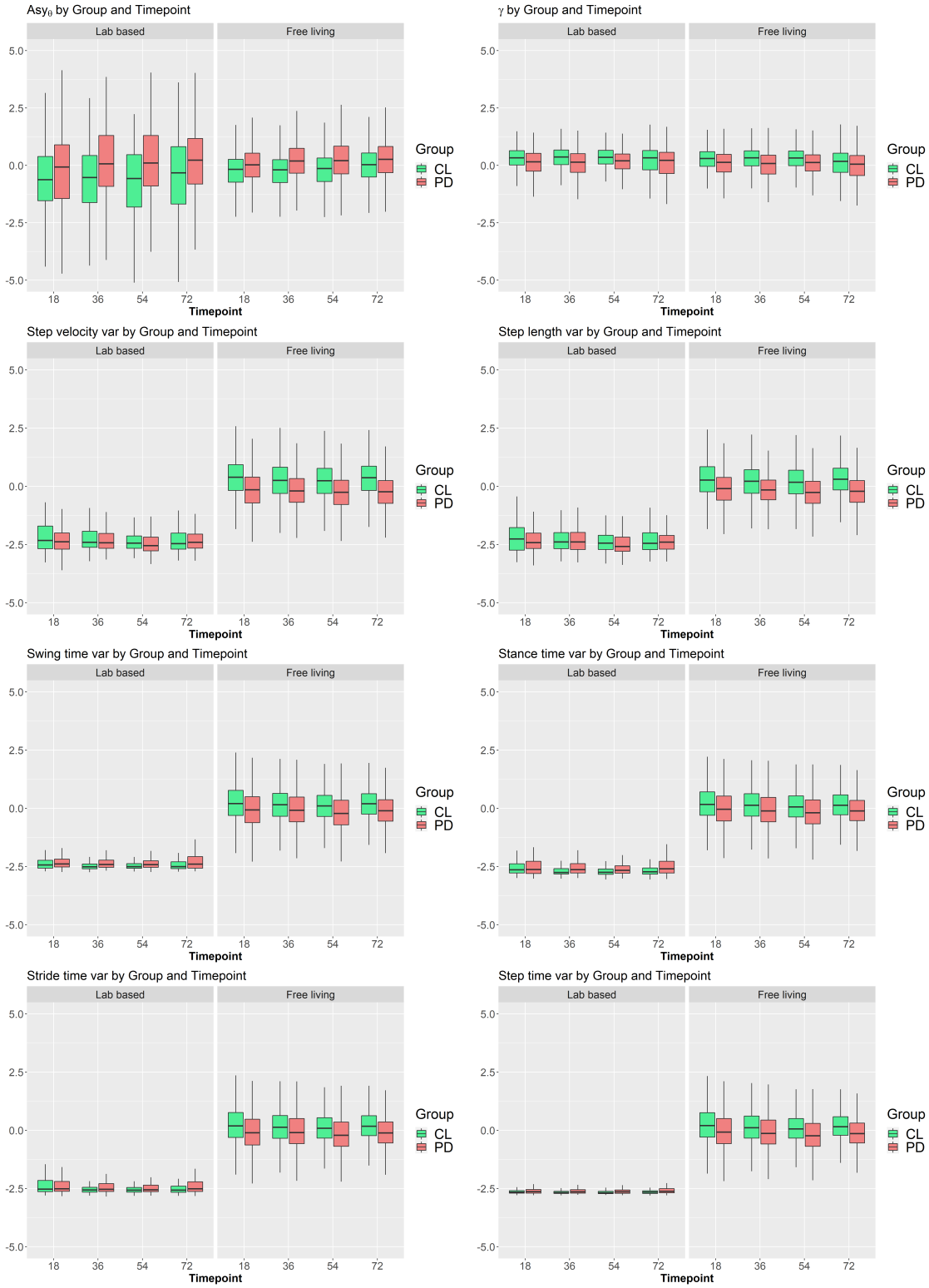

Figure 8.8: All Phase and ST box plots by disease groups. Lab-based and real world. 17-23 of 36

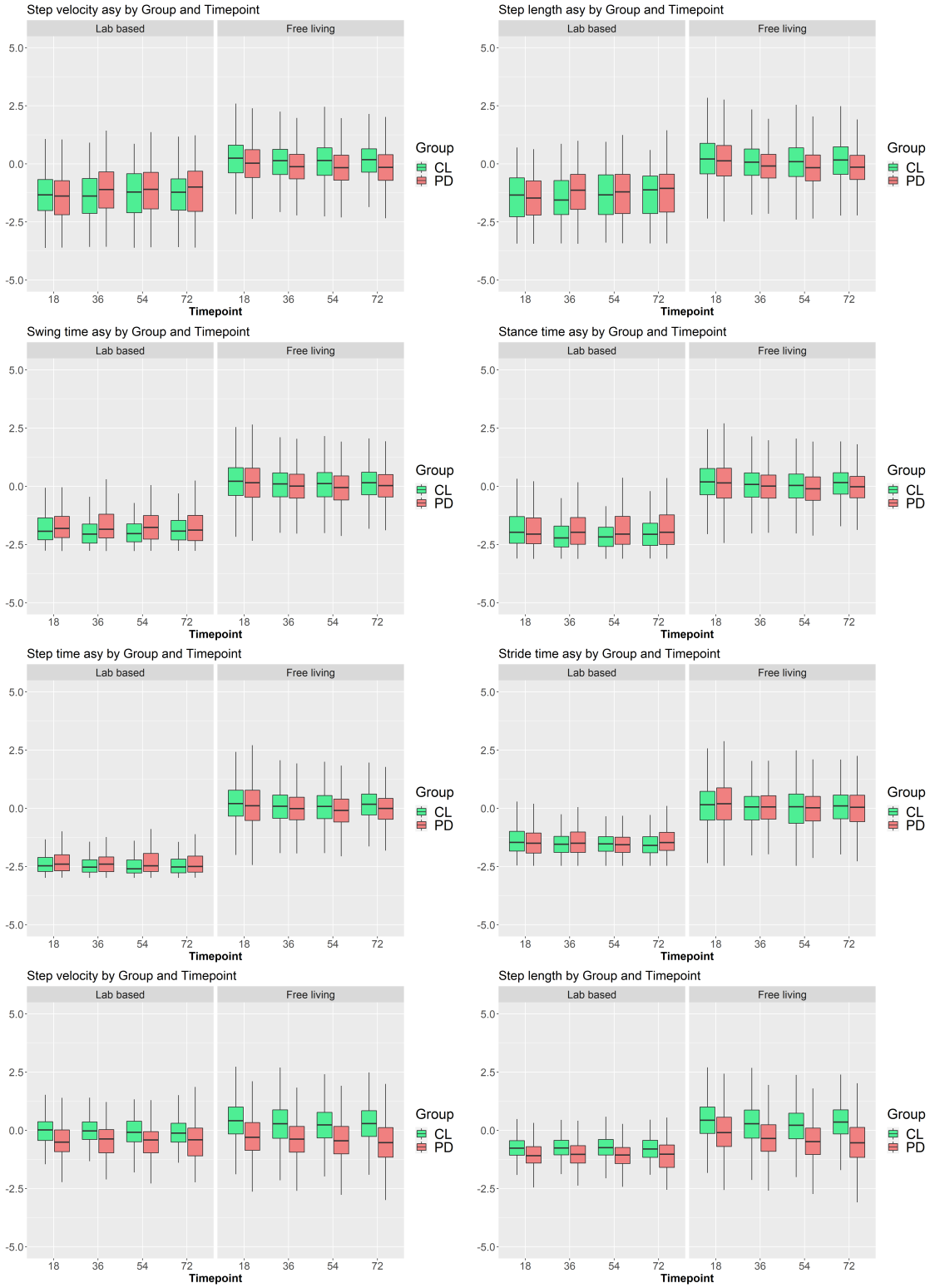

Figure 8.9: All Phase and ST box plots by disease groups. Lab-based and real world. 24-31 of 36

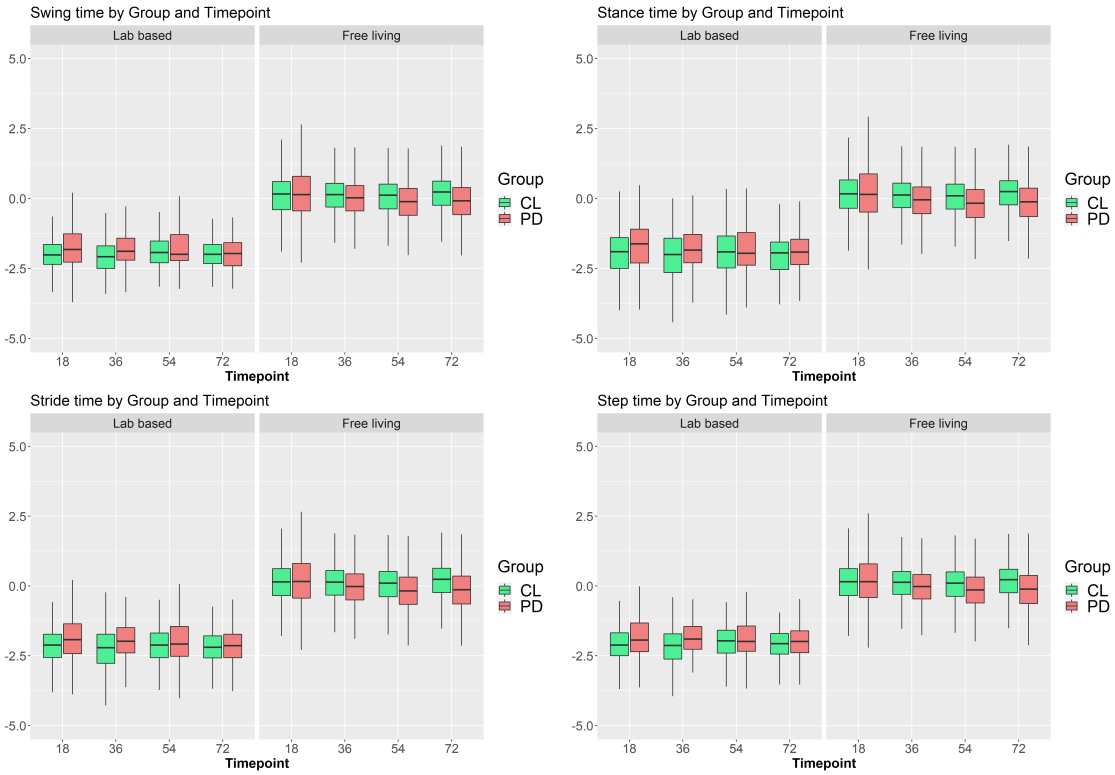

Figure 8.10: All Phase and ST box plots by disease groups. Lab-based and real world. 32-36 of 36

8.1.3 QQ-plots

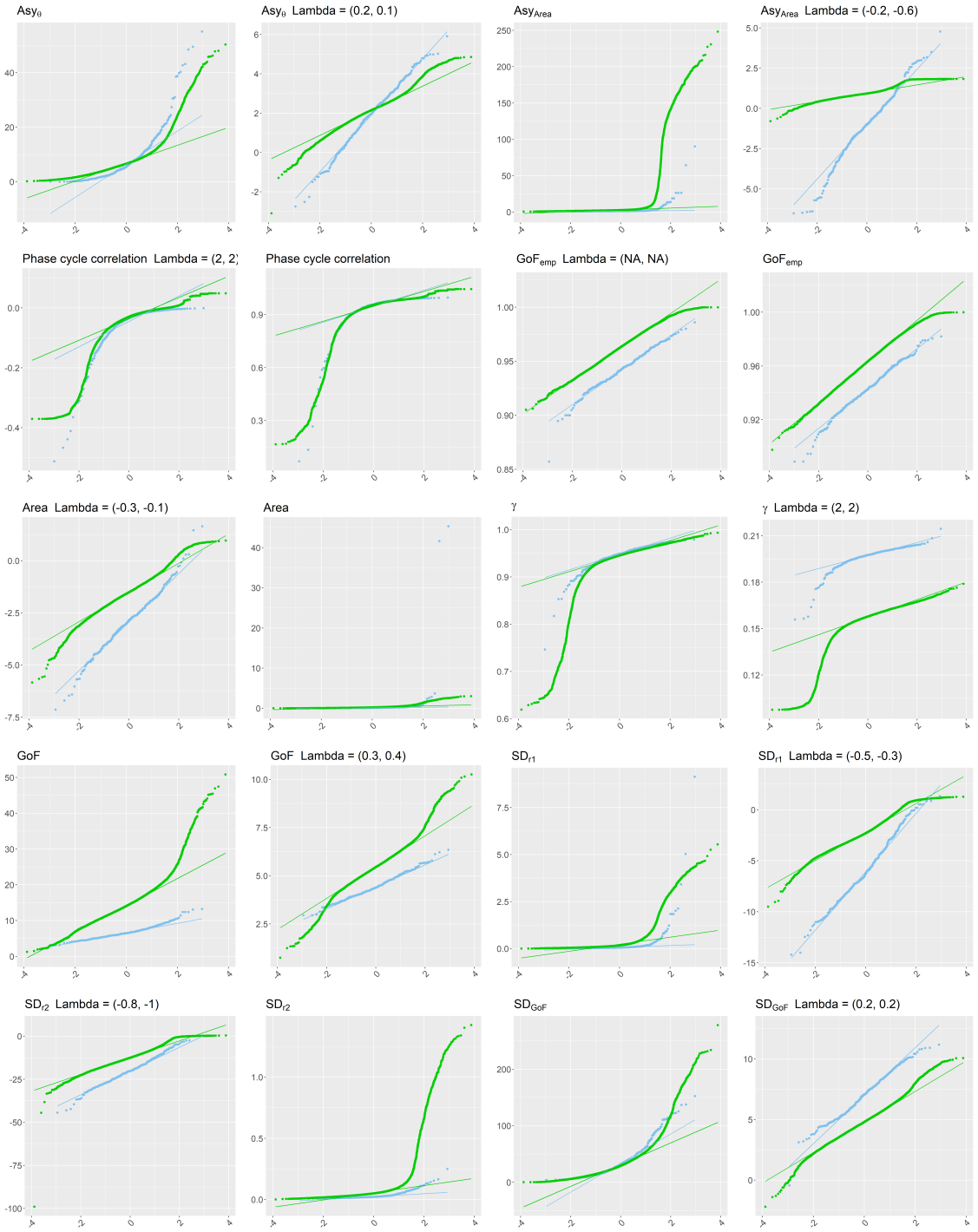

Figure 8.11: All Phase and ST QQ-plots for both Lab-based (blue) and real world (green). Raw features (column 1 and 3) and following Box–Cox transformation (columns 2 and 4). Estimated BC parameters shown in figure titles (Lab and real world respectively). Features 1-10 of 36

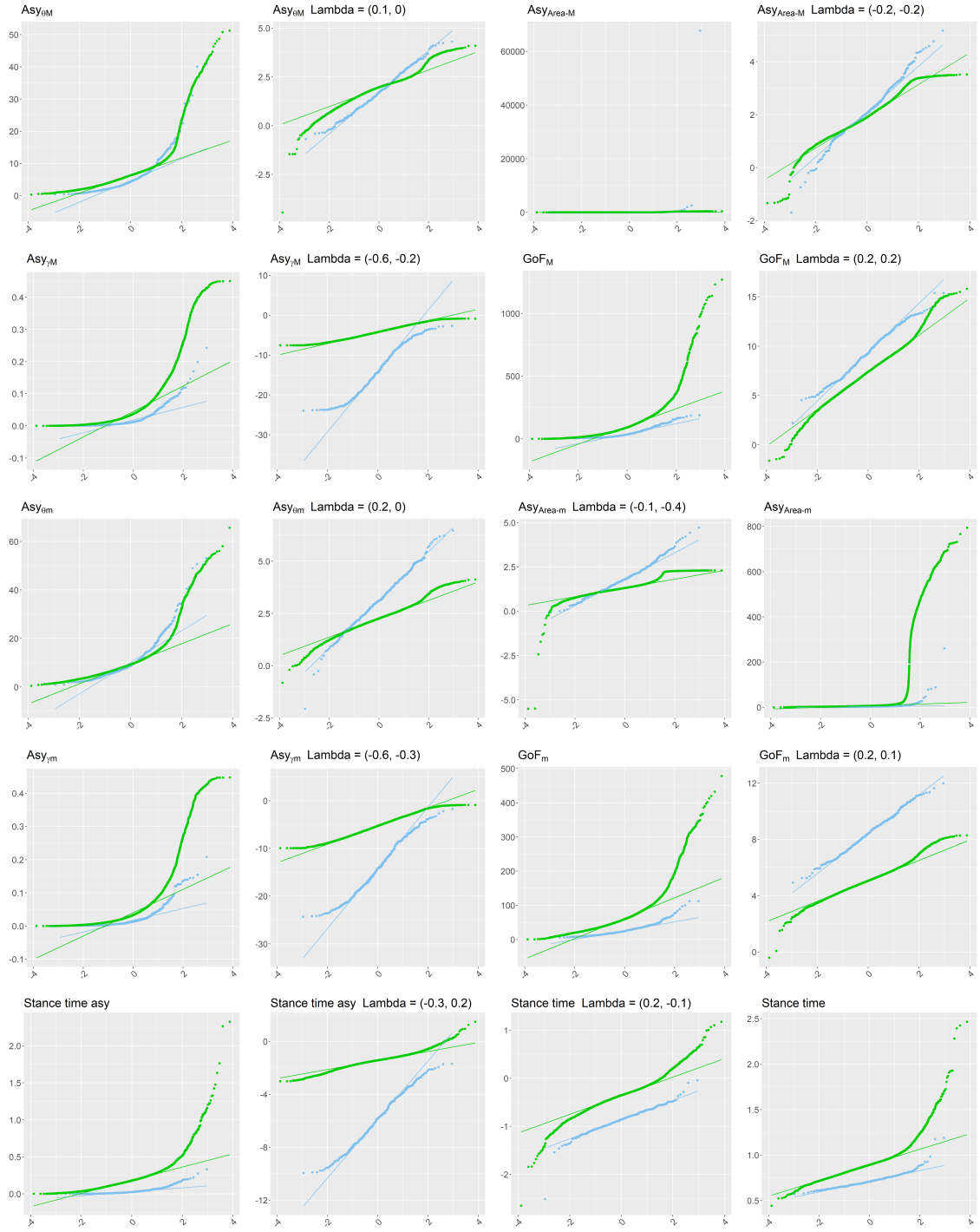

Figure 8.12: All Phase and ST QQ-plots for both Lab-based (blue) and real world (green). Raw features (column 1 and 3) and following Box–Cox transformation (columns 2 and 4). Estimated BC parameters shown in figure titles (Lab and real world respectively). Features 11-20 of 36

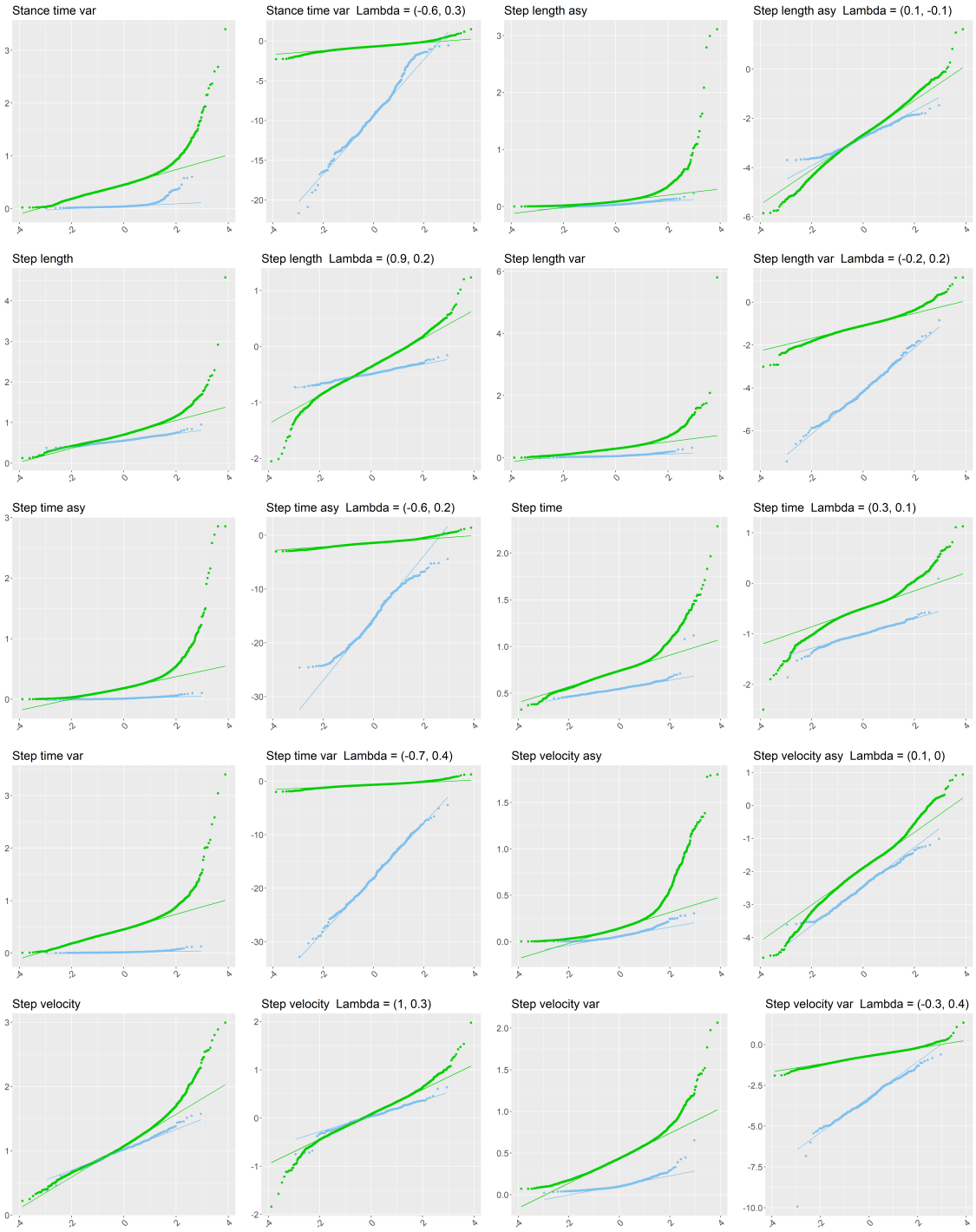

Figure 8.13: All Phase and ST QQ-plots for both Lab-based (blue) and real world (green). Raw features (column 1 and 3) and following Box–Cox transformation (columns 2 and 4). Estimated BC parameters shown in figure titles (Lab and real world respectively). Features 21-30 of 36

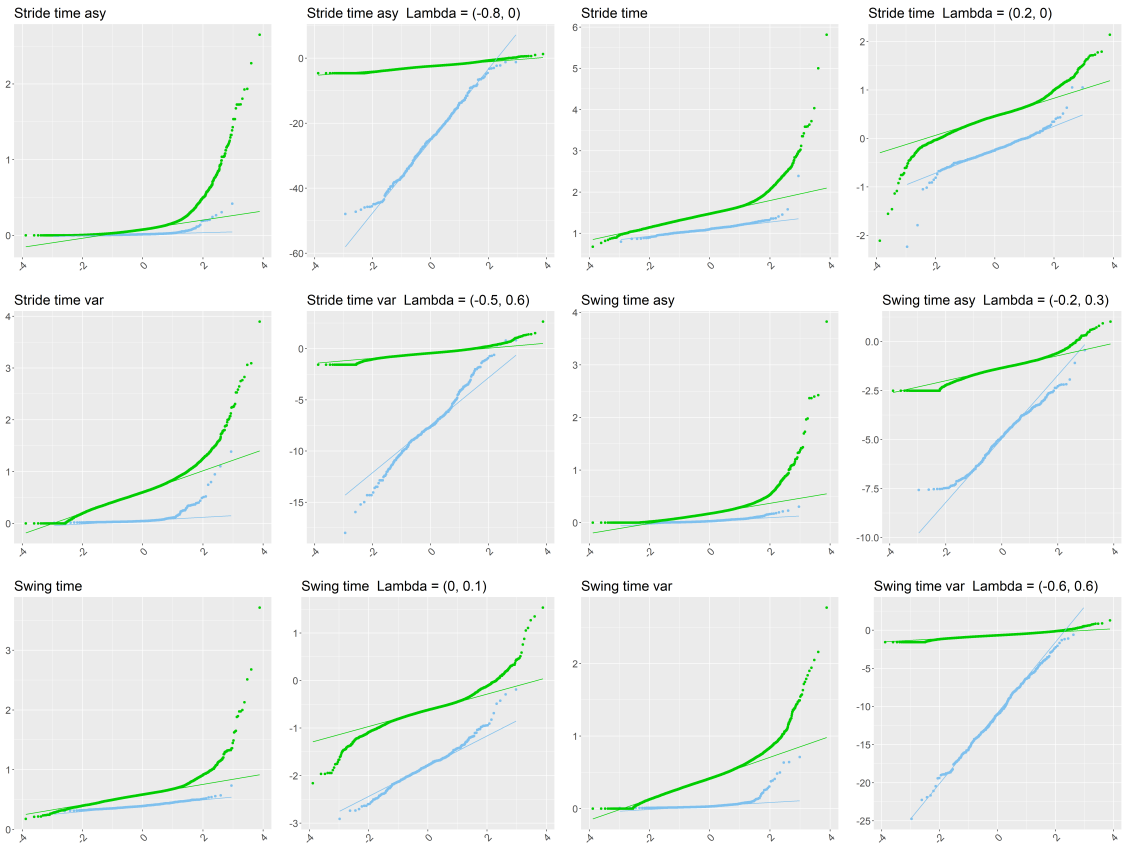

Figure 8.14: All Phase and ST QQ-plots for both Lab-based (blue) and real world (green). Raw features (column 1 and 3) and following Box–Cox transformation (columns 2 and 4). Estimated BC parameters shown in figure titles (Lab and real world respectively). Features 30-36 of 36

8.2 Confidence intervals

Fixed effect	95% Confidence interval
ST domain	
PC1	(0.22, 0.38)
PC2	(-0.25, -0.029)
PC3	(-0.46, -0.034)
PC4	(-1.08, -0.51)
Phase domain	
PC1	(-0.230, -0.067)
PC2	(0.33, 0.53)
PC3	(-0.58, -0.29)
PC4	(-0.43, -0.017)
All features	
PC1	(0.262, 0.399)
PC2	(0.061, 0.23)
PC3	(0.013, 0.22)
PC4	(-0.57, -0.29)

Table 8.1: Fixed effects Confidence intervals associated with Table 4.7

8.3 least squares ellipse fitting

8.3.1 derivation

$$\frac{\partial Cost(A)}{\partial b} = \sum_{i=1}^{n} 2x_i y_i (ax_i^2 + bx_i y_i + cy_i^2 + dx_i + ey_i + 1) = 0 \tag{8.1}$$

Assuming that the coefficient of xy in 2.1 is non-zero we wish to find the conic equation of the untilted ellipse 8.2. We can find the parameters of this untilted conic equation 8.2 by making a substitution to the previous tilted equation such that x is substituted with $Cx + Sy$ and y with $-Sx + Cy$ where $C = cos(\phi)$ and $S = sin(\phi)$ giving us the conic representation:

$$a(Cx+Sy)^2+b(Cx+Sy)(-Sx+Cy)+c(-Sx+Cy)^2+d(Cx+Sy)+e(-Sx+Cy)+F = 0$$

which gives an xy coefficient of $2aCS + (C^2 - S^2)b - 2cCS$

$$a'x^2 + c'y^2 + d'x + e'y + 1 = 0 \tag{8.2}$$

To find the value of ϕ which yields the untilted ellipse, we set this coefficient to zero and simplify:

$$2aCS - 2cCS + bcos(2\phi) = 0$$

$$\implies 2CS(a - c) + bcos(2\phi) = 0$$

$$\implies sin(2\phi)(a - c) + bcos(2\phi) = 0$$

$$\implies -sin(2\phi)(a - c)/bcos(2\phi) = 1$$

$$\implies \phi = \frac{arctan(b/(c - a))}{2}$$

Now the values of S and C can be found and the other constants a', c', d', e' can be similarly found as the coefficients of the other terms:

$$a' = aC^2 - bCS + cS^2$$

$$c' = aS^2 + bCS + cC^2$$

$$d' = dC - eS$$

$$e' = dS + eC$$

Re-writing equation 8.2 by completing the square twice gives:

$$a'(x + \frac{d'}{2a'})^2 + c'(y + \frac{e'}{2c'})^2 - \frac{d'^2}{4a'} - \frac{e'^2}{4c'} = 0$$

which can be written as

$$\frac{a'(x+\frac{d'}{2a'})^2}{l}+\frac{c'(y+\frac{e'}{2c'})^2}{l}=1 \tag{8.3}$$

where $l=\frac{d'^2}{4a'}+\frac{e'^2}{4c'}$.

From 8.3 we can compare with the geometric form 2.3 and read off the values: $x_0^u=-\frac{d'}{2a'}$, $y_0^u=-\frac{e'}{2c'}$, $r_1=\sqrt{|\frac{a'}{l}|}$ and $r_2=\sqrt{|\frac{c'}{l}|}$.

$$\begin{aligned}
a\Sigma x^4+b\Sigma x^3y+c\Sigma x^2y^2+d\Sigma x^3+e\Sigma x^2y&=-\Sigma x^2\\
a\Sigma x^3y+b\Sigma x^2y^2+c\Sigma xy^3+d\Sigma x^2y+e\Sigma xy^2&=-\Sigma xy\\
a\Sigma x^2y^2+b\Sigma xy^3+c\Sigma y^4+d\Sigma xy^2+e\Sigma y^3&=-\Sigma y^2\\
a\Sigma x^3+b\Sigma x^2y+c\Sigma xy^2+d\Sigma x^2+e\Sigma yx&=-\Sigma x\\
a\Sigma x^2y+b\Sigma xy^2+c\Sigma y^3+d\Sigma xy+e\Sigma y^2&=-\Sigma y
\end{aligned} \tag{8.4}$$

Where $\Sigma x^2y=\sum_{i=1}^{n}x_i^2y_i$ etc.

8.3.2 code

```
function [] = Ell_conic_fitting(x, y, fitted_ell)


mean_x = mean(x);

mean_y = mean(y);

x = x-mean_x;

y = y-mean_y;


x_1 = sum(x);

y_1 = sum(y);

x_2 = sum(x.^2);
```

```
y_2 = sum(y.^2);

x_3 = sum(x.^3);

y_3 = sum(y.^3);

x_4 = sum(x.^4);

y_4 = sum(y.^4);

xy = sum(x.*y);

x2y2 = sum((x.^2).*(y.^2));

xy_2 = sum(x.*(y.^2));

yx_2 = sum(y.*(x.^2));

xy_3 = sum(x.*(y.^3));

yx_3 = sum(y.*(x.^3));


A = [x_4 yx_3 x2y2 x_3 yx_2 ;

yx_3 x2y2  xy_3 yx_2 xy_2  ;

x2y2 xy_3 y_4 xy_2 y_3  ;

x_3 yx_2 xy_2 x_2 xy  ;

yx_2 xy_2 y_3 xy y_2 ];



B = [x_2 xy y_2 x_1 y_1]';

X = linsolve(A,B);


phi_hat = (atan(X(2) / (X(3) - X(1)))/2);


S = sin(phi_hat);

C = cos(phi_hat);
```

```
a = round(X(1), 5);

b = round(X(2), 5);

c = round(X(3), 5);

d = round(X(4), 5);

e = round(X(5), 5);


A = [a b, c, d, e];

X = [x.^2; x.*y; y.^2; x; y];


SS = sum((A*X).^2);

NEW_MSS = SS/length(x);

fprintf('NEW_MSS = %f', NEW_MSS)


if b^2 - (4*a*c) > 0

disp('Not ellipse!')

end


a_ = a*C^2 - b*C*S + c*S^2;

c_ = a*S^2 + b*C*S + c*C^2;

d_ = d*C -e*S;

e_ = d*S + e*C;


x_0u = mean_x -d_/(2*a_);

y_0u = mean_y -e_/(2*c_);
```

```
x_0 = x_0u*C + y_0u*S;

y_0 = x_0u*-S + y_0u*C;


l = (d_^2/(4*a_)) + (e_^2/(4*c_)) + 1;


h = sqrt(abs(l/a_));

k = sqrt(abs(l/c_));


M = max(h, k);

m = min(h, k);


end
```

Bibliography

[1] S. Del Din, A. Godfrey, B. Galna, S. Lord, and L. Rochester, "Free-living gait characteristics in ageing and parkinson's disease: impact of environment and ambulatory bout length," *Journal of neuroengineering and rehabilitation*, vol. 13, no. 1, pp. 1–12, 2016.

[2] S. Del Din, A. Godfrey, C. Mazzà, S. Lord, and L. Rochester, "Free-living monitoring of parkinson's disease: Lessons from the field," *Movement Disorders*, vol. 31, no. 9, pp. 1293–1313, 2016.

[3] S. Del Din, C. Kirk, A. J. Yarnall, L. Rochester, and J. M. Hausdorff, "Body-worn sensors for remote monitoring of parkinson's disease motor symptoms: Vision, state of the art, and challenges ahead," *Journal of Parkinson's disease*, no. Preprint, pp. 1–13, 2021.

[4] N. Scafetta, D. Marchi, and B. J. West, "Understanding the complexity of human gait dynamics," *Chaos: An Interdisciplinary Journal of Nonlinear Science*, vol. 19, no. 2, p. 026108, 2009.

[5] P. C. Grabiner, S. T. Biswas, and M. D. Grabiner, "Age-related changes in spatial and temporal gait variables," *Archives of physical medicine and rehabilitation*, vol. 82, no. 1, pp. 31–35, 2001.

[6] K. C. Moisio, D. R. Sumner, S. Shott, and D. E. Hurwitz, "Normalization

of joint moments during gait: a comparison of two techniques," *Journal of biomechanics*, vol. 36, no. 4, pp. 599–603, 2003.

[7] D. Chen, Y. Cai, X. Qian, R. Ansari, W. Xu, K.-C. Chu, and M.-C. Huang, "Bring gait lab to everyday life: Gait analysis in terms of activities of daily living," *IEEE Internet of Things Journal*, vol. 7, no. 2, pp. 1298–1312, 2019.

[8] C. A. McGibbon, "Toward a better understanding of gait changes with age and disablement: neuromuscular adaptation," *Exercise and sport sciences reviews*, vol. 31, no. 2, pp. 102–108, 2003.

[9] H. H. Atkinson, C. Rosano, E. M. Simonsick, J. D. Williamson, C. Davis, W. T. Ambrosius, S. R. Rapp, M. Cesari, A. B. Newman, T. B. Harris, *et al.*, "Cognitive function, gait speed decline, and comorbidities: the health, aging and body composition study," *The Journals of Gerontology Series A: Biological Sciences and Medical Sciences*, vol. 62, no. 8, pp. 844–850, 2007.

[10] K. S. Al-Zahrani and M. O. Bakheit, "A historical review of gait analysis," *Neurosciences Journal*, vol. 13, no. 2, pp. 105–108, 2008.

[11] G. A. Cavagna, F. P. Saibene, and R. Margaria, "External work in walking," *Journal of applied physiology*, vol. 18, no. 1, pp. 1–9, 1963.

[12] A. D. Kuo, "The six determinants of gait and the inverted pendulum analogy: A dynamic walking perspective," *Human movement science*, vol. 26, no. 4, pp. 617–656, 2007.

[13] A. Steindler, "A historical review of the studies and investigations made in relation to human gait," *JBJS*, vol. 35, no. 3, pp. 540–728, 1953.

[14] B. Galna, S. Lord, D. J. Burn, and L. Rochester, "Progression of gait dysfunction in incident parkinson's disease: impact of medication and phenotype," *Movement Disorders*, vol. 30, no. 3, pp. 359–367, 2015.

[15] S. Del Din, A. Godfrey, and L. Rochester, "Validation of an accelerometer to quantify a comprehensive battery of gait characteristics in healthy older adults and parkinson's disease: toward clinical and at home use," *IEEE journal of biomedical and health informatics*, vol. 20, no. 3, pp. 838–847, 2015.

[16] A. K. Golińska, "Poincaré plots in analysis of selected biomedical signals," *Studies in logic, grammar and rhetoric*, vol. 1, no. 35, pp. 117–127, 2013.

[17] A. Goshvarpour and A. Goshvarpour, "Diagnosis of epileptic eeg using a lagged poincare plot in combination with the autocorrelation," *Signal, Image and Video Processing*, vol. 14, no. 7, pp. 1309–1317, 2020.

[18] P. Esser, H. Dawes, J. Collett, and K. Howells, "Insights into gait disorders: walking variability using phase plot analysis, parkinson's disease," *Gait & posture*, vol. 38, no. 4, pp. 648–652, 2013.

[19] A. Cappozzo, U. Della Croce, A. Leardini, and L. Chiari, "Human movement analysis using stereophotogrammetry: Part 1: theoretical background," *Gait & posture*, vol. 21, no. 2, pp. 186–196, 2005.

[20] S. Del Din, E. Carraro, Z. Sawacha, A. Guiotto, L. Bonaldo, S. Masiero, and C. Cobelli, "Impaired gait in ankylosing spondylitis," *Medical & biological engineering & computing*, vol. 49, no. 7, pp. 801–809, 2011.

[21] C. Buckley, L. Alcock, R. McArdle, R. Z. U. Rehman, S. Del Din, C. Mazzà, A. J. Yarnall, and L. Rochester, "The role of movement analysis in diagnosing

and monitoring neurodegenerative conditions: Insights from gait and postural control," *Brain sciences*, vol. 9, no. 2, p. 34, 2019.

[22] I. Hillel, L. Avanzino, A. Cereatti, M. O. Rikkert, S. D. Din, P. Ginis, A. Mirelman, and J. M. Hausdorff, "Wearables reveal a gap between gait performance in the lab and during 24/7 monitoring in older adults," *Innovation in Aging*, vol. 3, no. Supplement_1, pp. S335–S335, 2019.

[23] W. Maetzler, L. Rochester, R. Bhidayasiri, A. J. Espay, A. Sánchez-Ferro, and J. M. van Uem, "Modernizing daily function assessment in parkinson's disease using capacity, perception, and performance measures," *Movement Disorders*, vol. 36, no. 1, pp. 76–82, 2021.

[24] A. Atrsaei, M. F. Corrà, F. Dadashi, N. Vila-Chã, L. Maia, B. Mariani, W. Maetzler, and K. Aminian, "Gait speed in clinical and daily living assessments in parkinson's disease patients: performance versus capacity," *npj Parkinson's Disease*, vol. 7, no. 1, pp. 1–11, 2021.

[25] S. Lord, B. Galna, J. Verghese, S. Coleman, D. Burn, and L. Rochester, "Independent domains of gait in older adults and associated motor and nonmotor attributes: validation of a factor analysis approach," *Journals of Gerontology Series A: Biomedical Sciences and Medical Sciences*, vol. 68, no. 7, pp. 820–827, 2013.

[26] I. Galperin, I. Hillel, S. Del Din, E. M. Bekkers, A. Nieuwboer, G. Abbruzzese, L. Avanzino, F. Nieuwhof, B. R. Bloem, L. Rochester, *et al.*, "Associations between daily-living physical activity and laboratory-based assessments of motor severity in patients with falls and parkinson's disease," *Parkinsonism & related disorders*, vol. 62, pp. 85–90, 2019.

[27] T. d. O. Sato, G.-Å. Hansson, and H. J. C. G. Coury, "Goniometer crosstalk compensation for knee joint applications," *Sensors*, vol. 10, no. 11, pp. 9994–10005, 2010.

[28] M. Dunne-Willows, P. Watson, J. Shi, L. Rochester, D. Del, *et al.*, "A novel parameterisation of phase plots for monitoring of parkinson's disease," 2019.

[29] M. Brennan, M. Palaniswami, and P. Kamen, "Do existing measures of poincare plot geometry reflect nonlinear features of heart rate variability?," *IEEE transactions on biomedical engineering*, vol. 48, no. 11, pp. 1342–1347, 2001.

[30] J. Piskorski and P. Guzik, "Geometry of the poincaré plot of rr intervals and its asymmetry in healthy adults," *Physiological measurement*, vol. 28, no. 3, p. 287, 2007.

[31] P. W. Kamen, H. Krum, and A. M. Tonkin, "Poincare plot of heart rate variability allows quantitative display of parasympathetic nervous activity in humans," *Clinical science*, vol. 91, no. 2, pp. 201–208, 1996.

[32] M. Fishman, F. J. Jacono, S. Park, R. Jamasebi, A. Thungtong, K. A. Loparo, and T. E. Dick, "A method for analyzing temporal patterns of variability of a time series from poincare plots," *Journal of applied physiology*, vol. 113, no. 2, pp. 297–306, 2012.

[33] G. Rigas, P. Bougia, D. Baga, M. Tsipouras, A. Tzallas, E. Tripoliti, S. Tsouli, M. Chondrogiorgi, S. Konitsiotis, and D. I. Fotiadis, "A decision support tool for optimal levodopa administration in parkinson's disease," pp. 1–6, 2010.

[34] P. L. Rosin, "A note on the least squares fitting of ellipses," *Pattern Recognition Letters*, vol. 14, no. 10, pp. 799–808, 1993.

[35] T. K. Khoo, A. J. Yarnall, G. W. Duncan, S. Coleman, J. T. O'Brien, D. J. Brooks, R. A. Barker, and D. J. Burn, "The spectrum of nonmotor symptoms in early parkinson disease," *Neurology*, vol. 80, no. 3, pp. 276–281, 2013.

[36] C. G. Goetz, B. C. Tilley, S. R. Shaftman, G. T. Stebbins, S. Fahn, P. Martinez-Martin, W. Poewe, C. Sampaio, M. B. Stern, R. Dodel, *et al.*, "Movement disorder society-sponsored revision of the unified parkinson's disease rating scale (mds-updrs): scale presentation and clinimetric testing results," *Movement disorders: official journal of the Movement Disorder Society*, vol. 23, no. 15, pp. 2129–2170, 2008.

[37] R. Rosin, H. Topka, and J. Dichgans, "Gait initiation in parkinson's disease," *Movement disorders: official journal of the Movement Disorder Society*, vol. 12, no. 5, pp. 682–690, 1997.

[38] C. J. Hass, D. E. Waddell, R. P. Fleming, J. L. Juncos, and R. J. Gregor, "Gait initiation and dynamic balance control in parkinson's disease," *Archives of physical medicine and rehabilitation*, vol. 86, no. 11, pp. 2172–2176, 2005.

[39] S. Furtado, A. Godfrey, S. Del Din, L. Rochester, and C. Gerrand, "The feasibility and validity of accelerometer-based physical functioning measurement after treatment for musculoskeletal tumors of the lower extremity.," 1997.

[40] A. Hickey, S. Del Din, L. Rochester, and A. Godfrey, "Detecting free-living steps and walking bouts: validating an algorithm for macro gait analysis," *Physiological measurement*, vol. 38, no. 1, p. N1, 2016.

[41] R. Z. U. Rehman, S. Del Din, Y. Guan, A. J. Yarnall, J. Q. Shi, and L. Rochester, "Selecting clinically relevant gait characteristics for classification

of early parkinson's disease: A comprehensive machine learning approach," *Scientific reports*, vol. 9, no. 1, pp. 1–12, 2019.

[42] T. C. Vu, J. G. Nutt, and N. H. Holford, "Progression of motor and nonmotor features of parkinson's disease and their response to treatment," *British journal of clinical pharmacology*, vol. 74, no. 2, pp. 267–283, 2012.

[43] C. S. Venuto, N. B. Potter, E. Ray Dorsey, and K. Kieburtz, "A review of disease progression models of parkinson's disease and applications in clinical trials," *Movement Disorders*, vol. 31, no. 7, pp. 947–956, 2016.

[44] E. Demir, C. Vasilakis, R. Lebcir, and D. Southern, "A simulation-based decision support tool for informing the management of patients with parkinson's disease," *International Journal of Production Research*, vol. 53, no. 24, pp. 7238–7251, 2015.

[45] A. Nieuwenhuys, E. Papageorgiou, K. Desloovere, G. Molenaers, and T. De Laet, "Statistical parametric mapping to identify differences between consensus-based joint patterns during gait in children with cerebral palsy," *PLoS One*, vol. 12, no. 1, p. e0169834, 2017.

[46] J. Warmenhoven, N. Bargary, D. Liebl, A. Harrison, M. A. Robinson, E. Gunning, and G. Hooker, "Pca of waveforms and functional pca: a primer for biomechanics," *Journal of Biomechanics*, vol. 116, p. 110106, 2021.

[47] M. É. Czeisler, J. F. Wiley, C. A. Czeisler, S. M. Rajaratnam, and M. E. Howard, "Uncovering survivorship bias in longitudinal mental health surveys," *medRxiv*, 2021.

[48] C. Mack, Z. Su, and D. Westreich, "Managing missing data in patient registries: addendum to registries for evaluating patient outcomes: a user's guide," 2018.

[49] S. Grace-Martin, "Data analysis with spss: A first course in applied statistics," *Statistics*, vol. 4, p. 27, 2010.

[50] G. Molenberghs, H. Thijs, I. Jansen, C. Beunckens, M. G. Kenward, C. Mallinckrodt, and R. J. Carroll, "Analyzing incomplete longitudinal clinical trial data," *Biostatistics*, vol. 5, no. 3, pp. 445–464, 2004.

[51] M. J. Azur, E. A. Stuart, C. Frangakis, and P. J. Leaf, "Multiple imputation by chained equations: what is it and how does it work?," *International journal of methods in psychiatric research*, vol. 20, no. 1, pp. 40–49, 2011.

[52] K. J. Lee and J. B. Carlin, "Multiple imputation for missing data: fully conditional specification versus multivariate normal imputation," *American journal of epidemiology*, vol. 171, no. 5, pp. 624–632, 2010.

[53] T. E. Raghunathan, P. W. Solenberger, and J. Van Hoewyk, "Iveware: Imputation and variance estimation software," *Ann Arbor, MI: Survey Methodology Program, Survey Research Center, Institute for Social Research, University of Michigan*, 2002.

[54] R. Bender and S. Lange, "Adjusting for multiple testing—when and how?," *Journal of clinical epidemiology*, vol. 54, no. 4, pp. 343–349, 2001.

[55] T. A. Craney and J. G. Surles, "Model-dependent variance inflation factor cutoff values," *Quality Engineering*, vol. 14, no. 3, pp. 391–403, 2002.

[56] T. S. Madhulatha, "An overview on clustering methods," *arXiv preprint arXiv:1205.1117*, 2012.

[57] J. H. Ward Jr, "Hierarchical grouping to optimize an objective function," *Journal of the American statistical association*, vol. 58, no. 301, pp. 236–244, 1963.

[58] G. J. Szekely, M. L. Rizzo, *et al.*, "Hierarchical clustering via joint between-within distances: Extending ward's minimum variance method," *Journal of classification*, vol. 22, no. 2, pp. 151–184, 2005.

[59] J. N. Mandrekar, "Receiver operating characteristic curve in diagnostic test assessment," *Journal of Thoracic Oncology*, vol. 5, no. 9, pp. 1315–1316, 2010.

[60] D. Ratnam, P. HimaBindu, V. M. Sai, S. R. Devi, and P. R. Rao, "Computer-based clinical decision support system for prediction of heart diseases using naïve bayes algorithm," *International Journal of Computer Science and Information Technologies*, vol. 5, no. 2, pp. 2384–2388, 2014.

[61] G. Lyons, K. Culhane, D. Hilton, P. Grace, and D. Lyons, "A description of an accelerometer-based mobility monitoring technique," *Medical engineering & physics*, vol. 27, no. 6, pp. 497–504, 2005.

[62] C. L. Geh, M. R. Beauchamp, P. R. Crocker, and M. G. Carpenter, "Assessed and distressed: white-coat effects on clinical balance performance," *Journal of psychosomatic research*, vol. 70, no. 1, pp. 45–51, 2011.

[63] J. Vickers, A. Reed, R. Decker, B. P. Conrad, M. Olegario-Nebel, and H. K. Vincent, "Effect of investigator observation on gait parameters in individuals with and without chronic low back pain," *Gait & posture*, vol. 53, pp. 35–40, 2017.

[64] C. Ladha, S. Del Din, K. Nazarpour, A. Hickey, R. Morris, M. Catt, L. Rochester, and A. Godfrey, "Toward a low-cost gait analysis system for clinical and free-living assessment," pp. 1874–1877, 2016.

[65] I. Hillel, E. Gazit, A. Nieuwboer, L. Avanzino, L. Rochester, A. Cereatti, U. Della Croce, M. O. Rikkert, B. R. Bloem, E. Pelosin, *et al.*, "Is every-

day walking in older adults more analogous to dual-task walking or to usual walking? elucidating the gaps between gait performance in the lab and during 24/7 monitoring," *European review of aging and physical activity*, vol. 16, no. 1, pp. 1–12, 2019.

[66] V. V. Shah, J. McNames, M. Mancini, P. Carlson-Kuhta, R. I. Spain, J. G. Nutt, M. El-Gohary, C. Curtze, and F. B. Horak, "Laboratory versus daily life gait characteristics in patients with multiple sclerosis, parkinson's disease, and matched controls," *Journal of neuroengineering and rehabilitation*, vol. 17, no. 1, pp. 1–12, 2020.

[67] A. K. Rao, G. Youdan Jr, X. Li, N. Fritz, L. Muratori, N. Inbar, T. Gurevich, J. Hausdorff, V. Poile, K. Marder, *et al.*, "Falls and life-space mobility in huntington disease," vol. 16, no. 4, pp. 1376–1377, 2019.

[68] S. Del Din, B. Galna, A. Godfrey, E. M. Bekkers, E. Pelosin, F. Nieuwhof, A. Mirelman, J. M. Hausdorff, and L. Rochester, "Analysis of free-living gait in older adults with and without parkinson's disease and with and without a history of falls: identifying generic and disease-specific characteristics," *The Journals of Gerontology: Series A*, vol. 74, no. 4, pp. 500–506, 2019.

[69] T. C. Pataky, M. A. Robinson, and J. Vanrenterghem, "Vector field statistical analysis of kinematic and force trajectories," *Journal of biomechanics*, vol. 46, no. 14, pp. 2394–2401, 2013.

[70] T. C. Pataky *et al.*, "Rft1d: Smooth one-dimensional random field upcrossing probabilities in python," *Journal of Statistical Software*, vol. 71, no. 7, pp. 1–22, 2016.

[71] T. C. Pataky, M. A. Robinson, and J. Vanrenterghem, "Region-of-interest anal-

yses of one-dimensional biomechanical trajectories: bridging 0d and 1d theory, augmenting statistical power," *PeerJ*, vol. 4, p. e2652, 2016.

[72] Y. Yun, H.-C. Kim, S. Y. Shin, J. Lee, A. D. Deshpande, and C. Kim, "Statistical method for prediction of gait kinematics with gaussian process regression," *Journal of biomechanics*, vol. 47, no. 1, pp. 186–192, 2014.

[73] C. Glackin, C. Salge, M. Greaves, D. Polani, S. Slavnić, D. Ristić-Durrant, A. Leu, and Z. Matjačić, "Gait trajectory prediction using gaussian process ensembles," pp. 628–633, 2014.

[74] D. J. Lizotte, T. Wang, M. H. Bowling, D. Schuurmans, *et al.*, "Automatic gait optimization with gaussian process regression.," vol. 7, pp. 944–949, 2007.

[75] N. Tambasco, S. Simoni, P. Nigro, F. P. Paoletti, E. Marsili, and P. Calabresi, "Morning akinesia in parkinson's disease: challenges and solutions," *Research and Reviews in Parkinsonism*, vol. 6, pp. 57–63, 2016.

[76] P. E. Castro, W. H. Lawton, and E. Sylvestre, "Principal modes of variation for processes with continuous sample curves," *Technometrics*, vol. 28, no. 4, pp. 329–337, 1986.

[77] R. Vautard, K. C. Mo, and M. Ghil, "Statistical significance test for transition matrices of atmospheric markov chains," *Journal of Atmospheric Sciences*, vol. 47, no. 15, pp. 1926–1931, 1990.

[78] M. Chikina, A. Frieze, and W. Pegden, "Assessing significance in a markov chain without mixing," *Proceedings of the National Academy of Sciences*, vol. 114, no. 11, pp. 2860–2864, 2017.

[79] J. M. Hausdorff, S. L. Mitchell, R. Firtion, C.-K. Peng, M. E. Cudkowicz, J. Y. Wei, and A. L. Goldberger, "Altered fractal dynamics of gait: reduced stride-

interval correlations with aging and huntington's disease," *Journal of applied physiology*, vol. 82, no. 1, pp. 262–269, 1997.

[80] S. Chastin and M. H. Granat, "Methods for objective measure, quantification and analysis of sedentary behaviour and inactivity," *Gait & posture*, vol. 31, no. 1, pp. 82–86, 2010.

[81] S. Del Din, B. Galna, S. Lord, A. Nieuwboer, E. M. Bekkers, E. Pelosin, L. Avanzino, B. R. Bloem, M. G. Olde Rikkert, F. Nieuwhof, *et al.*, "Falls risk in relation to activity exposure in high-risk older adults," *The Journals of Gerontology: Series A*, vol. 75, no. 6, pp. 1198–1205, 2020.

[82] C. Buckley, R. McArdle, B. Galna, A. Thomas, L. Rochester, and S. Del Din, "Evaluation of daily walking activity and gait profiles: a novel application of a time series analysis framework," in *2019 41st Annual International Conference of the IEEE Engineering in Medicine and Biology Society (EMBC)*, pp. 2482–2485, IEEE, 2019.

[83] S. Lord, B. Galna, and L. Rochester, "Moving forward on gait measurement: toward a more refined approach," *Movement Disorders*, vol. 28, no. 11, pp. 1534–1543, 2013.

[84] K. S. van Schooten, S. M. Rispens, P. J. Elders, P. Lips, J. H. van Dieën, and M. Pijnappels, "Assessing physical activity in older adults: required days of trunk accelerometer measurements for reliable estimation," *Journal of aging and physical activity*, vol. 23, no. 1, pp. 9–17, 2015.

[85] J. Wilson, L. Alcock, A. J. Yarnall, S. Lord, R. A. Lawson, R. Morris, J.-P. Taylor, D. J. Burn, L. Rochester, and B. Galna, "Gait progression over 6 years

in parkinson's disease: Effects of age, medication, and pathology," *Frontiers in aging neuroscience*, vol. 12, 2020.

[86] L. Rochester, K. Baker, A. Nieuwboer, and D. Burn, "Targeting dopa-sensitive and dopa-resistant gait dysfunction in parkinson's disease: Selective responses to internal and external cues," *Movement Disorders*, vol. 26, no. 3, pp. 430–435, 2011.